THE DYNAMICAL BEHAVIOUR OF FIXED OFFSHORE STRUCTURES USING THE WITTRICK-WILLIAMS ALGORITHM (NONLINEAR EIGENVALUE SOLUTION)

AHMED MAHMOUD
MAHER RAGAB

NOTICE

The quality of this microfiche is heavily dependent upon the quality of the original thesis submitted for microfilming. Every effort has been made to ensure the highest quality of reproduction possible.

If pages are missing, contact the university which granted the degree.

Some pages may have indistinct print especially if the original pages were typed with a poor typewriter ribbon or if the university sent us a poor photocopy.

Previously copyrighted materials (journal articles, published tests, etc.) are not filmed.

Reproduction in full or in part of this film is governed by the Canadian Copyright Act, R.S.C. 1970, c. C-30. Please read the authorization forms which accompany this thesis.

THIS DISSERTATION
HAS BEEN MICROFILMED
EXACTLY AS RECEIVED

AVIS

La qualité de cette microfiche dépend grandement de la qualité de la thèse soumise au microfilmage. Nous avons tout fait pour assurer une qualité supérieure de reproduction.

S'il manque des pages, veuillez communiquer avec l'université qui a conféré le grade.

La qualité d'impression de certaines pages peut laisser à désirer, surtout si les pages originales ont été dactylographiées à l'aide d'un ruban usé ou si l'université nous a fait parvenir une photocopie de mauvaise qualité.

Les documents qui font déjà l'objet d'un droit d'auteur (articles de revue, examens publiés, etc.) ne sont pas microfilmés.

La reproduction, même partielle, de ce microfilm est soumise à la Loi canadienne sur le droit d'auteur, SRC 1970, c. C-30. Veuillez prendre connaissance des formules d'autorisation qui accompagnent cette thèse.

LA THÈSE A ÉTÉ
MICROFILMÉE TELLE QUE
NOUS L'AVONS REÇUE

THE DYNAMICAL BEHAVIOUR OF FIXED OFFSHORE STRUCTURES USING THE WITTRICK-WILLIAMS ALGORITHM

(NONLINEAR EIGENVALUE SOLUTION)

by

Ahmed Mahmoud Maher Ragab, B.E.

A Thesis submitted in partial fulfilment
of the requirements for the degree of
Master of Engineering

Faculty of Engineering and Applied Science
Memorial University of Newfoundland

July 1978

St. John's Newfoundland, Canada

To My Parents

ABSTRACT

The dynamical behaviour of fixed offshore framed structures is studied using the Wittrick-Williams algorithm which considers the nonlinear eigenvalue problem. The effects of i) shear deformation and rotary inertia and ii) axial static loading (accounting for the self-weight of the structural members) are considered in this study of nonlinear free vibration and forced response to wave forces. The algorithm is also used for analysis of offshore structure by Modal Synthesis. The problem of rigid body modes in the modal synthesis is handled by vertical sectioning. The eigenvalue and eigenvectors obtained from using the algorithm (nonlinear free vibration values) are used to determine the linear forced response to ice forces, taking into account the non-proportionality of the damping matrix and the response quantities are obtained by a step-by-step integration method.

The members are assumed to be rigidly connected and the added water mass is assumed equal to the mass of the water displaced. The structural modelling is based on a two-dimensional representation of the three-dimensional tower assuming a constant dimension equal to the base length perpendicular to the plane. The distributed masses of the members in the plane of the frame are computed by summing up the structural mass, the mass of the water contained in the tube and the mass of the water displaced. The member masses in the plane perpendicualr to the frame are assumed to be lumped at the horizontal cross-brace levels.

The results of the study indicate that while the first two frequencies obtained from the Wittrick-Williams algorithm

formulation and linear eigenvalue agree closely, the effect of the algorithm is significant for the higher frequencies. Modal Synthesis enables solutions of large systems due to the reduced size matrices, partitioning and partial modal coupling. The results also highlight the significant effects of the axial static force in the dynamic tangent stiffness matrix in the response study of the offshore structure. Neglect of the off-diagonal terms in the non-proportional damping matrix does not affect the dynamic response values. Fields for further research include i) soil-structure interaction studies for gravity offshore structures, buried pipelines and ii) nuclear power plant structures.

ACKNOWLEDGEMENT

The author is very grateful to his supervisor, Dr. D.V. Reddy, Professor of Engineering and Applied Science, Memorial University of Newfoundland, for his inspiring guidance, valuable suggestions, motivation and continuous support with reference material throughout the project. Professor Reddy's painstaking efforts of careful supervision and criticism at every stage, enabled completion of the thesis in this form in a reasonably short period. Appreciation is expressed to Dr. M. Arockiasamy and Dr. W. Bobby for valuable ideas, references and enthusiastic support.

The author gratefully acknowledges the keen interest and encouragement of Dr. R.T. Dempster, Dean, Faculty of Engineering and Applied Science, and the generous finanical support offered by Memorial University of Newfoundland. Thanks are due to Dean F. Aldrich, Director of the School of Graduate Studies, and Professor M. El-Hawary former Chairman and Professor N. Wilson, present Chairman, Graduate Studies Committe, for their support. Mr. G. Somerton of N.L.C.S. (Newfoundland and Labrador Computer Services) helped in the Computer work. Finally the encouragement of my friends Mr. S. Tadros, and Mrs. G. Kerri is acknowledged.

TABLE OF CONTENTS

Page

LIST OF TABLES

LIST OF FIGURES

Figure | Page

CHAPTER I

INTRODUCTION

1.1 Statement of the Problem

The purpose of this investigation is to apply the Wittrick and Williams algorithm for free and forced vibration analyses of offshore structures. The effects of axial static load, shear deformation and rotary inertia are studied. The work also includes the application of modal synthesis and the use of a non-proportional damping matrix.

1.2 Layout

Chapter II reviews the literature on free and forced vibration of offshore framed structures, made up of members of distributed mass and stiffness, with reference to exact solutions using the Wittrick and Williams algorithm that take into account the effect of axial static load, shear deformation and rotary inertia.

Chapter III presents the study of the nonlinear eigenvalue problem. The application of the Wittrick and Williams algorithm for models with infinite degrees of freedom is described for the eigenanalysis of plane frame models of offshore structures including the effects of axial static load, shear deformation and rotary inertia.

Chapter IV describes the modal synthesis technique and the comparison of the results with those from a direct solution.

Chapter V presents the study of the frame response analysis to wave forces considering the exact solution of lateral vibration,

and including the effects of axial static load, shear deformation, rotary inertia and viscous damping. The effect of each parameter on the forced response displacements and member forces is studied.

Chapter VI presents the study of non-proportional damping matrix for offshore structures; the effect of neglecting off-diagonal terms for this matrix by diagonalization is investigated for response to random ice excitation.

Chapter VII compares the results obtained from the approximate and the exact solutions. In addition, the results obtained for free and forced vibration, neglecting secondary effects (shear deformation and rotary inertia and axial static load), are compared with those in which these effects are included. The conclusions and several recommendations for further research are presented at the end of the chapter.

CHAPTER II

LITERATURE REVIEW

2.1 Introduction

The topics reviewed are the analysis of infinite models with infinite properties using the Wittrick and Williams algorithm, including the effects of axial static load, shear deformation and rotary inertia. Other subjects covered are the modal synthesis technique, wave theory, Morison's equation, drag and inertia force coefficients, measurements of ice forces, and nonlinear damping.

2.2 NONLINEAR EIGENVALUE PROBLEM

2.2.1 The 'Infinite' Models

An infinite model is one in which some, or all of the nodal points, are connected not by massless springs as in the case of finite model but by continuous one-dimensional 'members' which may be regarded as line distributions of mass and stiffness. The term 'one-dimensional' does not necessarily imply that the line is straight, but merely that the differential equation governing its vibration involves only one independent spatial variable, namely distance measured along the line. The continuous members may represent straight or curved beams with up to six different stiffnesses included as required, namely two flexural and two shear stiffnesses plus the extensional and torsional stiffnesses. Vibration analysis of continuous beams or rigidly jointed plane frames using this type of model have been reported, for example, by Veletsos and Newmark (1), Simpson and Tabarrok (2), Armstrong (3),

and Williams and Wittrick (4). Plane grillages have been analysed in a similar way by Armstrong (5). The distributed mass and stiffness concept is also suitable for analysing the torsional oscillations of shaft systems and flywheels. It is not quite so obvious that such a modelling can account for certain types of prismatic structures which consist of a series of rectangular plates connected together along longitudinal edges; however, applications have been described by Williams and Wittrick (6), and Wittrick and Curzon (7). The structures include, for example, thin open section beams, thin tubes of polygonal section, panels with longitudinal stiffness, which are themselves thin-walled, and corrugated-core sandwich panels. If the ends of such structures are appropriately supported, all modes of vibration have displacements which vary sinusiodally in the longitudinal direction, with a half-wave-length equal to an integral fraction of the length.

Wittrick and Williams (8) have shown that the stiffness matrix may become infinite at certain frequencies, which will be infinite in number. This can be seen from the equation:

$$[K]\,[X] = [P], \qquad (2.1)$$

and its inverse

$$[X] = [K]^{-1}[P] \qquad (2.2)$$

where K is the dynamic stiffness matrix of the infinite model corresponding to the finite set of displacements X. If the system is constrained such that $X = 0$, the natural frequencies of the constrained system in general correspond to $\det [K]^{-1} = 0$,

which in turn implies that det [K] = ∞. Finally, Ref. 8 shows that the eigenvalue problem, [K] [X] = 0, may in exceptional circumstances have solutions for X = 0 but not for det [K] = 0. The only way of computing the natural frequencies of an infinite system has been to vary the frequency ω in small steps, calculating the determinant of K at each step, and to seek the values which make the determinant zero. In Ref. 8, the numerous disadvantages and pitfalls of the above procedure have been described. The algorithm, described later in this chapter, completely overcomes these dangers and difficulties.

2.2.2 Rayleigh's Theorem

The algorithm depends for its validity upon a theorem of Rayleigh (9) which may be stated as follows:

THEOREM 1. If one constraint is imposed upon a linearly elastic structure, whose natural frequencies of vibration arranged in ascending order of magnitude are ω_r, the natural frequencies ω'_r of the constrained structure are such that

$$\omega_{r-1} \leq \omega'_r \leq \omega_{r+1} \qquad r = 1, 2, 3$$

THEOREM 2. If one constraint is removed from a structure, the number of natural frequencies which lie below some fixed chosen frequency either remains unchanged or increases by one.

2.2.3 A Basic Theorem and Some Definitions Concerning Matrices

Wittrick and Williams (10) defined the sign count of any matrix S(K) as 'the number of negative elements on the diagonal

after reduction of the matrix to an upper triangular form K^{Δ}. This definition, based on the theorem given by Wilkinson (11), is stated as follows:

Theorem: The number of characteristic values λ_j, (j = 1, 2 ..... n) of the matrix H, which are less than some specified value λ^*, is equal to the number of reversals of sign between consecutive members of the sequence det $(H_r - \lambda^* I)$, where H_r is the leading principal sub-matrix of order r of H, r = 0, 1, 2 ..... n and det $(H_0 - \lambda^* I) = +1$ by definition.

2.2.4 Wittrick and Williams Algorithm

Wittrick and Williams (8, 10) extended the Sturm Sequence procedure and applied it to the nonlinear eigenvalue problem. The starting point of the eigenvalue problem is

$$[K]\ [X] = 0 \qquad (2.3)$$

where [K] is a (N x N) symmetrical matrix and [X] is (N x 1) vector of all the displacements of nodes. Partitioning Eqn. 2.3 leads to

$$\begin{bmatrix} K_{ii} & K_{io} \\ K_{io} & K_{oo} \end{bmatrix} \begin{bmatrix} X_i \\ X_o \end{bmatrix} = 0 \qquad (2.4)$$

where X_i is a (N-n) x 1 vector of the internal node displacements of the sub-structure, and X_o is a (n x 1) vector of displacements of the other nodes. Gaussian elimination was used to triangulate the above matrix. Then at the stage when all the rows in K_{ii} have

become pivotal, the matrix is

$$\begin{bmatrix} K_{ii}^{\Delta} & F \\ 0 & K_o \end{bmatrix}$$

where F is some rectangular matrix which is of no interest, and K_o is a symmetrical (n x n) matrix of smaller order than K and is given as

$$K_o = K_{oo}^T - K_{io}^T K_{ii}^{-1} K_{io} \qquad (2.5)$$

The triangulation is continued until the matrix reaches the form

$$K^{\Delta} = \begin{bmatrix} K_{ii}^{\Delta} & F \\ 0 & K_o^{\Delta} \end{bmatrix} \qquad (2.6)$$

In this case, the sign count of the above matrix is:

$$S(K) = S(K_{ii}) + S(K_o) \qquad (2.7)$$

The algorithm of Wittrick and Williams (8, 10) is as follows:

Theorem: Consider a structure having N degrees of freedom. Let X_o be any displacement vector of n (<N) degrees of freedom and the eigenvalue problem be defined by $K_o(\lambda)X_o = 0$, where K_o is the dynamic stiffness matrix corresponding to the displacement X_o. Let $J(\lambda^*)$ be the number of eigenvalues of the structure lying between 0 and some specified value λ^* for n constraints so that $X_o = 0$. Then it follows that

$$J(\lambda^*) = J_o(\lambda^*) + S[K_o(\lambda^*)] \qquad (2.8)$$

It is to be noted that the above equation remains valid as $N \to \infty$.

2.2.5 The Applications of the Algorithm to Infinite Systems

The algorithm enables the exact determination of the number of natural frequencies below any chosen frequency, without specifying their actual values. This knowledge gives all the natural frequencies, with no possibility of missing any; also the procedure will require far fewer iterations for a given accuracy. Moveover, as will be seen later, it automatically indicates the existence of the natural frequencies for which $X = 0$, rather than $\det[K] = 0$.

The algorithm was applied in Ref. 8 on two-dimensional framed structures similar to the frame discussed in detail in Ref. 2. In this application, one half of the frame with 12 degrees of freedom was used to investigate antisymmetrical vibrations. The 12 D-O-F represent 8 joint rotations and 4 sidesway displacements. Sketching of the variation of the determinant of the 12 x 12 dynamic stiffness matrix $K_{12}(\omega)$ associated with these 12 degrees of freedom gives a complete picture of the nature of the zero stiffness matrix, and the physical meaning associated with the determinant of the stiffness matrix approaching infinity. Ref. 4 gives the rules for finding all the required natural frequencies of any frame with members rigidly jointed at both ends (J_m), members attached elastically to foundations (J_e), and the number of frequencies of sub-structures. In addition, a simple and effective method converging on a specified natural frequency and based on the above results is described.

Another application of the algorithm is given in Ref. 10 to determine the natural frequencies of vibration of a marine dolphin structure with an infinite number of degrees of freedom. This structure is identical to the one discussed by Sainsbury and King (12), which was constructed in deep water at the Imingham Oil Terminal in England and suffered severe vibrations during ebb tides to vortex shedding from the piles. This application is concerned with two problems; first, the calculation of the natural frequencies of vibration of a dolphin of a given design, and, second, the problem of designing the piles to ensure that the fundamental frequency of vibration exceeds a specified value. Swannell (13) applied the algorithm to solve plane frame structures.

2.2.6 Secondary Effects on the Lateral Vibration

The effects of shear deformation and rotary inertia, axial static loading and viscous damping are studied in some text books. Timoshenko, Young and Weaver (14), Clough (15), Kolousek (16) and Thomson (17) give the effect of each parameter on the lateral vibration of motion. The solution of the differential equation of lateral vibration of a beam including the above parameters was solved by Swannell (18), and the results are presented in Appendix I. Tranberg (19) describe the effects of the above parameters on a single bay portal frame.

2.3 Modal Synthesis Technique

The concepts of modal synthesis were introduced by Hurty in a series of papers (20, 21, 22, 23), the first appearing in 1960.

Hurty's technique depends on partitioning the system into several parts, the constraints at the interfaces are set for each part, and the modal vectors are computed. These included the elastic normal modes, constraint modes, and rigid body modes. For each part, the generalized mass, stiffness, damping and force matrices are computed and the equations of motion set up. The transformation matrix [B] is formed for modal coupling by restoring geometric compatibility at the interfaces and used to establish the relation between the independent and the dependent co-ordinates. Hence, the synthesized total system equations are developed using the transformation matrix [B].

The technique, developed by Bajan, Feng and Jaszlics (24), involves modal coupling and modal substitution. The former couples the subsystem modes to obtain the total system modes, while the latter provides an iteration scheme for improving accuracy through error analysis. Goldman (25, 26) used rigid body modes and free-free elastic modes of the parts for synthesis. Modal coupling is effected by eliminating the internal force terms at connection interfaces from equations of motion through the compatibility relations. The technique developed by Gwin (27) involves empirical coupling for computing modal data of a space vehicle made up of a main structure and several branch structures.

2.4 Wave Force Analysis

2.4.1 Wave Theory

A wave theory, appropriate to the wave conditions under consideration, must be selected so that wave orbit velocities

and accelerations can be evaluated. Several such theories have been developed for various wave conditions. In relatively deep water, Stokes' Fifth Order Theory described by Skjelbreia and Hendrickson (28) is commonly used to describe steep non-linear waves. Hogben, Miller, Searle and Ward (29) have shown that the resulting distributions of particle velocities and accelerations are not very different from those predicted by the relatively simple Airy Linear Theory. Correspondingly, it has been found that in deep water, predictions of loading using Airy Linear Theory, but with integration of the forces up to the actual water surface, gives results which do not differ greatly from predictions based on Stokes Fifth Order Theory.

2.4.2 Morison Equation

The Morison equation (30) is adequate for evaluation of the wave force if:

(1) The diameter of the concerned structural member is small in relation to the wavelength to justify the assumption of uniform ambient acceleration, and there is no wave scattering due to the local influence of neighbouring components. For guidance, the criterion of diameter/wavelength $(D/\lambda) < 0.2$ is recommended by Hogben (31), based on the data of Chakrabarti and Tam (32), taking into consideration the wavelength range over which uniform acceleration can be assumed by reference to the corresponding range of uniformity of wave surface slope.

(2) The evaluation of the inertia force term in the Morison equation requires the mass coefficient to be known for the particular

shape of structural component and the corresponding direction of the acceleration vector. Mass coefficients for various simple geometrical shapes are given by Myers et al (33).

2.4.3 Drag and Inertia Force Coefficients

The drag force coefficient (C_d) was found equal to 0.60 by Evans (34) and Hudspeth (35) for data from the Gulf of Mexico. Rance (36) used $C_d = 0.6$ for high Reynolds numbers and a high Keulegan - Carpenter number in his pulsating water channel experiments. As the fluid motion around the cylinder is quasi-steady at high Keulegan - Carpenter numbers with post-critical Reynolds numbers, drag coefficients can be expected to be close to those of steady flow, which are in the range of 0.60-0.70. A constant value of $C_d = 0.60$ is therefore suggested for this regime. The inertia force coefficient value suggested , 1.5, is based on values given in Refs. 34 and 35.

For an inclined circular cylinder, Chakrabarti et al (37) suggested that the cross flow principle should be assumed (i.e. normal pressure force is assumed to be independent of tangential velocity), and the Morison equation used with the component of fluid velocity normal to the axis of the cylinder. This is the only information available on inclined cylinders in waves, no wave force coefficients were suggested because of the wide scatter in the derived values of the coefficients.

2.5 Ice Force Analysis

2.5.1 Measurement of Forces and Crushing Strength of Ice

Zubov (38), Korzhavin (39), and Drouin and Michel (40)

carried out analytical, experimental and field studies on the determination of static ice pressure on structures, primarily due to temperature fluctuations within the ice sheets. Korzhavin's comprehensive studies from 1933-1962 on the determination of ice pressures have been summarized by Michel (41). Blenkarn and Knapp (42) have described the anticipated ice conditions and maximum ice forces in the Grand Banks off the Coast of Newfoundland.

Kopaigorodski et al (43) made model studies on ice sheets to determine the mean ice pressure and variation of the values around the mean. It was concluded that sheets with small h/d (i.e. thickness to indentor width) ratios fail by instability while shear failure occurs for sheets with large h/d ratios. Hirayama et al (44, 45) suggested an empirical formula for ice pressures which takes into consideration the indentor shape and diameter, ice thickness, and the relative velocity between ice and the structure.

Afanas'ev (46) developed an empirical equation for loading on vertical surfaces based on experimental and theoretical studies. The American Petroleum Institute's (API) recommendation (47) indicates ice crushing strengths of 200 - 500 psi for the determination of ice forces.

2.5.2 Dynamic Ice Forces on Structures

Blumberg and Strader (48) analyzed an offshore monopod at Cook Inlet, Alaska, subjected to tidal current-driven ice loads for dynamic response. Assuming the primary structural response to ice floe excitation to be its fundamental mode of

vibration, Matlock, Dawkins and Panak (49) analyzed a cantilever pier, idealized as a damped single-degree-of-freedom system and subjected to postulated saw-tooth-type deterministic loading. The calculated response showed good agreement with earlier field measurements of Peyton (50). Sundararajan and Reddy (51) used the Matlock et al model to study the stochastic response of a single-degree-of-freedom (SDOF) model by the spectral technique. The force records used were the field measurements of Blenkarn (52) at Cook Inlet, Alaska. Ref. 50 concluded from field measurements of the responses of a pile subjected to the action of uniformly thick ice sheets that the force oscillations are predominant in the range of 1 Hz.

2.5.3 Dynamic Analysis of Fixed Offshore Structures to Ice Forces

Reddy and Cheema (53) used the power spectral density method for the determination of responses of an offshore structure modelled as multi-degree-of-freedom (MDOF) lumped mass system. The ice force records used were those of Blenkarp (42), determined from two instrumented structural devices - a strain gauged test pile driven into the ocean bottom adjacent to an existing temporary offshore drilling platform, and a field test beam hinged at both ends to the platform leg with a load cell measuring the reaction at the upper hinge. Reddy, Cheema and Swamidas (54) developed response spectra for ice forces and used these for analysing a three-dimensional offshore platform (modelled as a two-dimensional plane frame). The probable maximum dynamic response to impact loads of moving ice sheets was calculated assuming the added water mass to be equal to the mass of water

displaced as suggested by King (55). The ice-force records were digitised using the Nyquist Criterion, and the stationarity of the chosen ice-force records was verified by using the Kolomogorov-Smirnov criterion. The work included an extensive literature review ice-structure interaction. Reddy, Cheema, Swamidas and Haldar (56) used the power spectral density method for the response analysis of a framed tower taking into account the three-dimensionality. Swamidas and Reddy (57) analysed an offshore monopod tower considering ice-structure interaction by the finite element method. Instead of assuming the added water mass to be equal to the displaced water mass, the frequency dependence of the added water mass was taken into account based on the substructure concept of EATSW, a programme for Response of Axisymetric Tower Structures Surrounded by Water (58). The hydrodynamic interaction terms in the modal equations of motions of the structure are determined as solutions of the boundary value problems for the fluid domain. Ice force records were generated artificially following a method suggested by Swamidas, Reddy and Purcell (59) based on the similarity between the fluctuating parts of randomly varying ice-force records and seismic records. The work included the study of the influence of soil properties on the frequencies and responses.

2.6 The Non-Proportional Damping Matrix

For non-orthogonal or non-classical damping, the response can be determined by the classical normal mode method if the non-diagonal terms in the non-proportional damping matrix are

equal to zero. However, this simple diagonalization procedure may lead to significant errors. This procedure and the errors due to it have been studied in some detail. Thomson, Colkins and Caravani (60) determined the steady-state response of a three degree-of-freedom system with and without the approximate diagonalization procedure. Their plotted response curves indicated no errors in the resonant response. After discussing the diagonalization of the non-proportional daming matrix, Kronin(61) introduced correction terms (α) to improve the accuracy. Non-classical damping is used by setting

$$C = \alpha K + C'$$

where C' is a diagonal matrix and α = .02. Using Cronin's Correction Terms causes significant decreases in these errors.

Based on soil-structure interaction analyses, where an approximate diagonal damping matrix has been introduced, Beredugo (62) studied the coupled rocking - horizontal translation motion of a massive foundation embedded in an elastic half-space. Radiation damping causes coupling of the equations in the principal coordinates. Considering the steady state response of the foundation to harmonic forces, Beredugo showed that neglect of the off-diagonal terms has little effect on the amplitude of response. The paper presents the results for a footing resting on the surface of the soil and a similar one embedded in the soil. It is apparent from the form of the response curves that the embedment increases the radiation damping levels considerably. Although the effect

of the approximate diagonalization procedure on amplitudes is acceptably small, it is proportionately greater for the embedded footing.

Bielak (63) considers the coupled vibrations of a conventional multistorey shear building with a foundation resting on a viscoelastic half-space. The damping matrix for the structure with the foundation fixed is orthogonal to the eigenvectors of the fixed-base structure. However, when coupled vibrations of the complete system are considered, the matrix, which now includes frequency dependent terms from the radiation and internal damping of the rocking and horizontal translational modes of the foundation on the half-space, is not orthogonal to the eigenvectors of the coupled system. Considering the response of multi-storey structures to a harmonic free field surface acceleration, Ref. 63 showed that neglect of the off-diagonal terms, in the non-proportional damping matrix, has a small effect upon response amplitudes. The response of these structures to earthquakes requires the use of the Fast Fourier harmonic response, because of the frequency dependent damping terms. Thus it is concluded that if the harmonic response is not significantly affected by the approximate procedure of diagonalization, the response to earthquake will have comparable accuracy.

Clough and Mojtahedi (64) considered the coupled vibrations of a dam-foundation system caused by an earthquake, using the finite element method to idealize the dam and foundation cross-section. A standard value is assumed for the modal

damping ratios of the structure alone, and another value for the modal damping ratios of the foundation. However, for the coupled system, if different values are used for the two components, non-orthogonal damping occurs. The authors show that neglecting the off-diagonal terms from the non-proportional damping matrix leads to significant errors in the maximum response of the dam.

CHAPTER III

THE NONLINEAR EIGENVALUE PROBLEM

3.1 Introduction

An 'infinite model' is one in which some, or all of the components of the real structure are idealised as members which have continuous distributions of stiffness and mass. Thus the model has an infinite number of degrees of freedom, and consequently an infinite number of eigenvalues. Under these circumstances, the eigenvalue problem for a structure, assembled from partitioned sub-structures with n and N-n components, can be represented as

$$\begin{bmatrix} K_{ii} & K_{io} \\ K_{io}^T & K_{oo} \end{bmatrix} \begin{bmatrix} V_i \\ V_o \end{bmatrix} = 0 \qquad (3.1a)$$

where V_o is n x 1 vector of displacements of junctions between the continuous members of the sub-structures, V_i is a (N-n) x 1 vector of displacements of the internal nodes of the sub-structure. From the first of these equations

$$V_i = -K_{ii}^{-1} K_{io} V_o \qquad (3.1b)$$

The second equation then becomes

$$K_t(\omega) V_o = 0 \qquad (3.1c)$$

where

$$K_t(\omega) = K_{oo} - K_{io}^T K_{ii}^{-1} K_{io} \qquad (3.1d)$$

The matrix $K_t(\omega)$ is a symmetrical (n x n) matrix, called the dynamic tangent stiffness matrix, corresponding to the set of displacements V_o. The elements of the dynamic tangent stiffness matrix can be obtained by solving the differential equation governing the vibration of a continuous member. In general, the solution will be in terms of transcendental functions and the dynamic stiffness matrix of the member relating forces applied at its ends will have transcendental dependence on ω. This is reflected in the dynamic stiffness matrix of the system. The plotting of the determinant $|K_t(\omega)|$ against the square of the perturbing frequency (ω^2) will be discontinuous (Fig. 3.1). The values at the discontinuity points approach ± infinity.

In the following treatment, a three-dimensional fixed offshore structure is modelled as a plane frame with the contribution from the third direction lumped at the nodes. The nonlinear eigenvalue solution is first obtained neglecting the effects of shear deformation and rotary inertia, axial static load and the rotation of the lumped mass. In the following treatment, each one of the factors is considered separately and used in the nonlinear eigenvalue problem. The results are then compared to obtain parametic evaluations of the individual effects on the final solution.

As far as the author's knowledge goes, this is the first application of the nonlinear eigenvalue problem to an offshore structure.

3.2 The Dynamic Stiffness Matrices

Fig. 3.2 shows a typical prismatic beam-column member

in any two-dimensional framework. The end forces and moments vary sinusoidally with time and the amplitudes of the forces and displacements are [S] and [V] respectively. The relationship is of the form:

$$[S] = [K]\,[V] \qquad (3.2)$$

where [K] is the Dynamic Member Stiffness matrix

$$[S] = [S_{1x},\ S_{1y},\ m_1,\ S_{2x},\ S_{2y},\ m_2]$$

and

$$[V] = [V_{1x},\ V_{1y},\ \theta_1,\ V_{2x},\ V_{2y},\ \theta_2]$$

The differential equation for the free undamped vibration of a prismatic beam bending in a principal plane is (Fig. 3.3)

$$EI\ \partial^4 y/\partial x^4 + \rho A\ \partial^2 y/\partial t^2 = 0 \qquad (3.3)$$

where

$\rho A = m$ = mass/unit length,

ρ = mass density,

A = cross-sectional area,

and

EI = flexural rigidity

The displacement y is of the form

$$y = V\ \mathrm{Sin}\ (\omega t + \alpha)$$

where $\bar{V}$ is the amplitude of vibration, a function of position, ω is the frequency in radians/sec, and α is a term allowing for non-zero displacement at time $t = 0$.

Direct substitution into Eqn. 3.3 gives the ordinary differential equation

$$d^4\bar{V}/dx^4 - \rho A\omega^2\bar{V}/EI = 0 \qquad (3.4)$$

The general solution of this equation is:

$$\bar{V} = B_1 \operatorname{Sin}\lambda_1 x + B_2 \operatorname{Cos}\lambda_1 x + B_3 \operatorname{Sinh}\lambda_1 x + B_4 \operatorname{Cosh}\lambda_1 x \qquad (3.5)$$

where

$$\lambda_1^4 = m\omega^2/EI ,$$

and the constants of integration are evaluated from the boundary conditions (see Fig. 3.2):

$$x = 0,\ \bar{V} = V_{1y};\ x = L,\ \bar{V} = V_{2y}$$

$$x = 0,\ d\bar{V}/dx = \theta_1;\ x = L,\ d\bar{V}/dx = \theta_2$$

Differentiation of Eqn. 3.5 and direct substitution gives B_1, B_2, B_3 and B_4 as

$$\{B\} = [C]^{-1}\{V_F\} \qquad (3.6)$$

where

$$\{B\}^T = [B_1\ B_2\ B_3\ B_4],$$

$$\{V_F\}^T = [V_{1y}\ \theta_1\ V_{2y}\ \theta_2],$$

and

$$[C] = \begin{bmatrix} 0 & 1 & 0 & 1 \\ \lambda_1 & 0 & \lambda_1 & 0 \\ \text{Sin}\lambda_1 L & \text{Cos}\lambda_1 L & \text{Sinh}\lambda_1 L & \text{Cosh}\lambda_1 L \\ \lambda_1 \text{Cos}\lambda_1 L & -\lambda_1 \text{Sin}\lambda_1 L & \lambda_1 \text{Cosh}\lambda_1 L & \lambda_1 \text{Sinh}\lambda_1 L \end{bmatrix}$$

A relationship is now sought between the amplitudes of the end forces and $\{B\}$. It then becomes possible to write these amplitudes in terms of the corresponding displacements, $\{V_F\}$ as

$$M = -EId^2V/dx^2 = EI(\lambda_1^2 B_1 \text{Sin}\lambda_1 x + \lambda_1^2 B_2 \text{Cos}\lambda_1 x - \lambda_1^2 B_3 \text{Sinh}\lambda_1 x - \lambda_1^2 B_4 \text{Cosh}\lambda_1 x) \quad (3.7a)$$

and

$$S = dM/dx = EI(\lambda_1^3 B_1 \text{Cos}\lambda_1 x - \lambda_1^3 B_2 \text{Sin}\lambda_1 x - \lambda_1^3 B_3 \text{Cosh}\lambda_1 x - \lambda_1^3 B_4 \text{Cosh}\lambda_1 x) \quad (3.7b)$$

Again, use is made of the boundary conditions (Figs. 3.2 and 3.3):

$$x = 0 \; M = +m_1 ; \; x = L, \; M = -m_2,$$

and

$$x = 0 \; S = -S_{1y} ; \; x = L, \; S = +S_{2y}$$

which gives

$$\{S_F\} = [D] \{B\} \quad (3.8)$$

where

$$\{S_F\}^T = [S_{1y} \; m_1 \; S_{2y} \; m_2]$$

and

$$[D] = \begin{bmatrix} -\lambda_1^3 & 0 & \lambda_1^3 & 0 \\ 0 & \lambda_1^2 & 0 & -\lambda_1^2 \\ \lambda_1^3\mathrm{Cos}\lambda_1 L & -\lambda_1^3\mathrm{Sin}\lambda_1 L & -\lambda_1^3\mathrm{Cosh}\lambda_1 L & -\lambda_1^3\mathrm{Sinh}\lambda_1 L \\ -\lambda_1^2\mathrm{Sin}\lambda_1 L & -\lambda_1^2\mathrm{Cos}\lambda_1 L & \lambda_1^2\mathrm{Sinh}\lambda_1 L & \lambda_1^2\mathrm{Cosh}\lambda_1 L \end{bmatrix}$$

Hence

$$\{S_F\} = [K_F]\{V_F\} \qquad (3.9)$$

where

$$[K_F] = [D][C]^{-1}$$

The formal algebra implied by Eqn. 3.9 is straightforward and the results are stated in a convenient form of Dynamic Stiffness Functions in Appendix I.

In order to complete the derivation of the (6x6) member stiffness matrix, the amplitudes of the axial forces and displacements shown in Fig. 3.4 should also be considered. Again, classical theory gives the differential equation governing the axial motion as

$$EA\partial^2 u/\partial x^2 - \rho A\partial^2 u/\partial t^2 = 0 \qquad (3.10)$$

where u is the axial displacement, a function of position and varying sinsoidally with time. The amplitudes of motion, $\bar{u}$, are given by

$$EAd^2\bar{u}/dx^2 + \rho A\omega^2\bar{u} = 0 \qquad (3.11)$$

The general solution of this equation is

$$\bar{u} = A_1 \text{Sin}\alpha x + A_2 \text{Cos}\alpha x \qquad (3.12)$$

where

$$\alpha^2 = m\omega^2/EA$$

and the constants of integration are evaluated from the boundary conditions as

$$x = 0,\ \bar{u} = v_{1x};\ x = L,\ \bar{u} = v_{2x}$$

Hence

$$T = EA\bar{du}/dx = \alpha EA/\text{Sin}\alpha L\ [(v_{2x} - v_{1x}\ \text{Cos}\alpha L)$$

$$\text{Cos}\alpha x - v_{1x}\ \text{Sin}\alpha L\ \text{Sin}\alpha x] \qquad (3.13)$$

Using the boundary conditions

$$x = 0,\ T = -s_{1x} \text{ and } x = L,\ T = +s_{2x}$$

gives the results:

$$\{s_A\} = [k_A]\ \{v_A\} \qquad (3.14)$$

where

$$\{s_A\}^T = [s_{1x}\ s_{2x}],\ \{v_A\}^T = [v_{1x}\ v_{2x}]$$

and

$[k_A]$ is the coefficient matrix of axial Dynamic Stiffness Functions.

Eqn. 3.14, in conjunction with Eqn. 3.9, gives the full member

stiffness matrix $[k(\omega)]$ which is summarised in Appendix I.

3.3 The Determination of the Natural Frequencies

The natural frequency of the nonlinear eigenvalue problem of frame structure is determined from

$$[k_t(\omega)]\ [v] = 0$$

There are two solutions for the above equation:

(a) $|k_t(\omega)| = 0$, $v_o \neq 0$ is one set of solutions

(b) $|k_t(\omega)| = \infty$, $v_o = 0$ is not necessarily a trivial set of solutions but corresponds, sometimes to frame mode shapes whose nodes correspond to the nodes of the frame. Wittrick points out that $|k_t(\omega)| = \infty$ only when a term of $[k_t(\omega)]$ becomes infinite and that, physically, such an event occurs when any one or more of the elements of the frame is about to resonate. If it were "CLAMPED ENDED", i.e. $|k_t(\omega)| \to \infty$, with additional constraints at nodes to prevent displacement, the perturbing frequency ω, corresponds to a resonant frequency of the fully clamped structure. (A fully clamped structure behaves as a series of non-interacting individually fixed-ended elements).

Therefore, when $|k_t(\omega)| \to \infty$, it is normally implied that the actual, unclamped structure will resonate. However, it is possible occasionally that the stiffness of the real structure at 'pseudo-critical' values of the eigenparameter would be such that additional clamping forces necessary to prevent joint displacements would be zero. Hence, it is sometimes possible that at $|k_t(\omega)| \to \infty$ the real structure will resonate with all nodal

displacements zero in the corresponding eigenmode.

3.4 Wittrick and Williams Algorithm

Basic theorms relating to the solution procedure for types (a) and (b) in the previous section have been derived and published by Williams and Wittrick (4) and Wittrick and Williams (8, 10). An infallible search algorithm is available which determines the number of natural frequencies of the frame, either of type (a) or (b), which are less (i. e. have lesser frequency values) than any given perturbing frequency ω. These basic theorems are proven in general terms and the algorithm is easily states for the present purposes. The algorithm provides a powerful method for solving the strucutres with infinite degrees of freedom.

In the basic form, the algorithm states that:

$$J(\omega) = J_0(\omega) + s[k(\omega)] \tag{3.15}$$

where

$J(\omega)$ = No. of natural frequencies less in value than the perturbing frequency, ω, of the sinusoidally varying displacements,

$S[k(\omega)]$ = No. of the negative elements on the leading diagonal of $[k(\omega)]^{\Delta}$; $[k(\omega)]^{\Delta}$ is the upper triangular matrix obtained by applying the usual form of Gauss elimination to $k(\omega)$,

$J_0(\omega)$ = No. of 'clamped end' natural frequencies of individual members summed over all the members of the frame, which are less in value than the frequency ω.

Clamping these displacement components does not necessarily make $J_0(\omega)$ zero since it corresponds to clamping the joints of the plane of the frame, and the exact member equations (see Appendix

I) still allow each member an infinite number of degrees-of-freedom between joints. Thus

$$J_0(\omega) = \Sigma J_m(\omega) \tag{3.16}$$

where $J_m(\omega)$ is the number of eigenvalues between $\lambda = 0$ and $\lambda = \lambda_I$ for a component member with its ends clamped, while the summation extends over all members of the frame.

The plane frame member equations can be written as

$$\begin{aligned} k_{11}v_1 + k_{12}v_2 &= s_1 \\ k_{12}v_1 + k_{22}v_2 &= s_2 \end{aligned} \tag{3.17}$$

where v_i and s_i ($i = 1, 2$) are the element displacement and force vectors at end i of a member (amplitudes of quantities with sinusoidal time dependence in vibration problems), while k_{ij} ($i = 1, 2$; $j = 1, 2$) are (3x3) λ - dependent stiffness matrices. Appendix I gives formula for the elements of k_{ij} and defines the elements of v_i and s_i.

The usual direct assembly procedure enables $k(\omega)$ to be assembled from the $k^l_{ij}(\omega)$ of the members, where

$$k^l_{ij} = T^T k_{ij} T (i = 1, 2; j = 1, 2), \tag{3.18}$$

and T is the transformation matrix of Appendix I. $J(\omega)$ then follows from Eqs. 3.15 and 3.16, and the formulas for J_m in Appendix I.

Consider the plots of $|k_t(\omega)|$, Fig. 3.5, that can be obtained from any assumed structure. Suppose that λ_I is the first perturbing frequency of one member of the frame if that member were clamped.

Evaluations of $J(\omega)$ at the value λ just less than λ_I will give $J(\omega) = 5$ with $s[k(\omega)] = 5$ and $J_0(\omega) = 0$. This is self-evident because there are five critical perturbing frequencies corresponding to $|k_t(\omega)| = 0$, less in magnitude than λ_I, and, we have not reached λ_I; there have, as yet, been no values of λ which have as great as the lowest clamped-end perturbing frequency of any member of frame.

Suppose now we evaluate $J(\omega)$ at a value of λ just greater than λ_I. Suppose also, firstly, that one particular frame does not exhibit zero stiffness when $\lambda = \lambda_I$. This can be determined from the algorithm by noting that $J(\omega)$ remains equal to 5, being composed of $s[k(\omega)] = 4$ and $J_0(\omega) = 1$. In other words, a negative element will 'disappear' from the leading diagonal to 'compensate' for the increase in $J_0(\omega)$ (see Fig. 3.5(a)).

Suppose however, secondly, that one frame does exhibit zero stiffness when $\lambda = \lambda_I$. This would be obtained from the algorithm by noting that $J(\omega)$ has increased to 6 in crossing λ_J being composed of $s[k(\omega)] = 5$ and $J_0(\omega) = 1$. Obviously, the computer programme must be written to include tests which will identify the 'cause' of the increase of $J(\omega)$ as being an increase in $J_0(\omega)$ without a corresponding decrease in $s[k(\omega)]$, and that consequently a null mode occurs (see Fig. 3.5(b)).

The algorithm is therefore very elegant. A study of the 'comings and goings' of various negative elements on the leading diagonal of $[k_t(\omega)]^{\Delta}$ is in itself a fascinating mental exercise. The positions of the negative elements on the leading diagonal are important in facilitating the computation of the eigenmode

associated with each solution of $|k_t(\omega)| = 0$.

To calculate the eigenmode, it is necessary to set one of the displacement variables to unity, strike out the row in $[k_t(\omega)]$ which has the same row number as the column number corresponding to the unit displacement, and transfer the remaining set of simultaneous equations.

The important decision is about the displacement variable that should be set equal to unity if a haphazard choice is made, it is possible to erroneously set to a unity a displacement whose eigenmode value is truly zero and encounter considerable difficulty in finding the relative magnitudes of other modal displacements.

Swannell (18) suggested a procedure to overcome this in which the 'safe' displacement set to unity is the one corresponding to the position of the element on the leading diagonal of $[k_t(\omega)]^{\Delta}$ which changes from positive to negative as the particular eigenvalue is 'crossed' in the search.

3.5 Numerical Examples

a) Introduction

Two numerical examples are described to apply the Wittrick and Williams algorithm to offshore structures.

b) Example I

The structure investigated is a welded tubular steel frame, similar to that analysed by Carotis and Martin (65) for response to random wave forces in a medium water depth. Generally, the structure should be treated as a continuous system and the height of the structure will be set equal to the sum of the water depth

and the height above the water surface. In this example, a total height of 360 ft is assumed;60 ft above the still water line. A two-dimensional representation of the tower with fixed end bases and sectional properties of the members shown in Fig. 3.6 are given in Table 3.1. The structural members are assumed to be rigidly connected. A constant dimension equal to the base length of the planar frame is assumed in the third direction.

The masses per unit length of the members in the plane of the frame are computed by summing up the structural mass, the mass of the water contained in the tube, and the mass of water displaced. The masses of the members in the direction perpendicular to the plane are assumed to be lumped at horizontal cross base level joints and are shown in Fig. 3.6. The frame has 51 D-O-F, with two translations and one rotation at each joint.

Table 3.2 gives a comparison between the frequencies of the frame obtained by the programme given by Swannell (66) and the results obtained by Ref. 54. Table 3.3 gives the eigenmode shapes for the first three frequencies of some nodal points. The first frequency which represents the clamped end solution is 2.751 Hz.

Table 3.4 presents a study of the effects of including the axial load, shear deformation and rotary inertia for the first nine frequencies.

Example II

This is another example of a-two-dimensional frame model of an offshore tower with lumped masses accounting for the third dimension. The structure is a welded tubular steel frame, similar to that analysed statically by Feibush and Keith

(67). The total height is 420 ft with the water surface at a height of 365 ft. A two-dimensional representation of the tower with a fixed-end base is shown in Fig. 3.7 and the sectional properties of the members are given in Table 3.5. The members are assumed to be rigidly connected. A constant dimension equal to the base length of the planar frame is assumed in the third direction.

The modelling is similar to that in the previous example. Three degrees of freedom are assumed, joint-translations in the x and y directions and rotation about z axis, making up a total of 72 D-O-F for the frame.

Table 3.6 gives the comparison between the frequencies of the frame obtained by the programme given by Ref. 66 and the results obtained by Haldar, Swamidas, Reddy and Arockiasamy (68).

The first frequency, which represents the clamped end solution is 3.776 Hz.

CHAPTER IV

THE MODAL SYNTHESIS TECHNIQUE

4.1 Introduction

In this chapter the modal synthesis technique is applied to determine the frequencies of an offshore tower, by breaking the structure into substructures, analyzing the substructures individually and then re-assembling the total system using selected modal information from the substructures. The connection interfaces between parts should be simple with as few degrees of freedom involved as possible.

The main advantage of the modal synthesis is that the computer capability can be extended to large systems by reducing the size of matrices through partitioning and partial modal coupling.

4.2 Procedure

Hou (69) presented the technique of the modal synthesis as follows:

(A) Subsystem Analysis

The structural system is partitioned, and the free vibration analysis of the subsystems is carried out to obtain the normal frequencies $[\omega_i^2]$ and mode shapes $[\phi_i]$ using Swannell's (66) programme. The part of $[\phi_i]$ at the interfaces is designated $[\phi_{ic}]$. All mode shapes are normalized to unit generalized mass. For clarity of explanation, suppose a system is partitioned into two parts, A and B, which have n_A and n_B modes. Let n_r be the number of degrees-of-freedom at the connection interface. For

part A, the equation of motion is:

$$\{\ddot{x}_A\} + [\omega_A^2]\{x_A\} = [\phi_{Ac}]^T \{F_A\} \qquad (4.1)$$

where

$\{x_A\}$ = vector of generalized coordinates

and

$\{F_A\}$ = internal forces acting on the connection interface between parts.

The relation between the physical coordinates and the generalized coordinates is

$$\{y_A\} = [\phi_A]\{x_A\} \qquad (4.2)$$

Let $\{y_{Ac}\}$ be the part of $\{y_A\}$ on the connection interface, and the remaining part be $\{y_{Ar}\}$. Eqn. 4.2 can be partitioned as

$$\begin{Bmatrix} y_{Ar} \\ \hline y_{Ac} \end{Bmatrix} = \begin{bmatrix} \phi_{Ar} \\ \hline \phi_{Ac} \end{bmatrix} \{x_A\} \qquad (4.3)$$

Using similar expressions for part B, gives

$$\{\ddot{x}_B\} + [\omega_B^2]\{x_B\} = [\phi_B c]^T \{F_B\} \qquad (4.4)$$

As before

$$\{y_B\} = [\phi_B]\{x_B\} \qquad (4.5)$$

and

$$\begin{Bmatrix} y_{Br} \\ \hline y_{Bc} \end{Bmatrix} = \begin{bmatrix} \phi_{Br} \\ \hline \phi_{Bc} \end{bmatrix} \{x_B\} \qquad (4.6)$$

(B) Compatibility Conditions

The required conditions for geometric compatibility at the connection interface provide n_r equations as follows

$$\{y_{Ac}\} = \{y_{Bc}\} \tag{4.7}$$

or

$$[\phi_{Ac}]\{x_A\} = [\phi_{Bc}]\{x_B\} \tag{4.8}$$

Letting $n_A > n_r$, $[\phi_{Ac}]$ can be partitioned as

$$[\phi_{Ac}] = [\phi^s_{Ac} \mid \phi^r_{Ac}] \tag{4.9}$$

where $[\phi^s_{Ac}]$ is a square matrix of order equal to the number of degrees of freedom at the connection interface and $[\phi^r_{Ac}]$ contains the remainders. Thus, Eqn. 4.8 yields

$$[\phi^s_{Ac} \mid \phi^r_{Ac}] \left\{ \begin{array}{c} x^s_A \\ \hline x^r_A \end{array} \right\} = [\phi_{Bc}]\{x_B\}, \tag{4.10}$$

and

$$\{x^s_A\} = -[\phi^s_{Ac}]^{-1}[\phi^r_{Ac}]\{x^r_A\} + [\phi^s_{Ac}]^{-1}[\phi_{Bc}]\{x_B\} \tag{4.11}$$

This gives an expression for $(n_A + n_B)$ generalized coordinates $\{x\}$ in terms of $(n_A + n_B - n_r)$ independent coordinates $\{q\}$:

$$\{x\} = [T]\{q\} \tag{4.12}$$

where

$$\{x\} = \left| \begin{array}{c} x_A \\ \hline x_B \end{array} \right| = \left\{ \begin{array}{c} x^s_A \\ x^r_A \\ x_B \end{array} \right\} \tag{4.13}$$

$$\{q\} = \begin{Bmatrix} x_A^r \\ \hline x_B \end{Bmatrix} \tag{4.14}$$

$$[T] = \begin{bmatrix} -[\phi_{Ac}^s]^{-1}[\phi_{Ac}^r] & [\phi_{Ac}^s]^{-1}[\phi_{Bc}] \\ [I] & [0] \\ [0] & [I] \end{bmatrix} \tag{4.15}$$

(C) System Equations by Modal Coupling

The uncoupled modal information of the parts can be assembled as follows:

$$\begin{Bmatrix} \ddot{x}_A \\ \hline \ddot{x}_B \end{Bmatrix} + \left[\begin{array}{c|c} \omega_A^2 & 0 \\ \hline 0 & \omega_B^2 \end{array}\right] \begin{Bmatrix} x_A \\ \hline x_B \end{Bmatrix} = \left[\begin{array}{c|c} \phi_{Ac}^T & 0 \\ \hline 0 & \phi_{Bc}^T \end{array}\right] \begin{Bmatrix} F_A \\ \hline F_B \end{Bmatrix} \tag{4.16}$$

Substituting the compatibility condition given by Eqn. 4.12, and [illegible] then restoring symmetry gives

$$\begin{aligned} [T]^T [T] \{\ddot{q}\} + [T]^T \left[\begin{array}{c|c} \omega_A^2 & 0 \\ \hline 0 & \omega_B^2 \end{array}\right] [T] \{q\} \\ = [T]^T \left[\begin{array}{c|c} \phi_{Ac}^T & 0 \\ \hline 0 & \phi_{Bc}^T \end{array}\right] \begin{Bmatrix} F_A \\ \hline F_B \end{Bmatrix} \end{aligned} \tag{4.17}$$

Since the term on the right hand side of Eqn. 4.17 is equal to zero, this gives $(n_A + n_B - n_r)$ coupled system equations as

$$[m]\{\ddot{q}\} + [k]\{q\} = \{0\} \tag{4.18}$$

where

$[m]$ = pseudo-mass matrix = $[T]^T[T]$

and

$$[k] = \text{pseudo-stiffness matrix} = [T]^T \begin{bmatrix} \omega_A^2 & 0 \\ 0 & \omega_B^2 \end{bmatrix} [T]$$

4.3 The Analysed Structure

The platform analysed is similar to the Four-Pile Extended Cantilever (FPEC) platform considered by Hancock and Peevey (70). A FPEC platfrom is currently being designed for installation in West Cameron Block 605, offshore Louisiana. The water depth at the location is 300 ft. X braces are used to stiffen the jacket and the deck section incorporates two levels each measuring 73 x 104 ft. The leg spacing will be 45 x 60ft, thus establishing a 45 ft spacing between skid beams. The members are assumed to be rigidly connected, and the added water mass is assumed equal to the mass of the water displaced. The procedure for structural modelling is the same as that described in Chapter 3.

The dimensions of the platform are given in Fig. 4.1 and the member properties in Table 4.1.

4.4 Numerical Example

This example is intended to demonstrate the simplicity of the synthesis technique. A comparison of synthesized results with these obtained from the direct solution of the total system is presented.

To compute the dynamic properties through modal synthesis, partition the [illegible] to two identical parts by a vertical section, Fig. 4.2. The reason for using a vertical section is that the computer programme given by Ref. 66, can handle only stable structures. For a horizontal cut, the upper part of the platform

is a free-free structure with the problem of 'rigid body modes' which cannot be considered in the Swannell programme.

The frequencies and the mode shapes are determined for each part. Considering 15 mode shapes for each part, the order of the matrices $[\phi_{Ac}]$ and $[\phi_{Bc}]$ is (12 x 15) because the number of degrees of freedom interconnection points between parts A and B is 12 and the number of mode shapes is 15. Consider the partitioned matrix $[\phi_{Ac}]$ below:

$$[\phi_{Ac}]_{12 \times 15} = [\phi^{s}_{Ac}{}_{12 \times 12} \;\vdots\; \phi^{r}_{Ac}]_{12 \times 3}$$

The (30 x 18) transformation matrix [T] for the partial coupling can be computed by Eqn. 4.15. The computed (18 x 18) pseudo-mass and pseudo stiffness matrices, from Eqn. 4.17, are

$$[m] = [T]^{T}_{18 \times 30} \; [T]_{(30 \times 18)}$$

and

$$[k] = [T]^{T}_{18 \times 30} \begin{bmatrix} \omega_A^2 & 0 \\ 0 & \omega_B^2 \end{bmatrix}_{30 \times 30} [T]_{30 \times 18}$$

Modal analysis for this synthesized pseudo-system is carried out as indicated in Eqn. 4.18.

Table 4.2 gives a comparison of the frequencies between the synthesis results and those obtained from direct analysis for 15 degrees of freedom.

CHAPTER V

FORCED RESPONSE ANALYSIS

5.1 Introduction

For a structure with continuously distributed properties, the exact solution can be obtained for the governing partial differential equations of motion. The formal mathematical procedure, therefore, is to treat the infinite number of coordinates as independent variables.

In chapter III, the exact solution of the partial differential equation of free vibration was considered without taking into account the effect of axial force, shear deformation and rotary inertia and viscous damping. In this chapter, the same structure analysed in Example I of Chapter III, is considered for the analysis of dynamic response to wave forces. Also, the effects of the above-mentioned factors on the exact solution are considered individually. The solution of the partial differential equation of motion which includes the effects of axial force, shear deformation and rotary inertia and the viscous damping has been presented in Refs. 18 and 19.

5.2 Effect of Static Axial Load on Lateral Vibration

Whenever a beam is subjected to (time invariant) axial force N, the dynamic shear force and bending moment acting on its ends differ from those of a beam not sustaining such a force. This axial force produces yet another effect, namely a change of the frequency of free vibration; when it is compressive, the frequency

diminishes and when it is tensile it increases.

Consider the differential element of a member vibrating under the action of axial force (N) shown in Fig. 5.1. The conditions of equilibrium of forces acting on the element give:

$$S = N\, \partial y/\partial x + \partial M/\partial x \qquad (5.1)$$

$$\partial S/\partial x = p - m\, \partial^2 y/\partial t^2 \qquad (5.2)$$

where m is the mass/length of the member. From Eqs. 5.1 and 5.2, the final equation of motion, including the effect of axial force, is:

$$\partial^2/\partial x^2 \,(EI\, \partial^2 y/\partial x^2) + N\, \partial^2 y/\partial x^2 + m\, \partial^2 y/\partial t^2 = p \qquad (5.3)$$

The effect of static force due to the weight of structure for example, comes into play in slender members in which, fortunately, one can neglect the effects of shear deformation and rotary inertia.

5.3 Effect of Shear Deflection and Rotary Inertia and Lateral Vibration

The deflection of a member results not only from the longitudinal extension of fibres due to the normal stresses of bending, but also from transverse shear displacements of cross-sections due to shear stresses. Another factor which has an effect on the results of dynamic analysis is the rotary inertia. This effect is due to the rotation of the length elements of a member in vibration. The mass of the member is not concentrated on its gravity axis but is distributed across the member depth so that a vertical motion of the centre of gravity of the cross-section in the vertical direction

causes the cross-section to execute a rotary motion about its horizontal axis.

Consider the equilibrium of the differential element shown in Fig. 5.2. It is easy to see that during vibration a typical element of a beam performs not only a translatory motion but also rotates about an axis through its centre and perpendicular to the x-y plane. The angle of rotation, which is equal to the slope of deflection curve, is expressed by $\partial y/\partial x$; and the corresponding angular velocity and angular acceleration are given by

$$\partial^2 y/\partial x \partial t \quad \text{and} \quad \partial^3 y/\partial x \partial t^2$$

Therefore, the inertial moment of the element per unit length ($\bar{m}_I$) about an axis through its centre of the mass and perpendicular to the x-y plane will be

$$\bar{m}_I = \rho I \, \partial^3 y/\partial x \partial t^2$$

where ρ is the mass per unit volume ($\rho = m/A$), and I is the moment of inertia about this axis, which is perpendicular to the cross-section at the centre; thus

$$\bar{m}_I = m \, I/A \, \partial^3 y/\partial x \partial t^2 = m r^2 \, \partial^3 y/\partial x \partial t^2 \qquad (5.4)$$

in which $r^2 = I/A$ is the radius of gyration of the cross section.

The moment-equilibrium relationship of the forces acting on the differential element shown in Fig. 5.2a, gives

$$\partial M/\partial x = S + m r^2 \, \partial^3 y/\partial x \partial t^2 \qquad (5.5)$$

The force equilibrium in the y-direction gives

$$\partial S/\partial x = p - m\, \partial^2 y/\partial t^2 \qquad (5.6)$$

Substituting the shearing force S from Eqn. 5.5 into Eqn. 5.6, leads to

$$\partial/\partial x\, (\partial M/\partial x - mr^2\, \partial^3 y/\partial x \partial t^2) = P - m\, \partial^2 y/\partial t^2 \qquad (5.7)$$

From elementary flexural theory, the moment-curvature relationship is

$$M = EI\, \partial^2 y/\partial x^2 \qquad (5.8)$$

Using this above expression in Eqn. 5.7, gives

$$EI\, \partial^4 y/\partial x^4 = P - m\, \partial^2 y/\partial t^2 + mr^2\, \partial^4 y/\partial x^2 \partial t^2 \qquad (5.9)$$

This is the differential equation for the transverse vibration of prismatic beams, in which the third term on the right side represents the effect of rotary inertia.

A still more accurate differential equation is obtained if in addition to the rotary inertia, the deflection due to shear is also taken into account. The slope of the deflection curve depends not only on the rotation of cross sections of the member but also on the shear deformation. Let $\partial y/\partial x$ denote the slope of the deflection curve when the shearing force is neglected, and β the angle of shear at the neutral axis in the same cross section. The total slope of the element is

$$\alpha = \partial y/\partial x + \beta \qquad (5.10)$$

From elementary flexure theory, the bending moment and shear force are given by the following equations

$$S = KAG\beta = KAG\,(\alpha - \partial y/\partial x), \tag{5.11}$$

and

$$M = EI\,\partial\alpha/\partial x. \tag{5.12}$$

in which k is a numerical factor depending on the shape of the cross section, A is the cross-sectional area, and G is the modulus of rigidity. Differentiating Eqn. 5.11 and substituting into the ventical-equilibrium relationship Eqn. 5.6 leads to

$$KAG\,(\partial\alpha/\partial x - \partial^2 y/\partial x^2) = P - m\,\partial^2 y/\partial t^2 \tag{5.13}$$

Differentiating Eqn. 5.12 and substituting it together with the shear-distortion expression into Eqn. 5.5 gives

$$EI\,\partial^2\alpha/\partial x = KAG\,(\alpha - \partial y/\partial x) + mr^2\,\partial^2\alpha/\partial t^2 \tag{5.14}$$

Finally, the rotation α can be evaluated from Eqn. 5.13 and substituted into Eqn. 5.14, leaving the transverse displacement y as the only dependent variable. In order to simplify the resulting expression, it will now be assumed that the physical properties of the beam do not vary along its length. In this case, solving Eqn. 5.13 for $\partial\alpha/\partial x$ leads to

$$\partial\alpha/\partial x = \partial^2 y/\partial x^2 + 1/KAG\,(P - m\,\partial^2 y/\partial t^2) \tag{5.15}$$

Differentiating Eqn. 5.14 with respect to x, and substituting expressions for the appropriate derivatives of $\partial\alpha/\partial x$ from Eqn.

5.15 leads finally to

$$EI\,\partial^4 y/\partial x^4 - (P - m\,\partial^2 y/\partial t^2) - m r^2\,\partial^4 y/\partial x^2 \partial t^2 + EI/KAG\,(P - m\,\partial^2 y/\partial t^2) - m r^2/KAG\,\partial/\partial t^2 \quad (5.16)$$
$$(P - m\,\partial^2 y/\partial t^2)$$

where

$EI\,\partial^4 y/\partial x^4 - (P - m\,\partial^2 y/\partial t^2)$ = Elementary Case,

$-mr^2\,\partial^4 y/\partial x^2 \partial t^2$ = Rotary inertia,

$EI/KAG\,\partial^2/\partial x^2\,(P - m\,\partial^2 y/\partial t^2)$ = shear distortion,

and

$-mr^2/KAG\,\partial^2/\partial t^2\,(P - m\,\partial^2 y/\partial t^2)$ = combined shear distortion and rotary inertia

5.4 Effect of Viscous Damping on Lateral Vibration

In the foregoing formulations of the equations of motion of beam-type members, no consideration was given to mechanisms which absorb energy from the structure during its dynamic response. Two types of viscous (velocity - dependent) damping can be incorporated, into the formulation without difficulty. These types, shown in Fig. 5.3, include a viscous resistance to absolute velocity, and viscous resistance to strain velocity. If the viscous resistance to absolute velocity is represented by $c(x)$, the corresponding damping forces is $f_D(x) = c(x)\,\partial y/\partial t$. From the equilibrium of the forces in the vertical direction

$$\partial S/\partial x = P - m\,\partial^2 y/\partial t^2 - c(x)\,\partial y/\partial t \quad (5.17)$$

Similarly, if the resistance to strain velocity is represented by c_s, the damping stress is $\sigma_D = c_s \partial\varepsilon/\partial t$ where ε is the local normal strain. Assuming that the strains vary linearly over the section (Navier's hypothesis), it is easy to show that a damping moment is given by

$$M_D(x) = \int \sigma_D y dA = c_s I(x) \partial^3 y/\partial x^2 \partial t \qquad (5.18)$$

Incorporating this damping moment into the moment equilibrium relationship Eqn. 5.18, and substituting into Eqn. 5.17, leads to the differential equation of motion including damping:

$$\partial/\partial x^2 (EI \partial^2 y/\partial x^2 + c_s I \partial^3 y/\partial t \partial x^2) + m \partial^2 y/\partial t^2 + c(x) \partial y/\partial t = P \qquad (5.19)$$

5.5 Wave Force Calculations

For any type of structure, the wave force can be calculated using the Morison equation (30) given by:

$$F = 1/2 \rho c_D A U|U| + \rho V c_M dU/dt \qquad (5.20)$$

In this equation, it is assumed that the fluid forces on a fixed body in an steady flow are given by the linear superposition of a drag force with drag coefficient, c_D, dependent on the square of the velocity, U^2, and acting on the projected frontal area A, and an inertia force with inertia coefficient, c_M, dependent on the acceleration du/dt, and the volumetric displacement, V.

In this chapter, it is assumed that the wave forces are horizontal and the members on which they act are circular cylinders. For this case, Eqn. 5.20 takes the original form

suggested by Ref. 30.

$$\bar{F} = 1/2\ \rho c_D D\ u|u| + \rho\pi\ D^2/4\ c_M\ \partial u/\partial t \qquad (5.21)$$

where $\bar{F}$ is the force per unit length on a cylinder of diameter D, and u is the horizontal component of the water velocity. The values of the drag force coefficient, c_D, and the inertia force coefficient, c_M, are calculated using the data from the Gulf of Mexico given by Ref. 34. The wave shown in Fig. 5.4 has a height, H, of 60 ft and the time of duration, T, of 12 sec..

The wave forces acting on the frame members are treated as concentrated loads at the horizontal cross base level joints on one side of the idealized planar frame in Fig. 5.5.

5.6 Sequence of Operations

The sequence of operations required for response evaluation is listed below:

(1) Input properties of the idealized finite-elemented structure.

a) Size of frame is described by the number of members (NM), number of joints (NJ), number of bases (NB), number of additionally constrained joints (NACJ), and the number of different member sections used to make up the assembly (NSEC).

b) Joint Co-ordinates

c) Section Properties such as the second moment of area I, cross sectional area, A, first moment of section above or below the neutral axis, Q, which is the parameter of the effect of shear distortion, width of the section at the neutral axis, B, mass per unit length, M, Young's Modulus of Elasticity, E, and

the Modulus of Rigidity, G.

d) Member Data for each member four data items are required, describing member connectivity and pins, section type, and static axial load (N).

e) Lumped Masses are described by giving the joints number at which they are located, the magnitudes of the masses and the mass moments of inertia.

f) Base Numbers indicate the fixed position joints of the frame.

g) Additionally Constrained Joints

(2) Form the dynamic tangent stiffness matrix

(3) Set up the equation of motion

(4) Solve to evaluate nodal point displacements.

5.7 Numerical Example

This example demonstrates how to obtain the forced response displacements from the exact solution of the partial differential equations of motion of structure having infinite continuously distributed properties. The frame considered is the same as that analysed in Chapter III Example I. The equations of motion of this structure are

$$[k_t(\omega)]\ \{x\} = \{F(t)\} \qquad (5.22)$$

where $k_t(\omega)$ is the dynamic tangent stiffness matrix (given in Appendix II) which takes into account the effects of axial force, shear deformation and rotary inertia and the viscous damping, $\{x\}$ is the vector of the finite set of amplitutes of modal point displacements, and $[F(t)]$ is the vector of the dynamic wave forces.

The solution involves first obtaining the eigenvalues and eigenvectors given by

$$[k_t(\omega)] = 0 \qquad (5.23)$$

Eqn. 5.22 is then normalized using the weighted modal matrix $[\phi]$ for the first three eigenmodes. The relation between the modal coordinates, $[y]$, and the geometric coordinates $[x]$ is

$$\{x\} = [\phi]\ \{y\} \qquad (5.24)$$

The dynamic equations are solved for the first three mode shapes by the superposition method to obtain the modal displacements. The nodal displacements of the structure are then obtained using Eqn. 5.24.

To obtain the effect of damping on the results of the dynamic response, two values of the damping parameter, c_o, 0.15 and 0.7 are used in this analysis. The individual effects of the axial load, the shear deformation and rotary inertia on the response displacements are also considered. The effects of all these above-mentioned factors are compared by plotting them on the time-history graph (Fig. 5.6 to 5.14). The maximum horizontal and vertical displacements for nodes 15 and 19, obtained from the time-history graph, are given in Table 5.1. The maximum axial force, shear force, and bending moment for member 1 at node 1, obtained from the time history, are given in Table 5.2. The maximum values of the horizontal displacements at nodes 14 and 19 for different values of damping are given in Table 5.3.

CHAPTER VI

THE NON-PROPORTIONAL DAMPING MATRIX

6.1 Introduction

For any structure, if there is no reasonable degree of homogeneity in the energy loss mechanisms of the different parts of the structure, the differences in the absorption rates for each part will make the distribution of damping forces quite different from the distributions of elastic and inertial forces during free vibrations. A damping mechanism of this type, called 'Non-proportional Damping' induces coupling between the modal coordinates.

This chapter considers the determination of the dynamic response of offshore platforms to random ice forces using the non-proportional damping matrix. The equations of motion are coupled and the dynamic response is computed for the model by integrating these simultaneous equations. The results, obtained from the solution of the coupled equations, are compared with the results of decoupled equations of the same model in which the diagonalization was considered for damping matrix.

6.2 Basic Assumption and Procedure

For a system of n degrees of freedom, the equations of motion in matrix form are:

$$[M]\{\ddot{X}\} + [C]\{\dot{X}\} + [K]\{X\} = \{f(t)\} \qquad (6.1)$$

The eigenvalues and eigenvectors of the system are easily computed

from the undamped equation,

$$|K_t(\omega)| = 0 \tag{6.2}$$

using a computer programme given by Ref. 66.

Eqn. 6.1 is normalized using the weighted modal matrix $[\phi]$. The relation between the modal coordinates $\{Y\}$ and the structure coordinates $\{X\}$ is

$$\{X\} = [\phi]\{Y\} \tag{6.3}$$

Premultiplying by $[\phi]^T$, gives

$$[\phi]^T[M][\phi]\{Y\} + [\phi]^T[C][\phi]\{Y\} + [\phi]^T[K][\phi]\{Y\} = \phi^T\{f(t)\} \tag{6.4}$$

The matrices $[\phi]^T[M][\phi] = [I]^D$ and $[\phi]^T[K][\phi] = [\omega^2]^D$ are diagonal; in general $[\phi]^T[C][\phi] = [\bar{C}]$ will not be a diagonal matrix. Assuming $[\bar{C}]$ to be non-diagonal, Eqn. 6.4 can be rewritten as

$$[I]^D\{\ddot{\bar{Y}}\} + [\bar{C}]\{\dot{\bar{Y}}\} + [\omega^2]^D\{\bar{Y}\} = \{F(t)\} \tag{6.5}$$

simultaneous integration is used to get the solution for Eqn. 6.5 (Appendix II) which is a coupled equation. The full damping matrix $[\bar{C}]$ of Eqn. 6.5 is then replaced by a diagonal matrix $[\bar{C}]^D$, and the set of uncoupled equations is written as

$$[I]^D\{\ddot{Y}\} + [\bar{C}]^D\{\dot{Y}\} + [\omega^2]^D\{Y\} = \{F(t)\} \tag{6.6}$$

The solution of Eqn. 6.5 is designated $\{\bar{Y}\}$, and that of Eqn. 6.6 by $\{Y\}$.

6.3 Evaluation of Non-proportional Damping Matrix

Non-proportional damping can be expressed in terms of an explicit C; thus a means of defining the non-proportional damping matrix must be developed regardless of which analysis procedure is used. Rayleigh damping is given by a linear combination of the mass and stiffness matrices as

$$[C] = a_o[M] + a_1[K] \tag{6.7}$$

As this matrix satisfies the orthogonality condition, the resulting damping can be specified by modal damping ratios. The relationship between the proportionality constants, a_o and a_1, and the damping ratio of the nth mode is

$$\zeta_n = a_o/2\omega_n + a_1\omega_n/2 \tag{6.8}$$

where ω_n is the modal frequency. Thus, these constants can be determined by specifying damping ratios for two modes in terms of corresponding model frequencies, and then solving the two simultaneous equations of Eqn. 6.8. Generally, the two frequencies in this evaluation should be the lowest; the other important modes will then have reasonable values. If the damping values are different for the various parts of the structure, the constants, a_o and a_1, must be determined for each part, using appropriate damping ratios, and solving simultaneously the resulting pair obtained from Eqn. 6.8. The frequencies to be used in these equations are the undamped frequencies of the entire structure.

When the constants a_0 and a_1 have been defined for each different part of the structure, the damping matrix for each part is determined from the mass and stiffness matrices of that part by an equation equivalent to Eqn. 6.7. Then the damping matrix for the complete structure is obtained by assembling matrices for the parts.

6.4 Consistent Mass Matrix

For the non-uniform straight beam segment shown in Fig. 6.1, in which the two nodal points for assembly are located at the ends, there are three degrees of freedom at each node, for axial and transverse plane displacements.

The arbitary deflected shapes due to unit displacements of each type at the left end of the element, satisfying the nodal compatibility and continuity requirements. These are cubic Hermitian polynomials which may be expressed as

$$\begin{aligned}
\psi_1(x) &= 1 - (x/\ell) \\
\psi_2(x) &= 1 - 3(x/\ell)^2 + 2(x/\ell)^3 \\
\psi_3(x) &= x(x/\ell - 1)^2 \\
\psi_4(x) &= x/\ell \\
\psi_5(x) &= 3(x/\ell)^2 - 2(x/\ell)^3 \\
\psi_6(x) &= x^2/\ell\ (x/\ell - 1)
\end{aligned} \tag{6.9}$$

The deflected shape of the element in terms of its nodal displacements is

$$v(x) = \psi_1(x)\, v_1 + \psi_2(x)\, v_2 + \psi_3(x)\, v_3 + \psi_4(x)\, v_4 + \psi_5(x)\, v_5 + \psi_6(x)\, v_6 \tag{6.10}$$

where the numbered degrees of freedom are related to those shown in Fig. 6.1 as follows

$$\begin{Bmatrix} v_1 \\ v_2 \\ v_3 \\ v_4 \\ v_5 \\ v_6 \end{Bmatrix} = \begin{Bmatrix} u_a \\ y_a \\ \theta_a \\ u_b \\ y_b \\ \theta_b \end{Bmatrix} \tag{6.11}$$

For a unit angular acceleration of the left end, $\ddot{v}_3 = \ddot{\theta}_a = 1$, accelerations developed along its length can be written as

$$\ddot{v}(x) = \psi_3(x)\, \ddot{v}_3 \tag{6.12}$$

which can be obtained from Eqn. 6.10. From d'Alembert's principle, the inertia force is given by

$$f_I(x) = m(x)\, \ddot{v}(x) = m(x)\, \psi_3(x)\, \ddot{v}_3 \tag{6.13}$$

The associated mass influence coefficients are defined by the nodal inertia forces which can be determined from the distributed inertia force of Eqn. 6.13 using the principle of virtual displacements as follows:

$$P_a\, \delta v_a = \int_0^{\ell} f_I(x)\, \delta v(x)\, dx \tag{6.14}$$

where δv_a = vertical virtual displacement,

P_a = external nodal force,

$f_I(x)$ = distributed inertial forces

The internal virtual displacements, $\delta v(x)$, are expressed in terms of the interpolation function, and substituted into Eqn. 6.13 to give

$$m_{13} = \int_o^{\ell} m(x)\ \psi_1(x)\ \psi_3(x)\ dx \qquad (6.15)$$

The mass influence coefficient, m_{ij}, of an arbitrary beam segment can therefore be written as

$$m_{ij} = \int_o^{\ell} m(x)\ \psi_i(x)\ \psi_j(x)\ dx \qquad (6.16)$$

Which constitute the elements of the consistent-mass matrix.

For a beam with uniformly distributed mass, the consistant matrix is

$$\begin{Bmatrix} f_{I1} \\ f_{I2} \\ f_{I3} \\ f_{I4} \\ f_{I5} \\ f_{I6} \end{Bmatrix} = m\ell/420 \begin{bmatrix} 140 & 147 & 21\ell & 70 & 63 & -14\ell \\ & 156 & 22\ell & 63 & 54 & -13\ell \\ & & 4\ell^2 & 14\ell & 13\ell & -3\ell^2 \\ & & & 140 & 147 & -21\ell \\ & & & & 156 & -22\ell \\ & & & & & 4\ell^2 \end{bmatrix} \begin{Bmatrix} \ddot{v}_1 \\ \ddot{v}_2 \\ \ddot{v}_3 \\ \ddot{v}_4 \\ \ddot{v}_5 \\ \ddot{v}_6 \end{Bmatrix}$$

where m = the mass/unit length of the member. and f_{I1} = inertia force in direction 1 and so on.

6.5 Ice-Force Loading

Swamidas and Reddy (59) generated artificial ice-force time histories modifying the available field records given by Blenkarn (52). The method, based on the similarity between the fluctuating parts of randomly varying ice-force records and seismic records, uses a nonstationary random process obtained from filtering a shot noise through a second order filter. The structural response can be studied using any appropriate time-history of ice-force loading obtained from either actual or computed records. In this investigation, the generation of artificial ice-force records is used to overcome the deficiencies due to the scantiness of available field records, and to obtain more realistic estimates of the loading function.

Both ice and earthquake loadings will induce significant cyclic stresses and stains in the soil. There are some important differences in the nature of loading, such as the time scale and the number of cycles. The duration of a strong earthquake is

measured in seconds with the periods ranging from 0.1 to 2 sec, while the duration of ice loading may extend to hours, or even days, with periods ranging from 0.5 to 2 sec. Hence, the number of significant loading cases may be larger for ice than for earthquakes in most cases, which may have an important effect for a site where both ice and earthquake loadings occur. Some of the methods, which were originally developed for soil responses for earthquake loading by Seed and Idriss (71), are applied to study the responses to ice loading.

The formula developed by Afanas'ev (46) is used for estimating the mean of the ice-force records. The maximum ice force developed when an ice-cover is cut through by the vertical column of the tower is given by

$$P = mKBh\sigma_o \tag{6.17}$$

where m = shape coefficient equal to 0.90 for a semi circular one

$$K = [5\ h/B + 1]^{1/2} \text{ for } \leq B/h \leq 6 \tag{6.18}$$

[for B/h > 6 the values are obtained from the graph in Ref. 46]

B = width of the resisting structure,

h = thickness of the ice-sheet,

and

σ_o = uniaxial compressive strength of ice

The typical total (mean and fluctuating) force record for the framed tower is shown in Fig. 6.2. The mean part of the force on the framed tower is assumed to be produced by the impact of a moving ice floe of constant thickness of 1.5 ft and the random

part is generated artifically as described in Ref. 59.

6.6 Numerical Example

The structure analyzed in Chapters III and IV is also used to demonstrate the evaluation of the non-proportional damping matrix for an offshore tower (Fig. 6.3).

The first stage in the solution involves the formulation of a discretized physical model, the evaluation of its mass and stiffness matrices and the effective ice force vector in the discretized coordinates. The total mass matrix [M] for the structure is

$$[M]_T = [M]_L + [M]_D \qquad (6.19)$$

where $[M]_L$ is the lumped mass matrix of the planar frame, and $[M]_D$ is the consistent mass matrix for the distributed mass of the members. The eigenvalues and eigenvectors of the system are determined from the undamped free vibration case.

To evaluate the non-proportional damping matrix for the first three modes, different values of damping ratios are assumed for each group of members with identical properties. Constant damping ratios to account for the members perpendicular to the planar frame are assumed at the lumped mass locations. The values of the damping ratios for the lumped masses and for each of the groups are given in Table 6.1.

The constants, a_o and a_1, are determined for each of the damping ratios, and the damping matrices for member groups are obtained by substitution in Eqn. 6.7. The distributed damping

matrix $[C]_D$ is then obtained by assembling the damping matrices of the individual members. In order to obtain the total non-proportional matrix for the structure, $[C]_T$, the damping matrices, [C], for each lumped mass are first calculated as

$$[C] = [2\ \zeta\ \omega] \tag{6.20}$$

where ζ = the damping ratio of the lumped mass which was assumed constant for all the modes, and ω = the lowest natural frequency of the structure. $[C]_T$ is obtained as

$$[C]_T = [C]_D + [C]_L \tag{6.21}$$

where $[C]_L$ is the diagonal damping matrix for all the lumped masses.

The equations of motion in matrix form for the frame structure with 51 D-O-F are

$$[M]_T \{\ddot{X}\} + [C]_T \{\dot{X}\} + [K] \{X\} = \{f(t)\} \tag{6.22}$$

where the order of the mass, damping and stiffness matrices is (51 x 51).

The weighted modal matrix $[\phi]$ is formed using the first three modes of the eigenvector; this matrix is then used to normalize Eqn. 6.22. The results of this normalization gives the equation of motion for the model structure Eqn. 6.5.

For the damping ratios given in Table 6.1, the normalized non-proportional damping matrix of the model is determined as

$$[\bar{C}] = \begin{bmatrix} 1.0564 & .0322 & -.007 \\ .0322 & 1.4734 & .1562 \\ -.007 & .1562 & 2.402 \end{bmatrix}$$

This is used in Eqn. 6.5 to obtain the modal response (coupled) $\{\bar{Y}\}$ by simultaneous integration. The full damping matrix is then diagonalized by ignoring its off-diagonal terms, i. e.

$$[\bar{C}]^D = \begin{bmatrix} 1.0564 & & \\ & 1.4734 & \\ & & 2.402 \end{bmatrix}$$

The matrix $[\bar{C}]$ in Eqn. 6.5 is then replaced by matrix $[\bar{C}]^D$ to set up the decoupled Eqs. 6.6. The solution of these equations gives the modal response vector $\{Y\}$.

In order to obtain the displacement responses for the structure, the modal coordinates $\{\bar{Y}\}$ and $\{Y\}$ are multiplied by the weighted modal matrix $[\phi]$. The displacements obtained are designated $\{\bar{X}\}$, and $[X]$ respectively. These results are then compared by plotting them on the time history graph (Figs. 6.4 and 6.5).

The above procedure is again applied using different damping ratio values for the members, while keeping the damping ratios for the lumped masses locations constant. The damping ratios used are 0.4 and 0.05, and the values given in Table 6.2 and 6.3 respectively. Time-histories are also obtained for the different values of the damping ratios for the member (Figs. 6.6 to 6.9). Table 6.4 gives the maximum horizontal displacements for nodes 14 and 19, obtained from the time-history graph for different values of damping.

CHAPTER VII

DISCUSSION AND CONCLUSIONS

7.1 Introduction

The results for free and forced vibration of plane frame models with distributed mass have been presented taking into account the effects of axial static load, shear deformation and rotary inertia, mass moment of inertia, and viscous damping. The comparison between the frequencies obtained by Direct Solution and the Modal Synthesis Technique is also presented. The study includes the effect of neglecting the off-diagonal terms from the non-proportional damping matrix on the maximum horizontal response displacement.

7.2.1 Frequencies

While the first two frequencies obtained from the exact solution by considering the differential equation of the lateral vibration of plane frame model with infinite properties are very close to those obtained by approximate solutions, the agreement is not good for higher frequencies. The approximate frequencies are about one and half times the exact values. This is seen from the results in Tables 3.2 and 3.6. The frequencies of the frame do not change by inclusion of the effects of the mass moment of inertia and viscous damping. However, the frequencies decrease by 2.0% when the effects of shear deformation and rotary inertia are included. Inclusion of the axial static loading

changes the frequencies by 30% to 50%. This can be easily seen from the results in Table 3.4. From Table 4.2, it is observed that the frequencies obtained from the modal synthesis technique are close to those obtained by direct solution.

7.2.2 Displacements

The axial static load has a major influence on structural response to forces, owing to the large decrease in the fundamental as well as the higher frequencies. From Table 5.1, it is observed that the maximum horizontal and vertical displacements at deck level are twice those when the axial load is excluded; including the effect of shear deformation and rotary inertia increases these displacements by 10% and 20% respectively. It is also seen from the dynamic response to ice force loading that the maximum horizontal displacement at the deck level, obtained from the solution of the coupled equations of motion, is very close to that obtained from the decoupled equations considering the diagonalization of the non-proportional damping matrix.

7.2.3 Forces

From Table 5.2, it is observed that the effect of shear deformation and rotary inertia increases the axial force by 6%, the shear force by 10%, and the bending moment by 25%.

The effect of self weight (axial direction) produces significant changes in the response of the structure; the axial force is increased by 10%, the shear force by 250% and the

bending moment by 200%.

7.3 Conclusions

The following conclusions are drawn from this study:

(1) The first two fundamental frequencies of the frame obtained by the exact solution of lateral vibration of the frame model with infinite properties are very close to the frequencies obtained from approximate solutions.

(2) The frequencies of the higher modes are influenced significantly when the exact solution of the differential equation of lateral vibration is considered.

(3) The modal synthesis technique extends the computer capability to large systems by reducing the size of matrices through partitioning and partial modal coupling. This technique is also useful if a design change in one part of the structure necessitates the modification of the modal data of the changed part. The changed modal data can then be coupled to the remaining unchanged parts.

(4) The effect of static axial loading on free and forced vibration analyses is most pronounced for slender members of the frame models in which fortunately, the effects of shear deformation and rotary inertia can be neglected.

(5) For non-orthogonal or non-classical damping cases, the response can be determined by the classical normal mode method if the non-diagonal terms in the non-proportional damping matrix are equated to zero. However, this simple diagonalization procedure may lead to errors. A study of these errors, indicates

that the approximate diagonalization procedure will not cause serious errors in major response quantities.

7.4 Contributions

1. Exact solution for free lateral vibration of a three-dimensional fixed-offshore tower modelled as a plane frame with infinite degrees of freedom.

2. Exact solution for the forced response of an offshore tower subjected to wave forces.

3. Investigation of the influence of various effects such as axial static loading, shear deformation and rotary inertia on free vibration behaviour, and also the dynamic response of an offshore tower subjected to wave loading.

4. Application of the Modal Synthesis Technique to offshore towers.

5. Study of the effect of neglecting the off-diagonal terms in the non-proportional damping matrix on the dynamic response displacement of an offshore tower subjected to ice loading.

7.5 Recommendations for Further Research

(1) Determination of exact solutions for free and forced vibration to other kinds of offshore structures, eg. gravity platforms and pipelines.

(2) Application of the exact solution of free and forced vibration to other kinds of environmental loading, eg. random ice forces.

(3) Development of exact solutions for free and forced vib-

ration of the soil-structure interaction by considering the model of the soil as a spring system.

(4) Study the influence of shear deformation, rotary inertia and axial static load in the structural members on the stresses in the soil and also on the displacements at the foundations.

(5) Application of the modal synthesis technique to the problem of soil-structure interaction.

(6) Study of the effect of neglecting off-diagonal terms from the non-proportional damping matrix of a soil-structure model, with the soil damping ratio different from that for the structure.

(7) Frequency domain analysis for earthquake response of offshore structures considering soil-structure interaction.

TABLES AND FIGURES

Table 3.1 Properties of Member Groups for Offshore Tower shown in Fig. 3.6.

Member	Cross Sectional Area (ft^2)	Moment of Inertia (ft^4)	Mass/Length (slug/ft)
A	.224	.0818	12.65
B	1.658	2.0726	56.40
C	.501	1.0853	7.64
D	1.297	.9814	47.47
E	.202	.0602	10.52
F	.807	.9595	12.30
G	.180	.0424	8.63

Table 3.2 Frequencies of the Offshore Tower shown in Fig. 3.6
(Unit: Hz)

Mode	Algorithm	Ref. 54
1	0.993	1.0279
2	1.810	1.8133
3	2.17	3.5128

Table 3.3 Mode Shapes for Offshore Tower shown in Fig. 3.6.

Joint No.	Deformation	Mode 1	Mode 2	Mode 3
3	x	-.7389	.3382	-.118
	y	.014	.0000017	.0602
	Rot.	.0155	.000438	-4.814
5	x	-1.86	.600	.551
	y	.565	-.00624	.059
	Rot.	.0247	-.0112	-.0410
6	x	-3.10	.837	.780
	y	.0516	0.00004	.163
	Rot.	.0192	.00177	-.141
8	x	-4.50	.987	.1116
	y	.894	.0153	-.0673
	Rot.	.0516	.00338	.0305
9	x	-5.86	1.08	1.61
	y	.0799	0.00002	.0018
	Rot.	.0474	.00297	.0298

Table 3.3 - Continued

Joint No.	Deformation	Mode 1	Mode 2	Mode 3
11	x	-7.12	1.11	1.90
	y	.949	.0397	.0199
	Rot.	+.0586	-.0083	-.0356
12	x	-8.65	1.06	1.99
	y	.106	.00003	.106
	Rot.	+0.196	-.0046	-.0195
14	x	-9.88	1.00	2.00
	y	.808	.0395	.0604
	Rot.	.318	.037	.0686
16	X	-26.3	-.838	-1.21
	y	.977	.05309	.0874
	Rot.	.544	.0145	.0214
19	x	-27.6	-.944	1.31
	y	1.000	.05309	.0871
	Rot.	.739	.00165	-.0014

Table 3.4 Frequencies for Offshore Tower shown in Fig. 3.6
(Unit: Hz)

Frequency No.	Excluding Shear Deformation, Rotary Inertia & Axial Load	Including Shear Deformation & Rotary Inertia	Including Axial Load (Compression)
1	.9947	.97917	.7149
2	1.810	1.8084	.9636
3	2.1759	2.1559	1.0258
4	2.2536	2.2381	1.2278
5	2.7510	2.7355	1.5231
6	2.8443	2.8287	1.6319
7	3.1395	3.1240	1.6786
8	3.5281	3.5126	1.7251
9	3.5903	3.5592	1.7407

Table 3.5 Section Properties for Different Groups of Members for Tower shown in Fig. 3.7.

Member	Cross-Sectional Area (ft^2)	Moment of Inertia (ft^4)	Mass/Length (slug/ft)
A	10.8	255	740
B	9.09	216.3	718.0
C	0.918	1.40	54.5
D	0.734	0.783	37.0

Table 3.6 Frequencies for Offshore Tower shown in Fig. 3.7. (Unit: Hz)

Mode	Algorithm	Ref. 68
1	0.500	0.501
2	1.963	2.14
3	3.201	4.63

Table 4.1 Section Properties of the Two Member Groups for the Tower shown in Fig. 4.1

Member	Cross-Sectional Area (ft^2)	Moment of Inertia (ft^4)	Mass/Length (slug/ft)
A	1.658	2.0726	56.4
B	0.224	0.0818	12.65

Table 4.2 Frequencies for Tower shown in Fig. 4.1
(Unit: Hz)

Mode	Modal Synthesis	Direct Solution by the Programme of Ref. 66
1	0.84	0.74
2	1.13	1.01
3	1.50	1.37
4	2.50	2.47

Table 5.1 Maximum Values for Horizontal and Vertical Displacements in Joints 15 and 19

Factor	Displ. at Joint 15 (ft)		Displ. at Joint 19 (ft)		Time (sec)
	Vertical	Horizontal	Vertical	Horizontal	
Excluding P & Q	$-.132 \times 10^{-2}$	-.041	$+.14 \times 10^{-2}$	-.043	3.0
Including Q	$-.16 \times 10^{-2}$	-.045	$+.17 \times 10^{-2}$	-.048	3.0
Including P	$+.22 \times 10^{-2}$	-.087	$+.32 \times 10^{-2}$	-.0915	3.0

Q = shear distortion effect

P = axial static load effect

Table 5.2 Maximum Values for Axial Load, Shear Force and Bending Moment for Member 1 at Node 1

Factor	Axial Force (kips)	Shear Force (lbs)	Bending Moment (kips ft)	Time (sec)
Excluding P & Q	-199.0	-216.0	-24.1	3.0
Including Q	-212.0	-236.0	-30.1	3.0
Including P	-222.0	-710.0	-73.3	3.0

Q = shear distortion effect

P = axial static load effect

Table 5.3 Maximum Values for Horizontal Displacements at Joints 14 and 19

Damping Coefficient, c_o	Displacements (ft)	
	Joint 14	Joint 19
0.0	.0386	.0455
0.15	.0383	.045
0.70	.0379	.043

Table 6.1 Damping Ratios (ζ) for the Members and Lumped Mass Locations

Members	
A, E, G	.04
B	.10
F, C	.06
D	.08
Lumped Masses	.07

Table 6.2 Damping Ratios (ζ) for the Members and Lumped Mass Locations

Members	
A, E, G	.016
B	.04
F, C	.024
D	.032
Lumped Masses	.07

Table 6.3 Damping Ratios (ζ) for the Members and Lumped Mass Locations

Members	
A, E, G	.002
B	.005
F, C	.003
D	.004
Lumped Masses	.07

Table 6.4 Maximum Values for Horizontal Displacements for Different Damping Values

Damping Values	Time (sec)	Joint 14 (in)		Joint 19 (in)	
		Coupled	Decoupled	Coupled	Decoupled
Table 6.1	.5	1.65	1.61	3.510	3.47
Table 6.2	.5	1.8	1.77	3.86	3.78
Table 6.3	.5	2.25	2.20	4.08	4.01

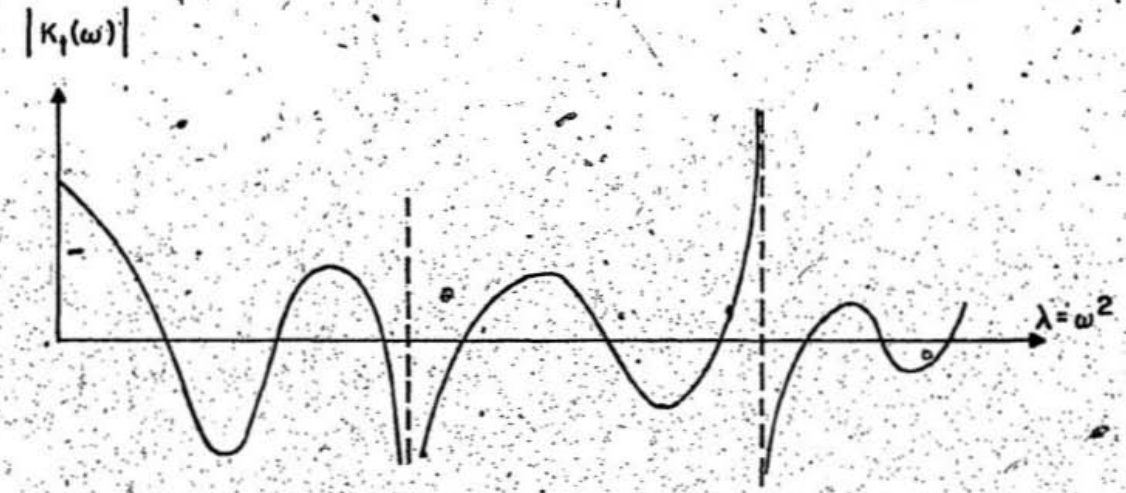

Fig. 3.1 Relationship Between Dynamic Stiffness and Eigenvalues In the Nonlinear Formulation

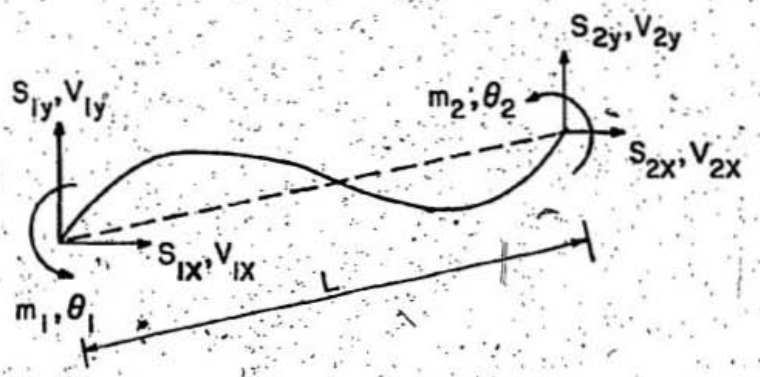

Fig. 3.2 Member End Displacements and Forces

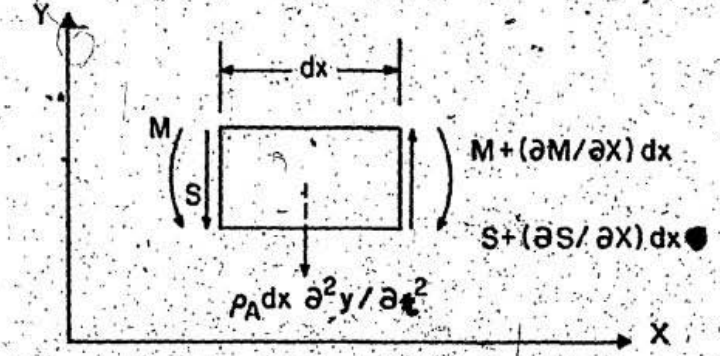

Fig. 3.3 Transverse Forces on a Prismatic Element

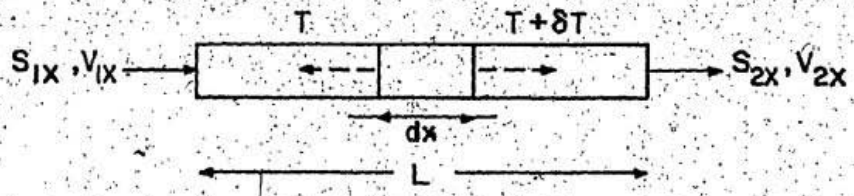

Fig. 3.4 Axial End Forces and Displacements

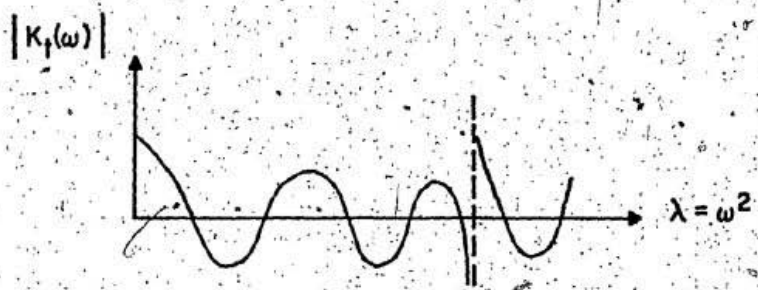

Fig. 3.5 a

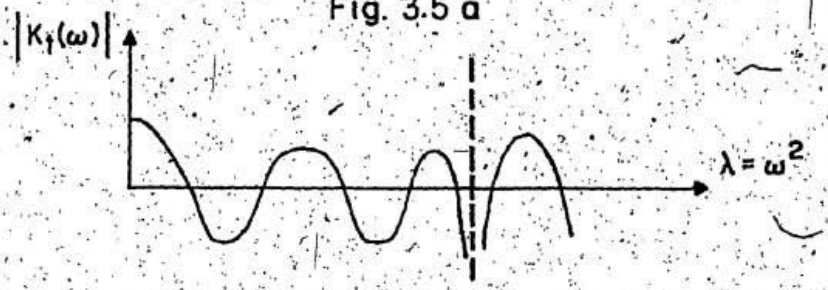

Fig. 3.5 b

Definition Sketch for the Wittrick and Williams Algorithm

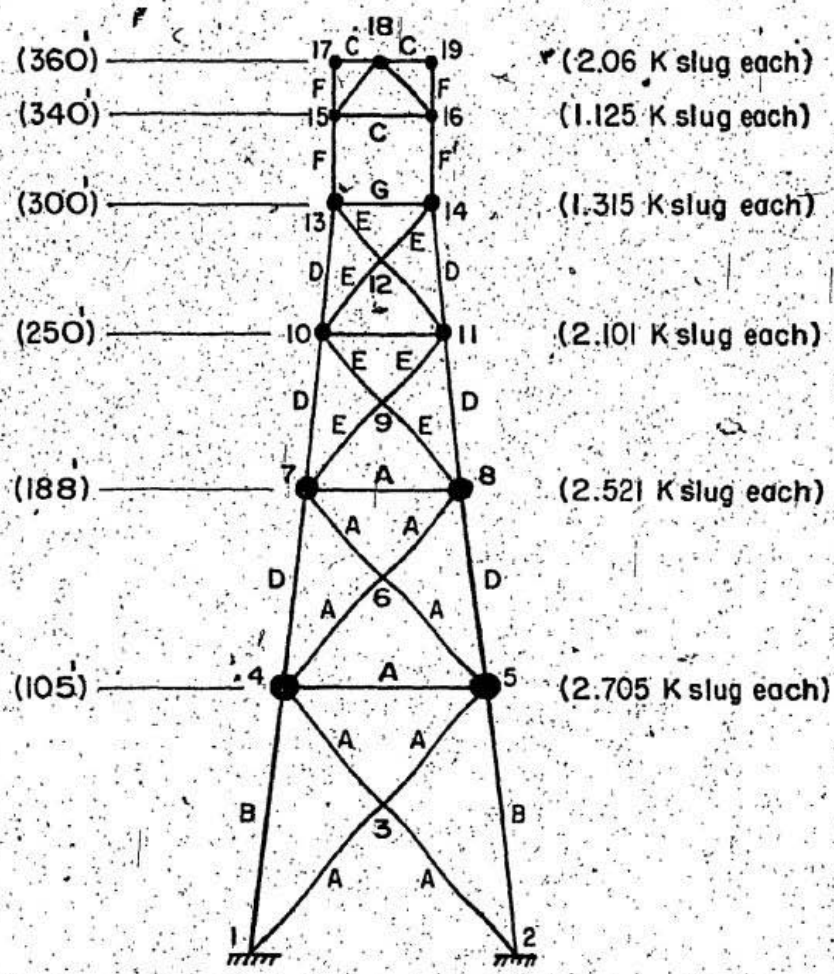

Fig. 3.6 Modelling of Framed Offshore Structure

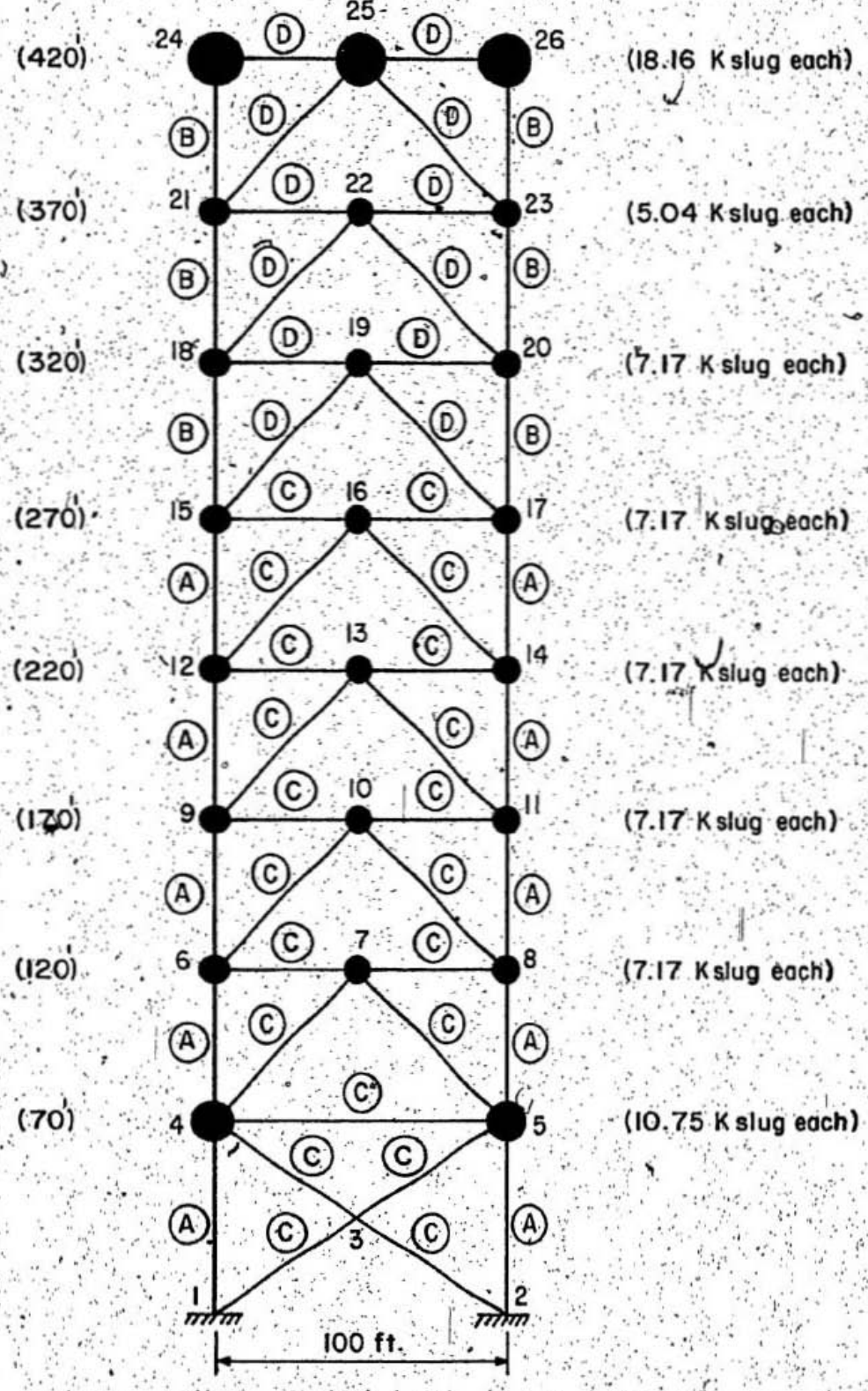

Fig. 3.7 Modelling of Framed Structure System.

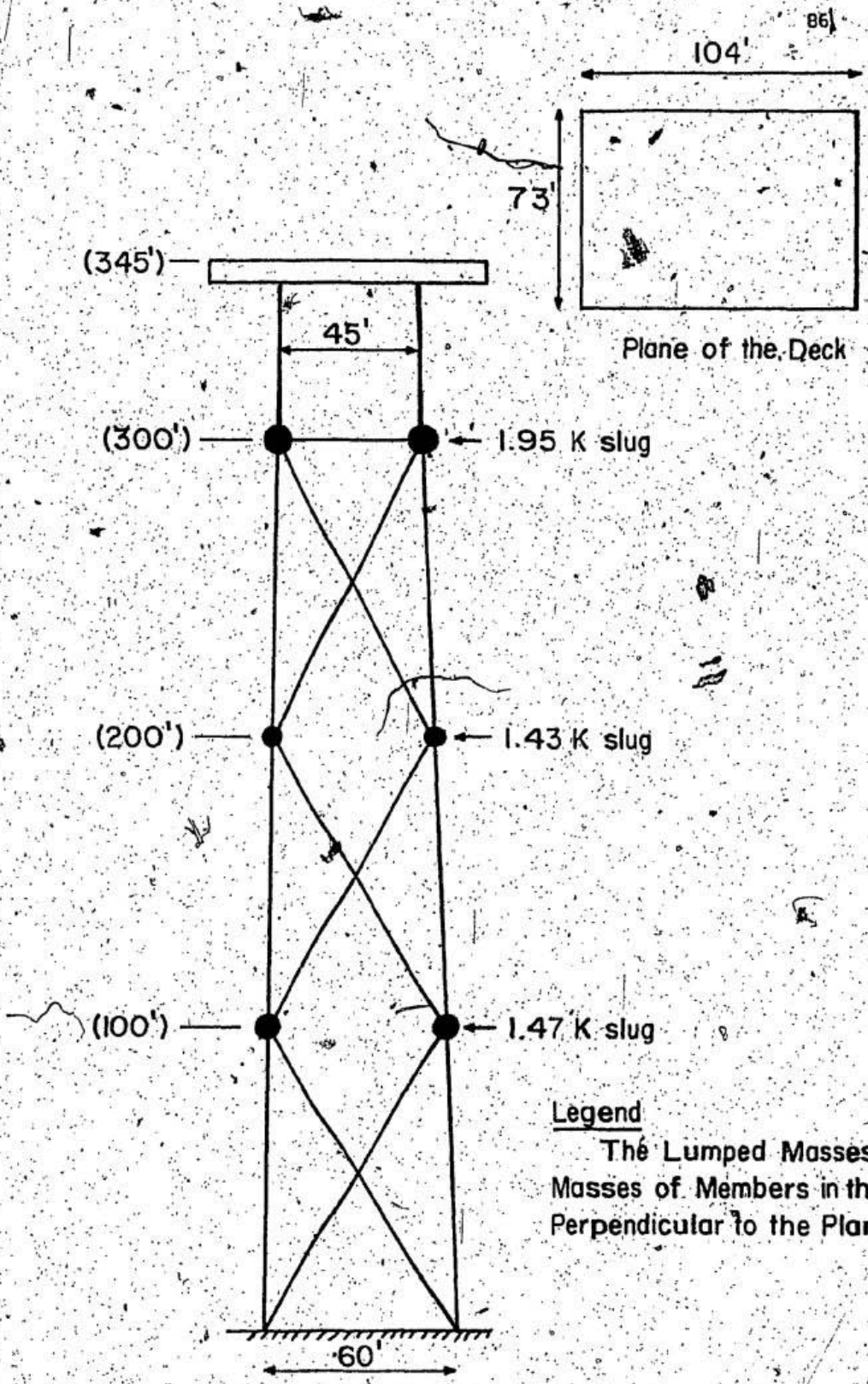

Fig. 4.1 Offshore Platform: Two Dimensional Frame

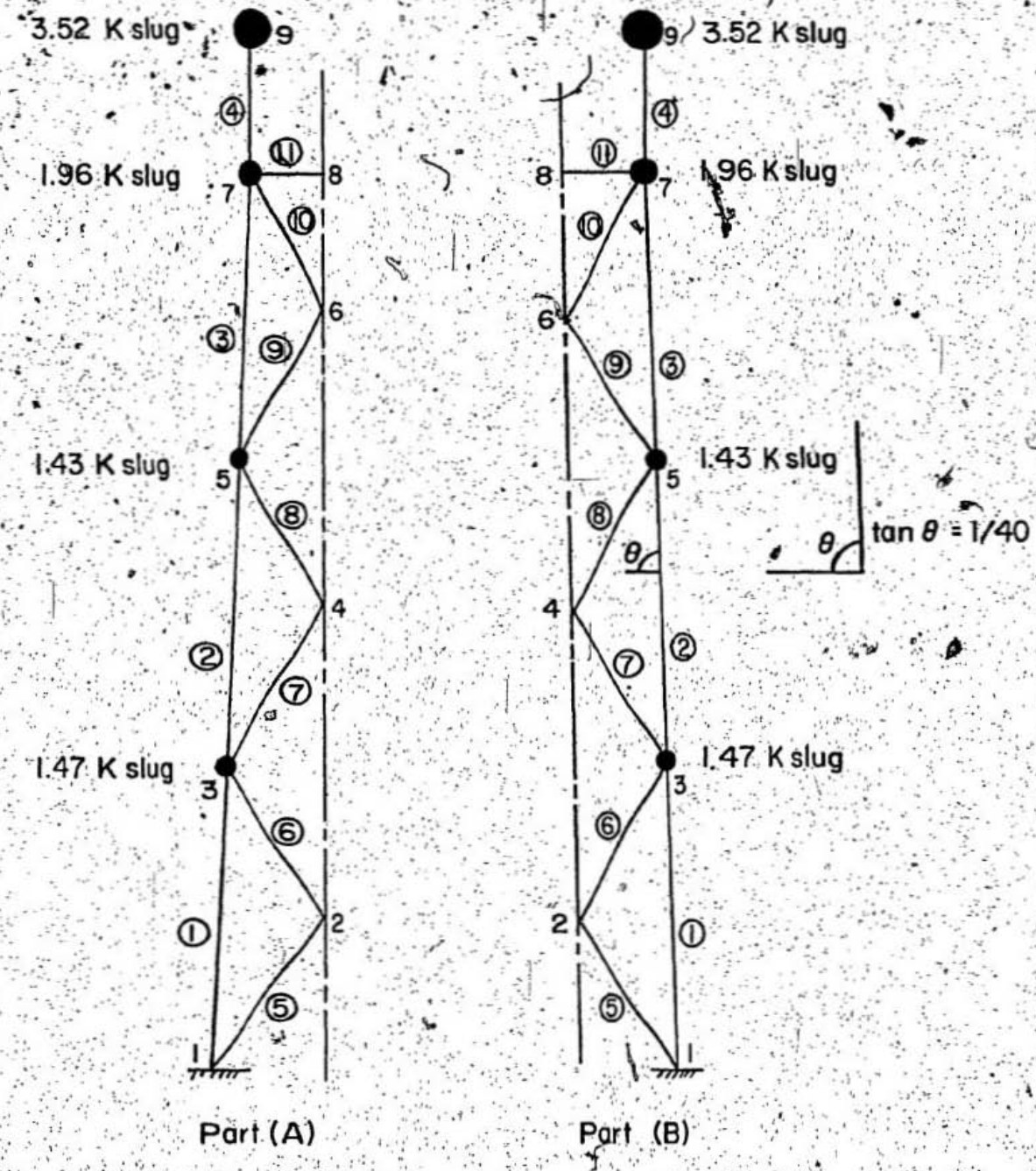

Fig. 4.2 Sub-Structures of the Offshore Platform

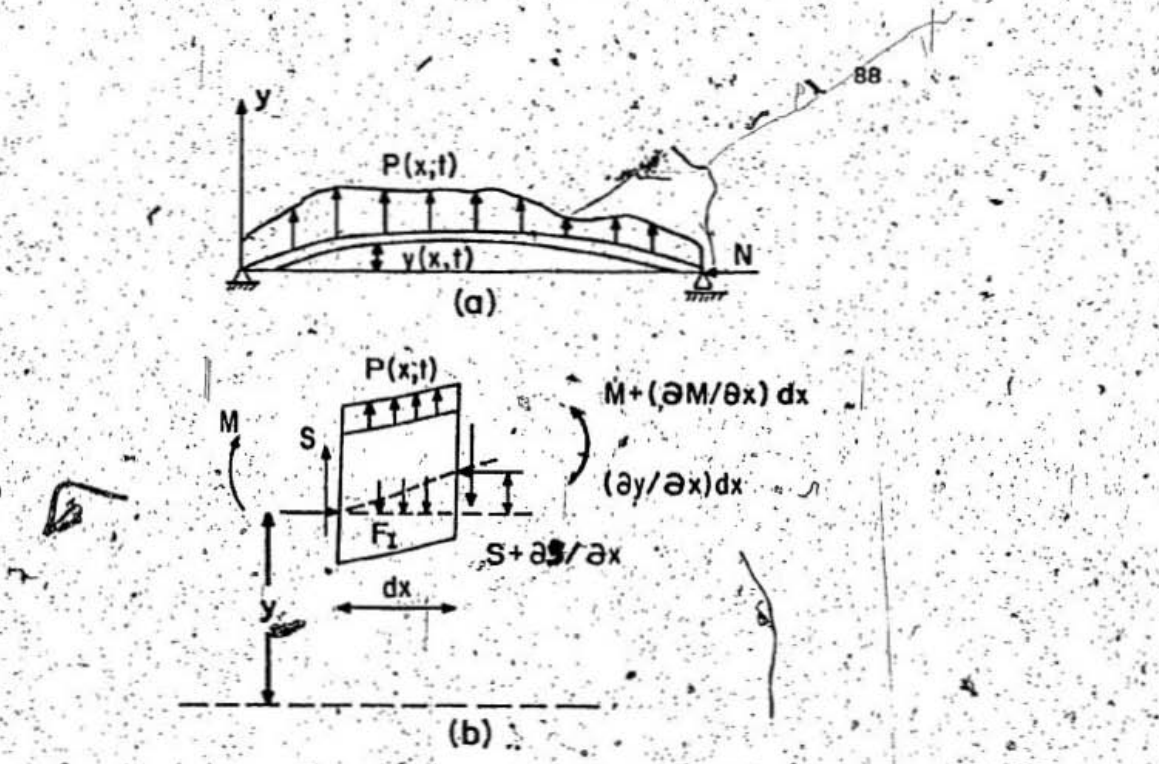

Fig. 5.1 Beam with Static Axial Force and Dynamic Lateral Load a) Beam Deflection Profile b) Forces on Differential Element

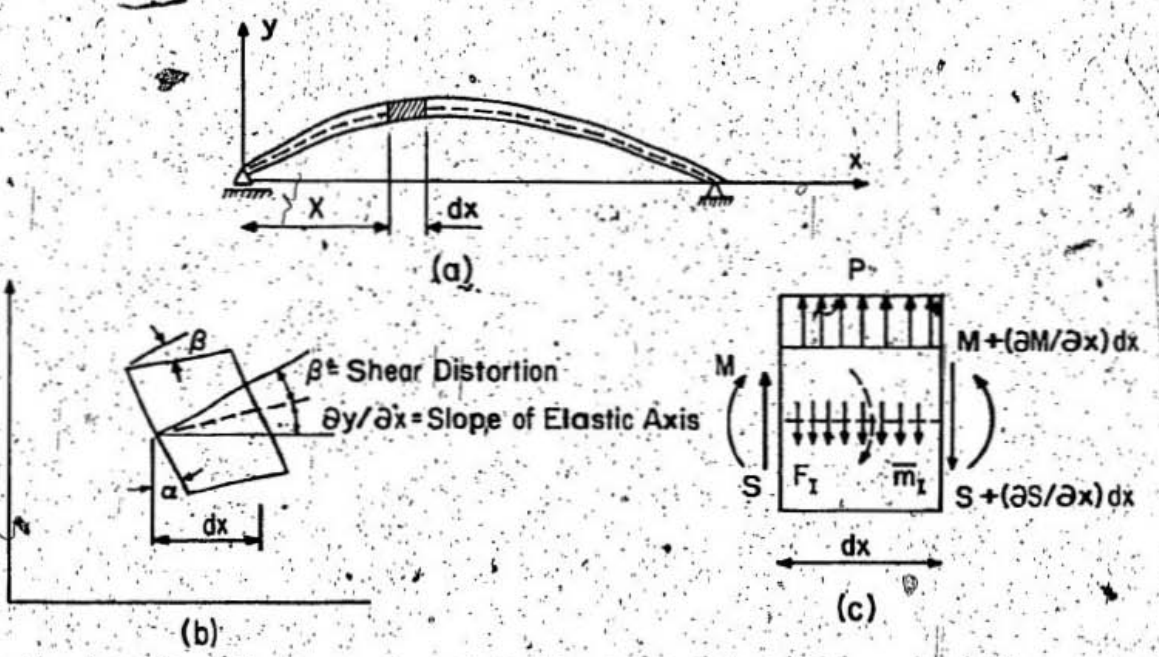

Fig. 5.2 Effects of Shear Distortion and Rotary Inertia a) Deflection Profile b) Deformations of Differential Element c) Forces on Differential Element

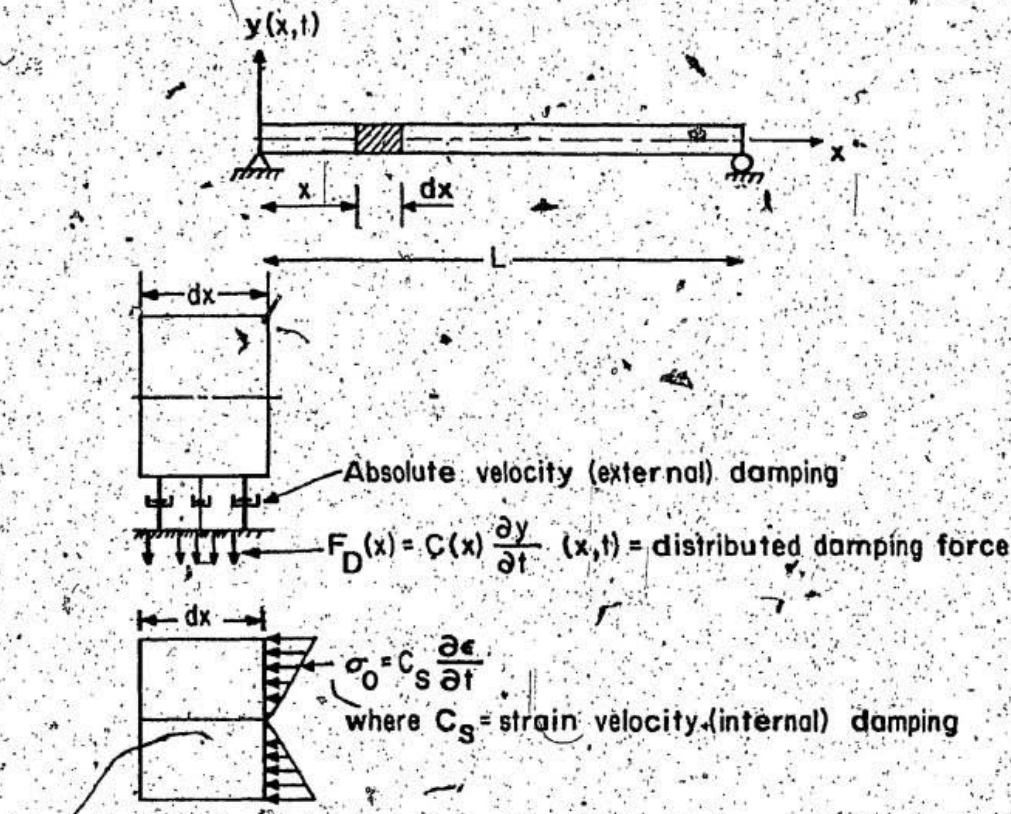

Fig. 5.3 Viscous Damping Mechanisms in a Beam

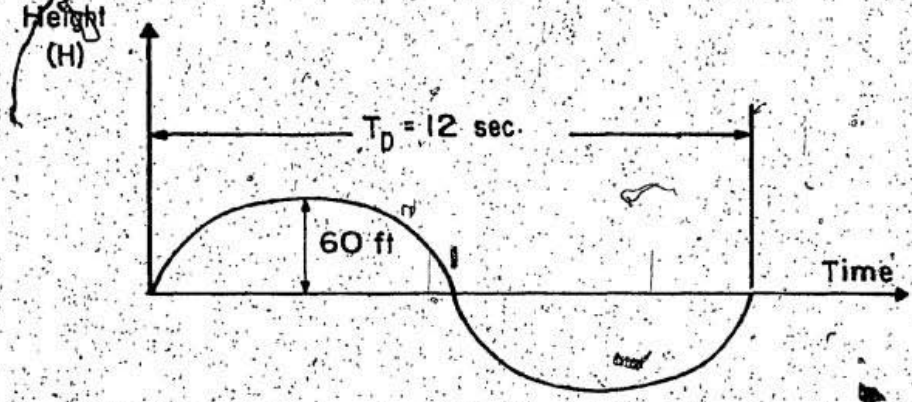

Fig. 5.4 Wave Height vs. Time

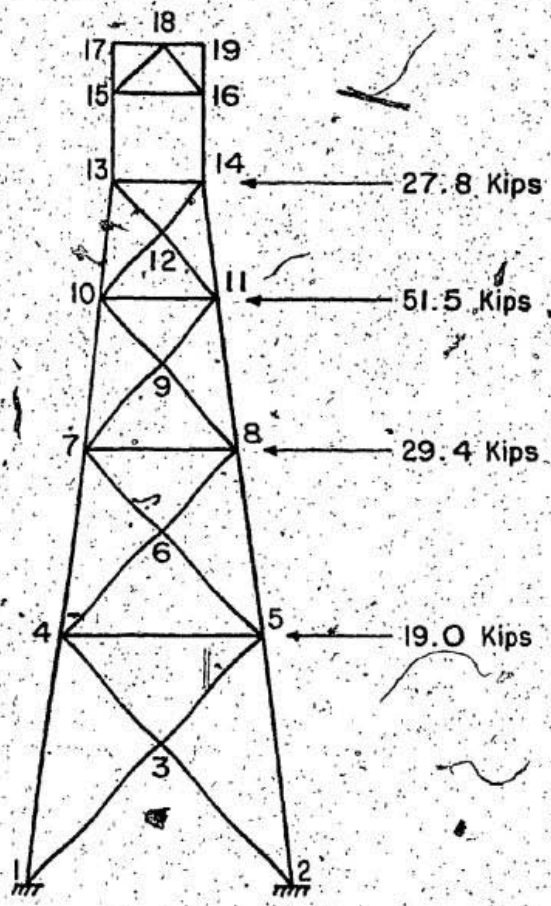

Fig. 5.5 Wave Forces Acting on the Frame

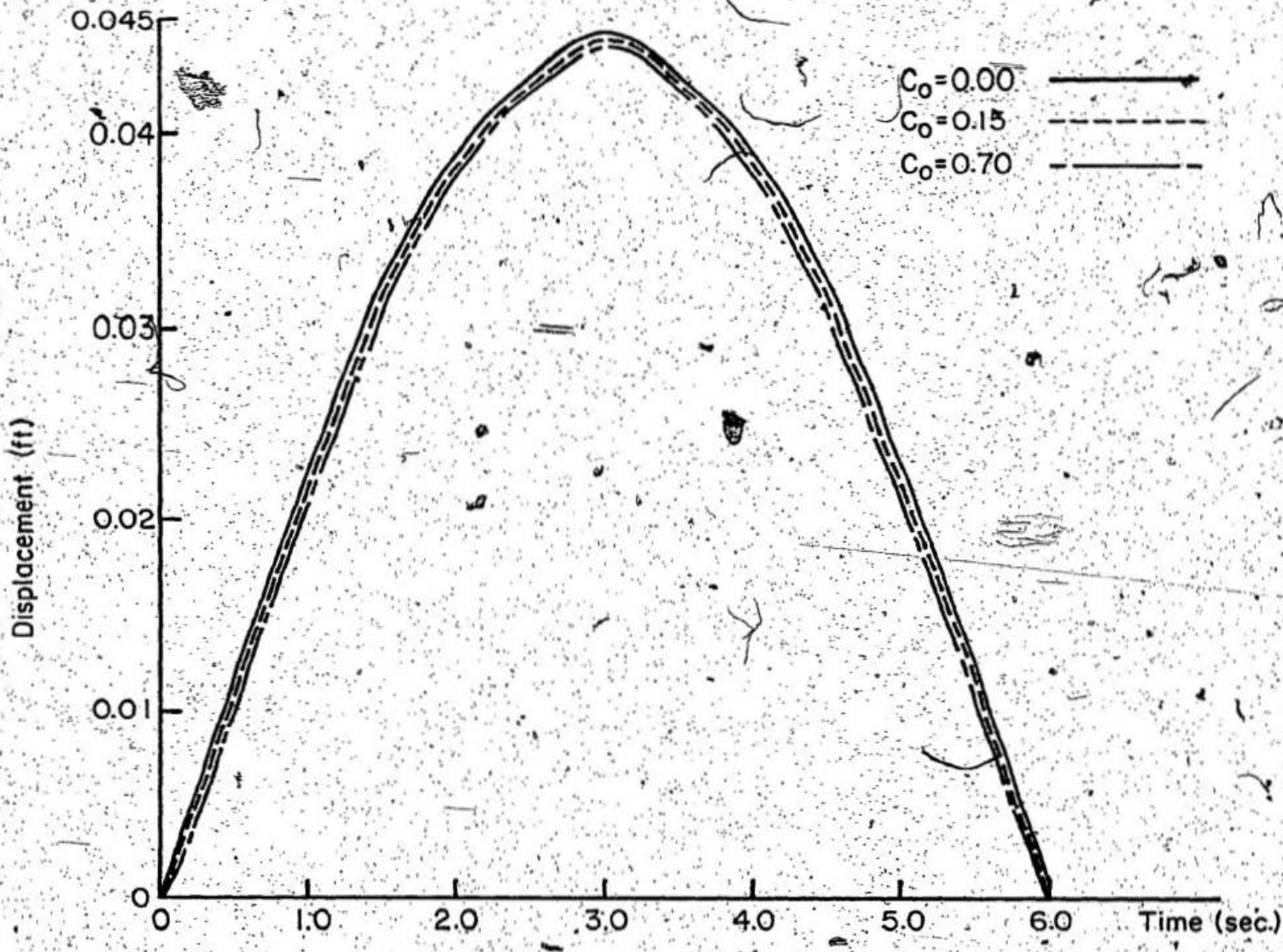

Fig. 5.6 Time-History for the Horizontal Displacement at Node 19.

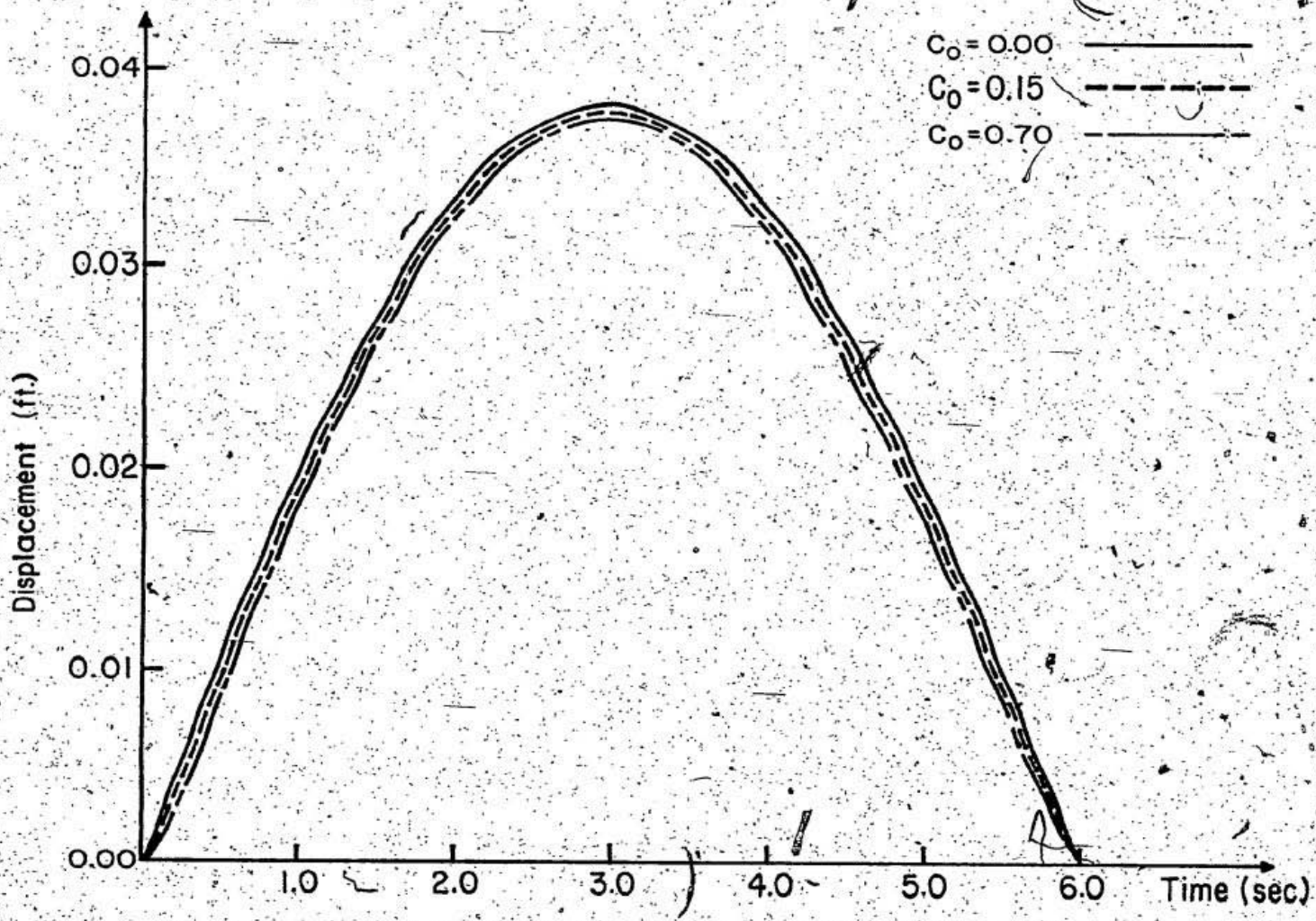

Fig. 5.7 Time – History for the Horizontal Displacement at Node 14

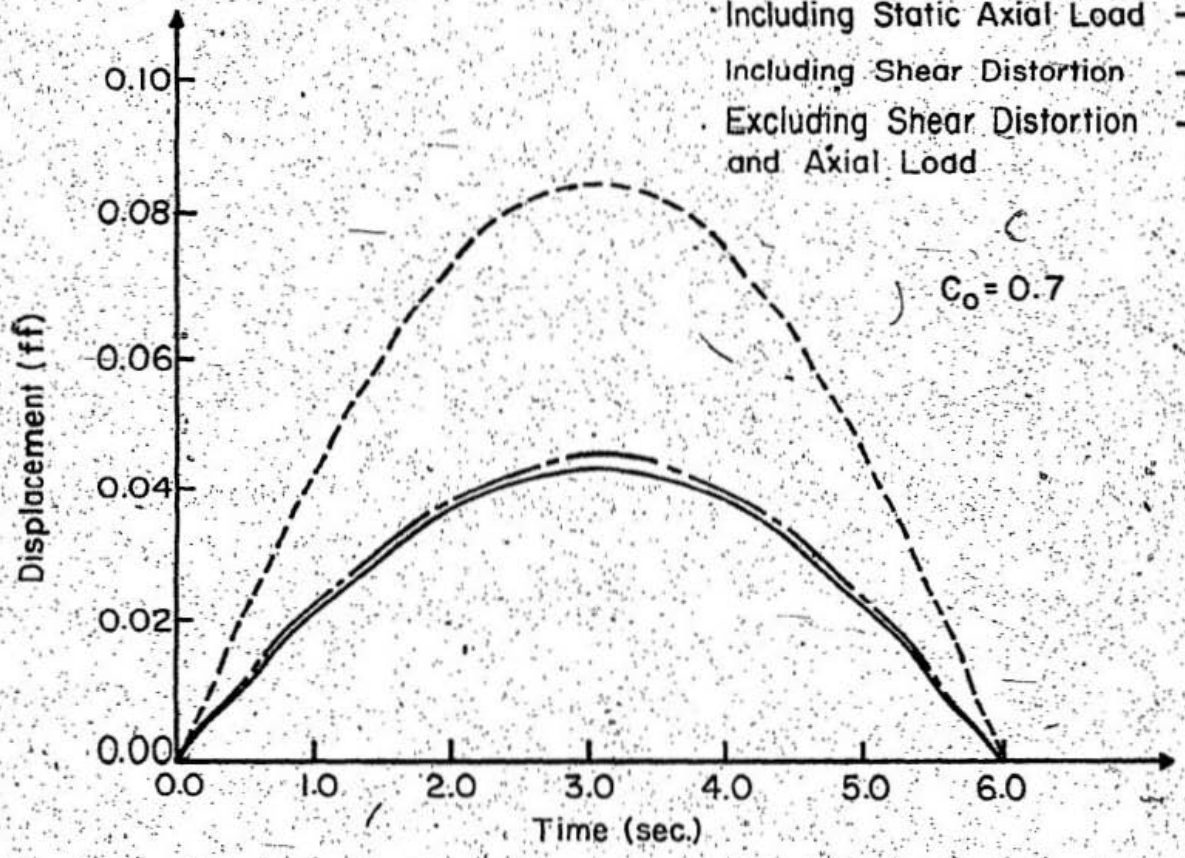

Fig. 5.8 Time-History for the Horizontal Displacement at Node 15

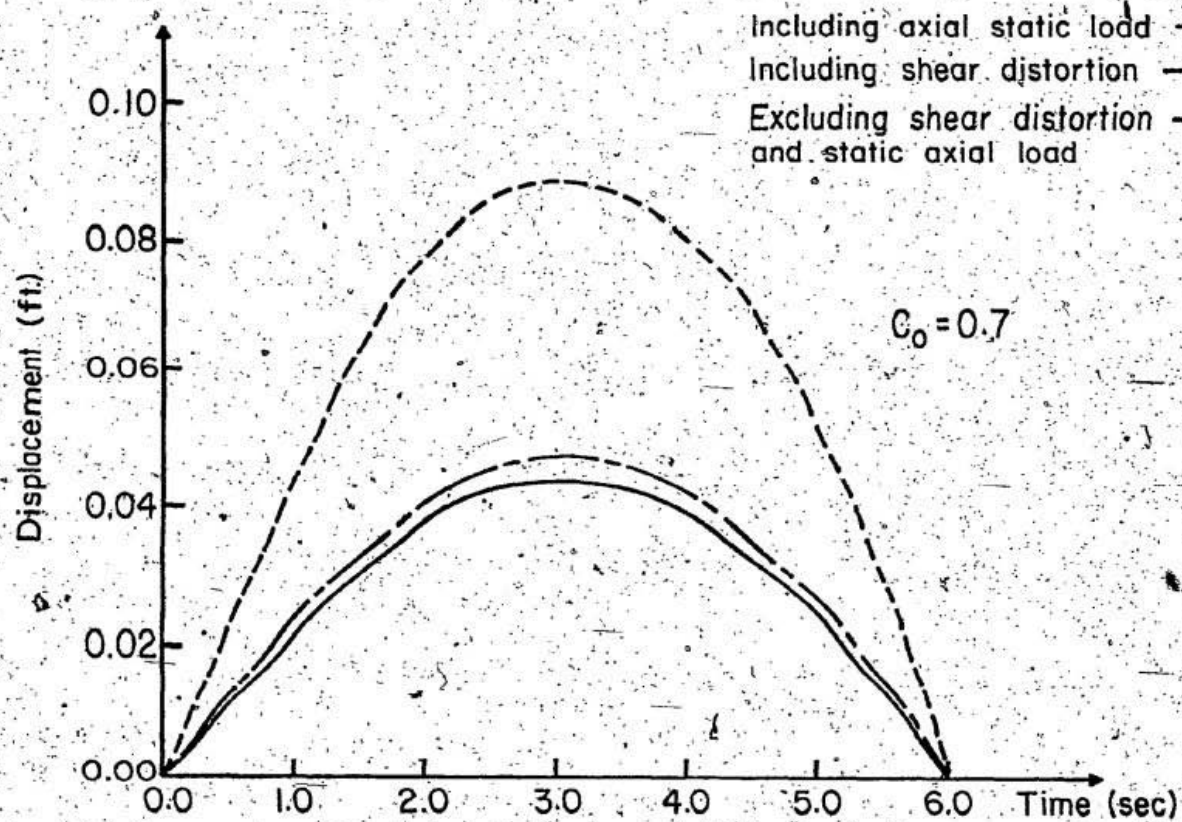

Fig. 5.9 Time – History for the Horizontal Displacement at Node 19

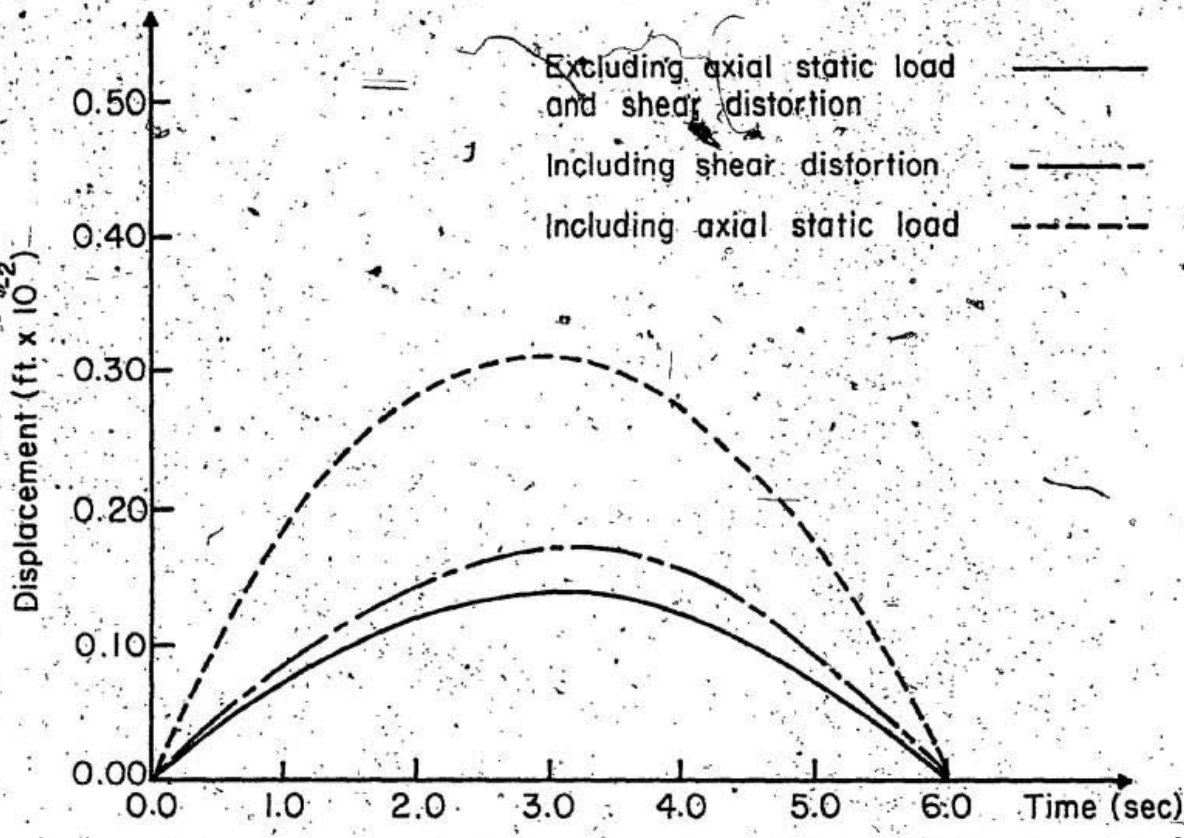

Fig. 5.10 Time-History for the Vertical Displacement at Node 19

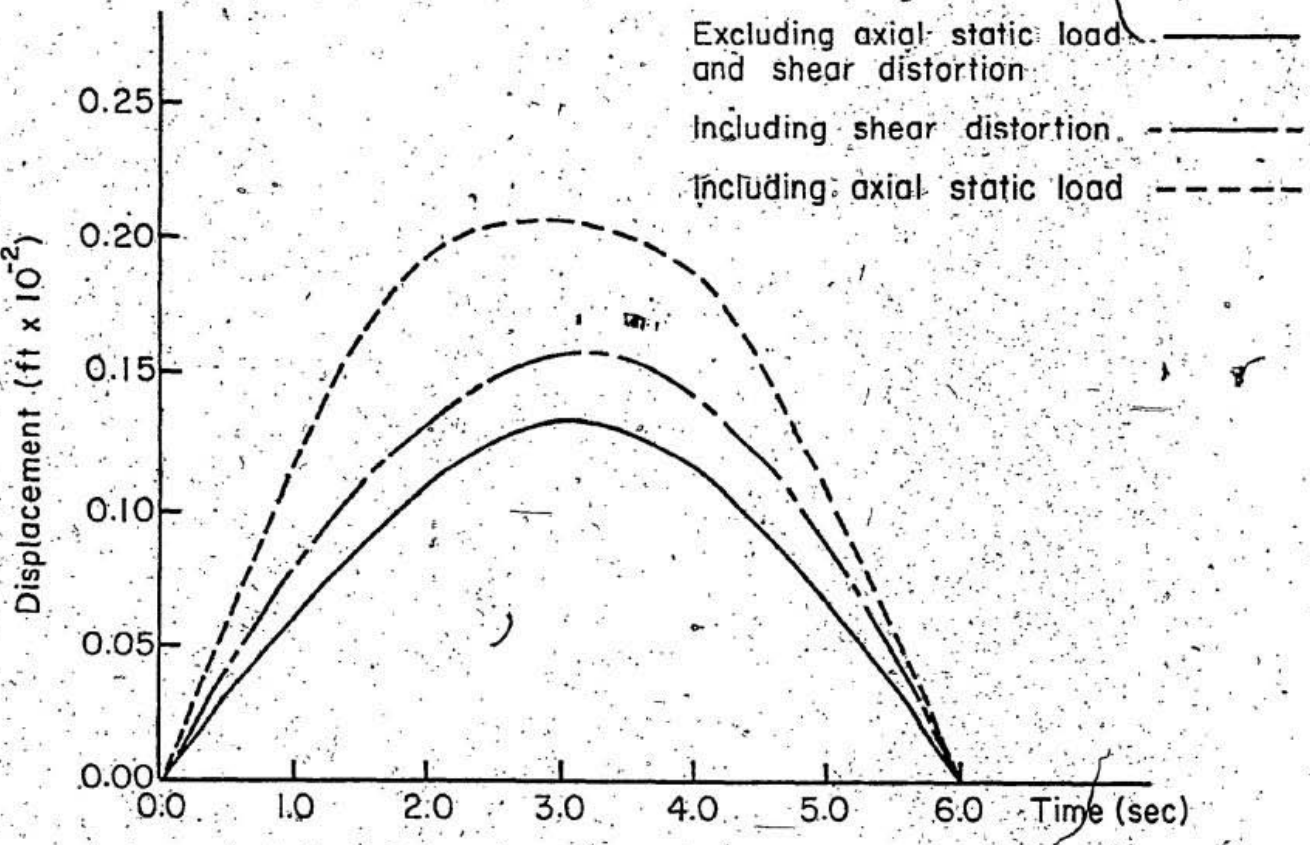

Fig. 5.11 Time-History for the Vertical Displacement at Node 15

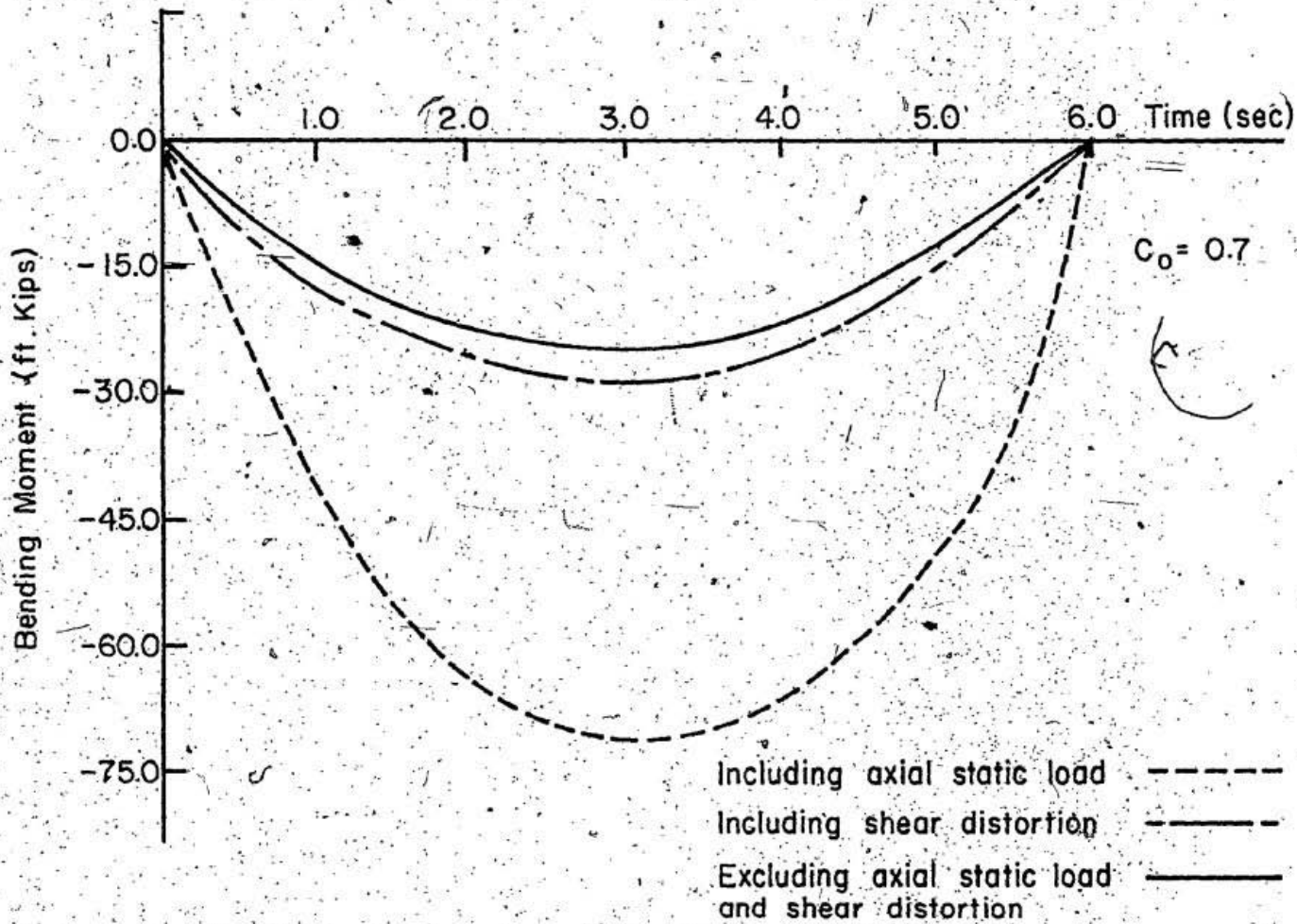

Fig. 5.12 Time-History for Bending Moment in Member 1 at Node 1

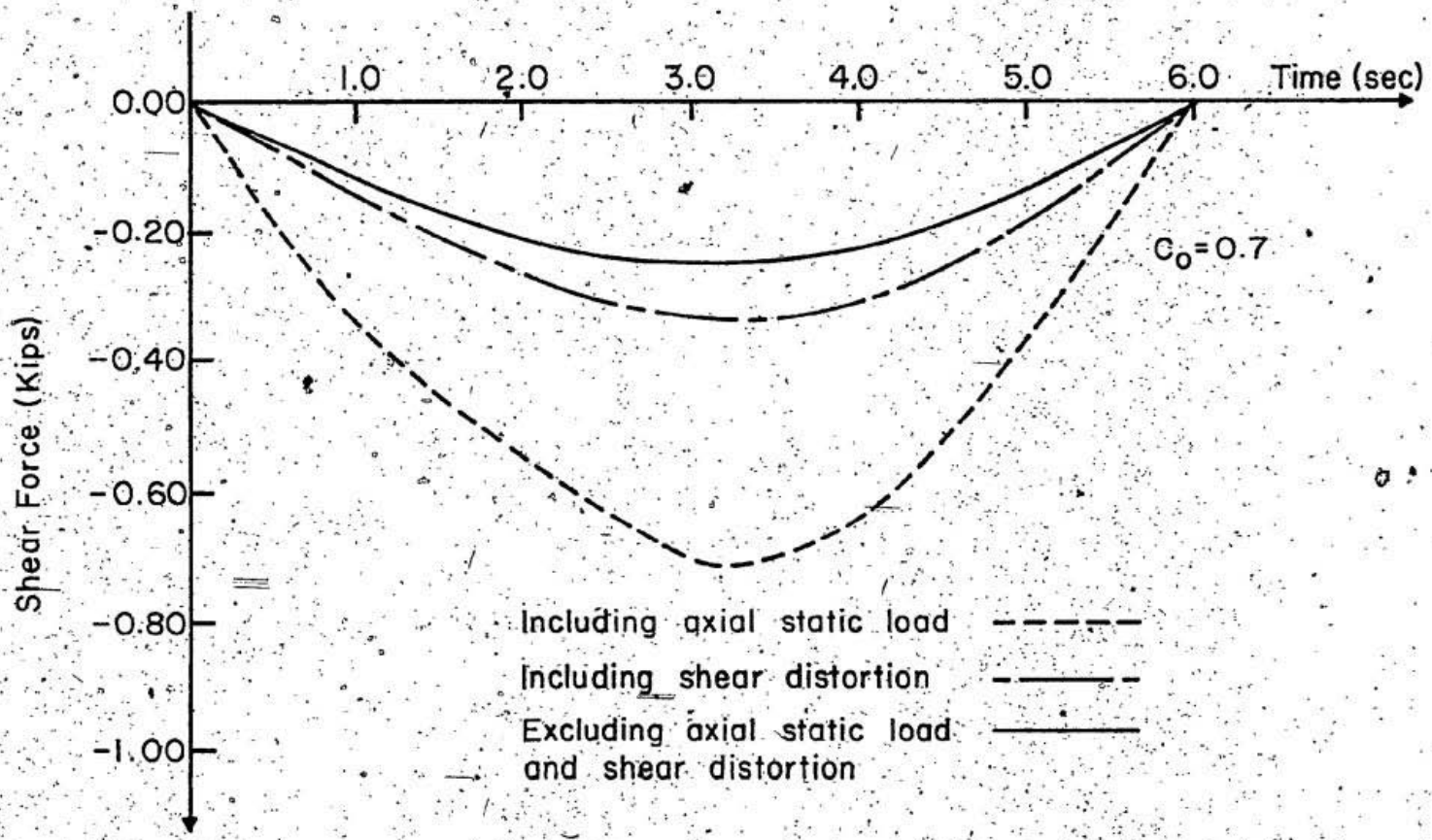

Fig. 5.13 Time-History for the Shear Force in Member 1 at Node 1

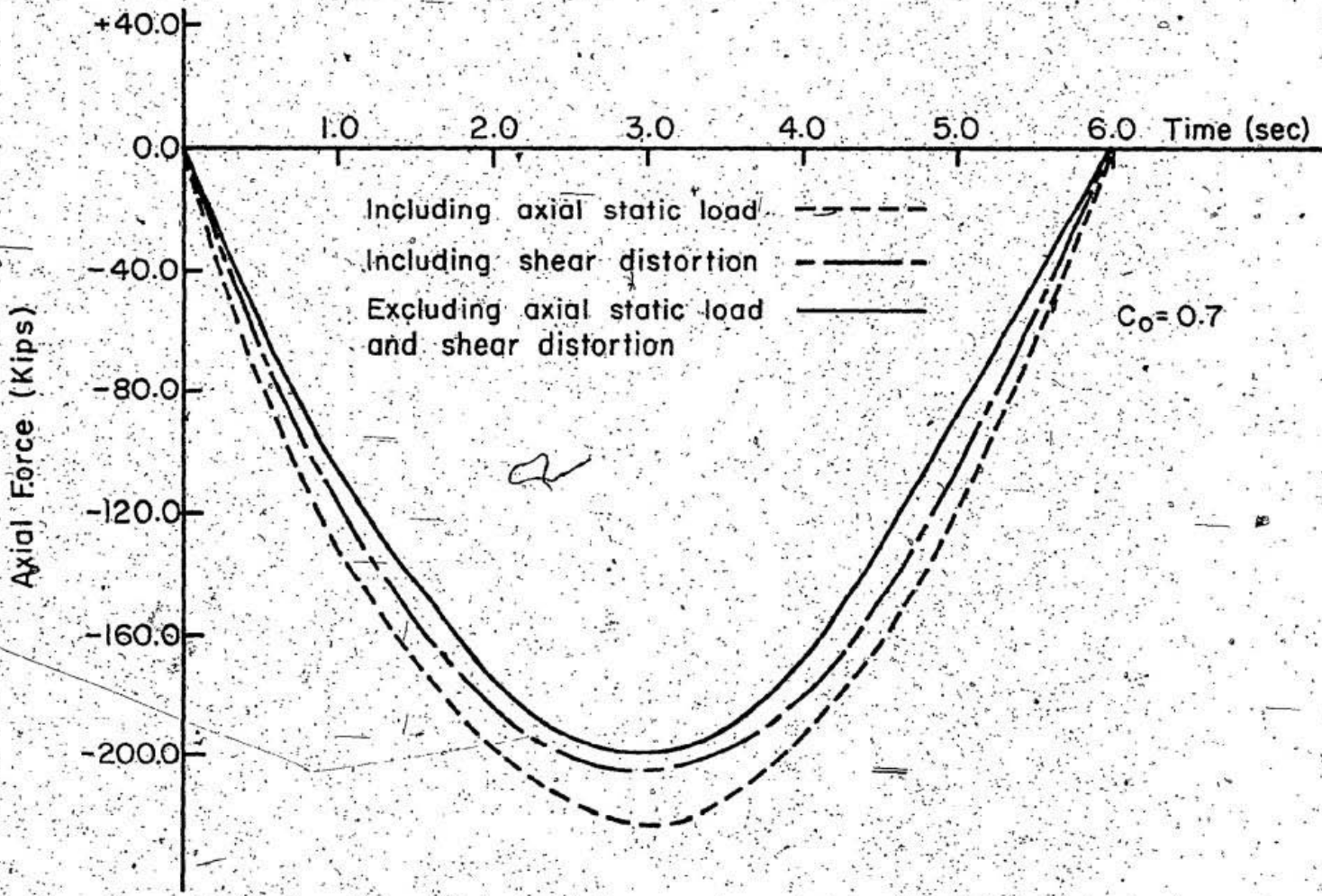

Fig. 5.14 Time-History for the Axial Force in Member 1 at Node 1

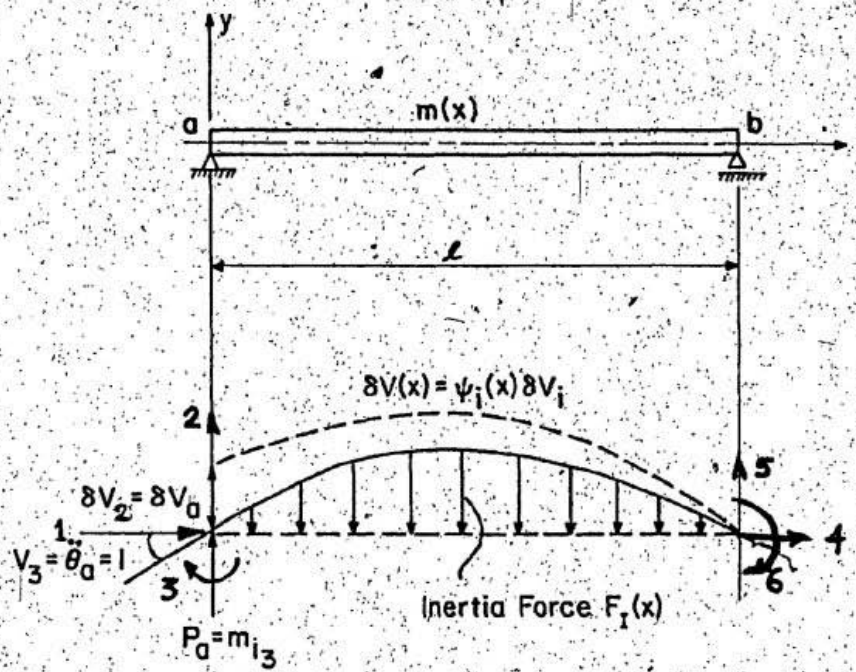

Fig. 6.1 Node Subjected to Real Angular Acceleration and Virtual Translation

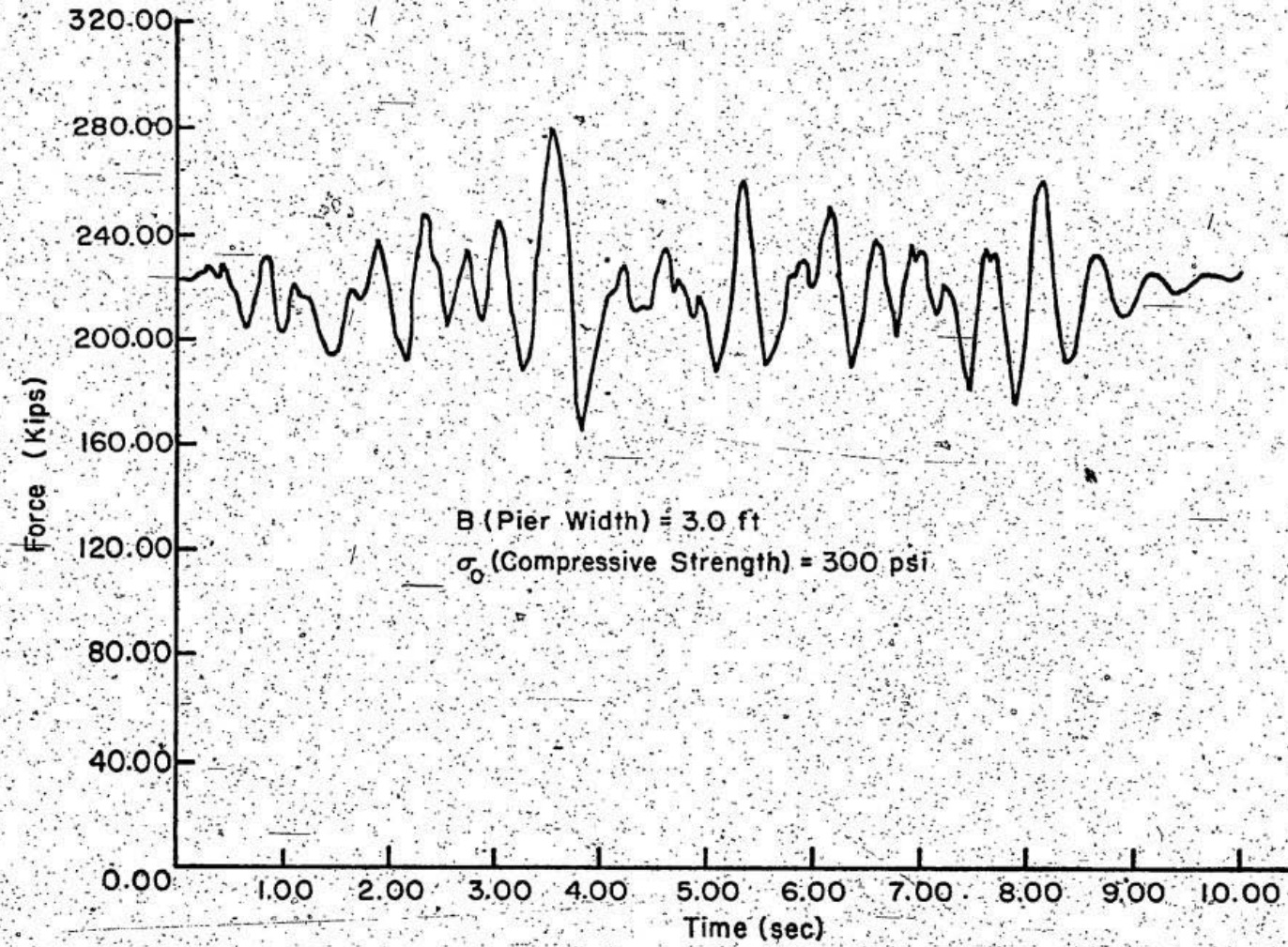

Fig. 6.2 Typical Artificially-Generated Ice-Force Records (Force vs. Time) (Ref. 52)

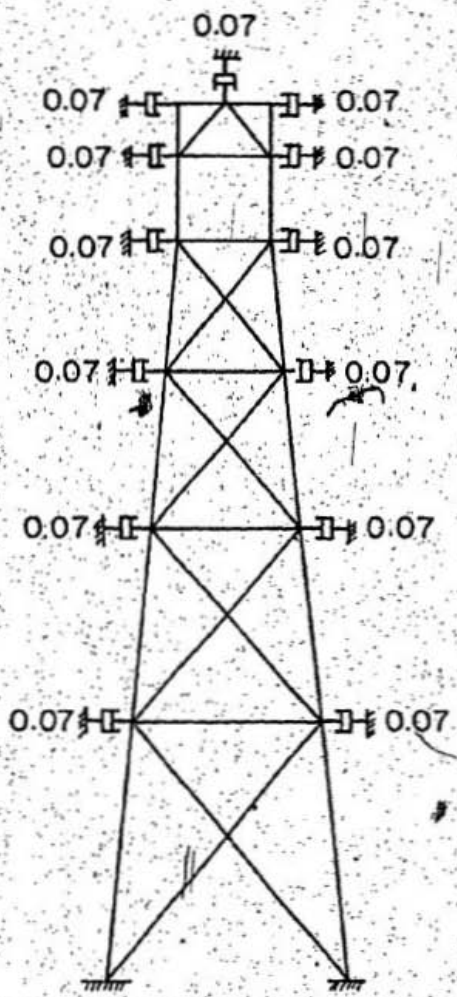

Fig. 6.3 Location of Dampers to Simulate Member Damping in the Direction Perpendicular to the Planar Frame

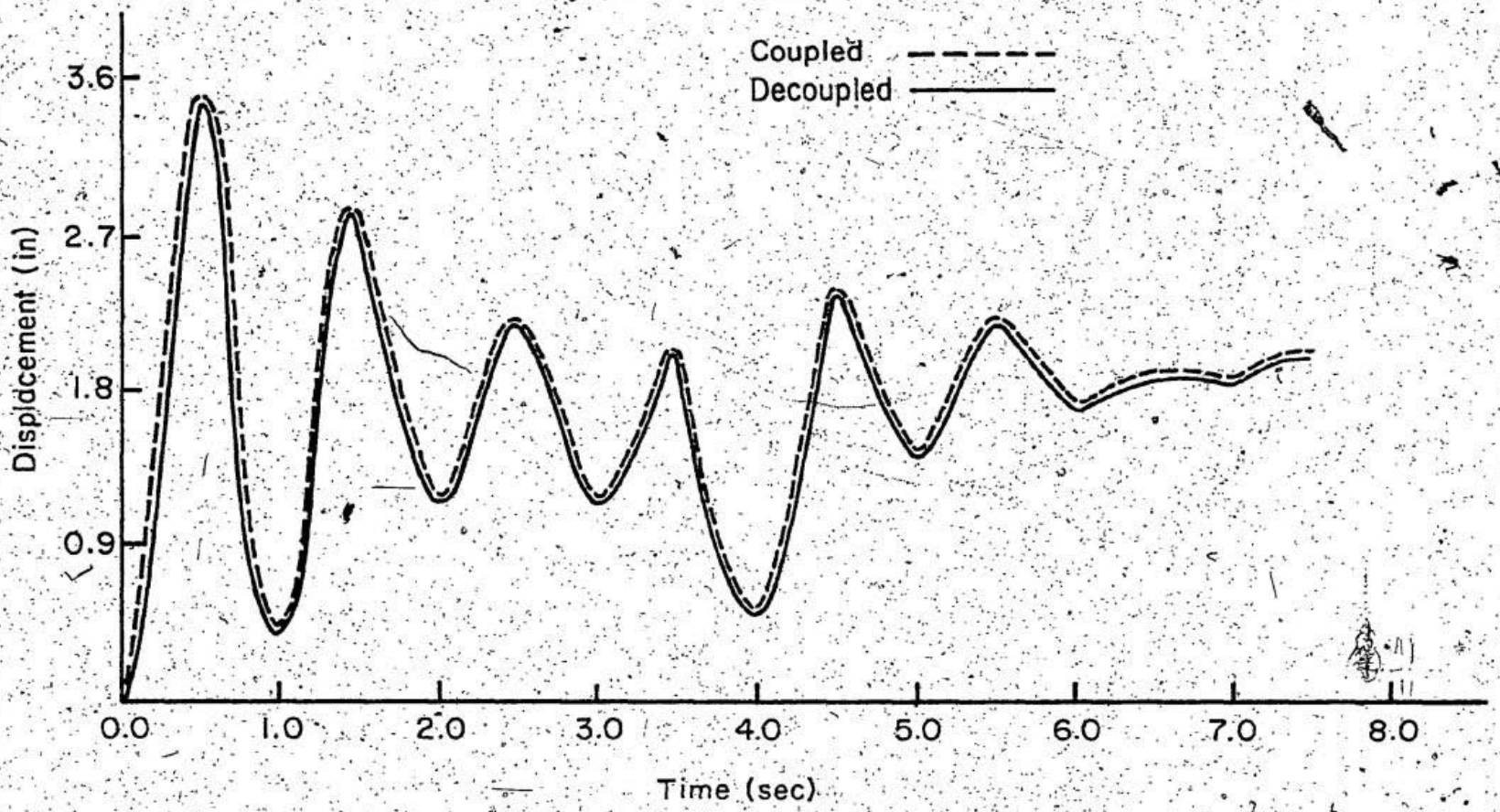

Fig. 6-4 Time-Histories for Horizontal Displacement at Node 19 for the Damping Ratios Given in Table 6.1

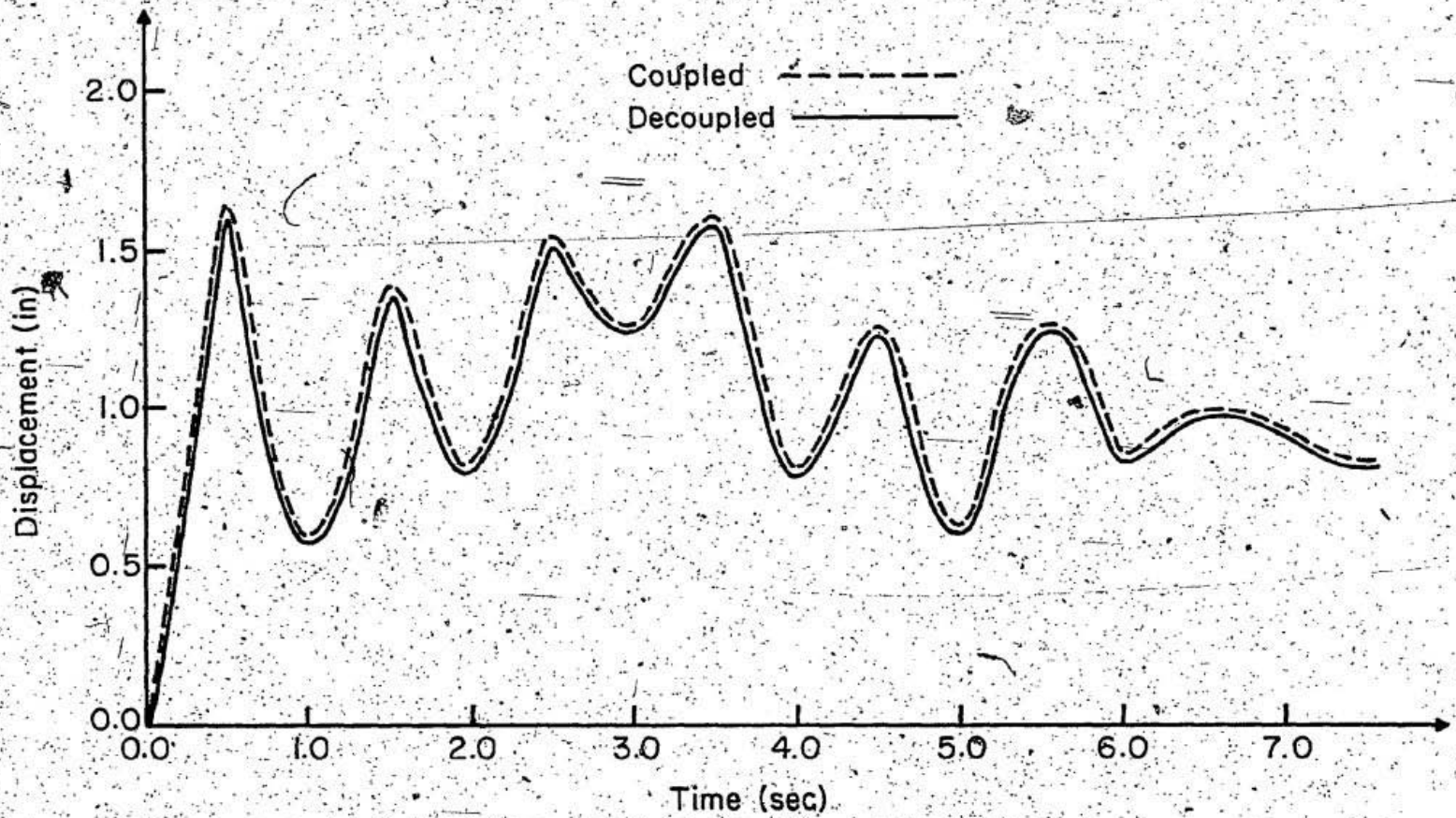

Fig. 6.5 Time-Histories for Horizontal Displacement at Node 14 for the Damping Ratios Given in Table 6.1

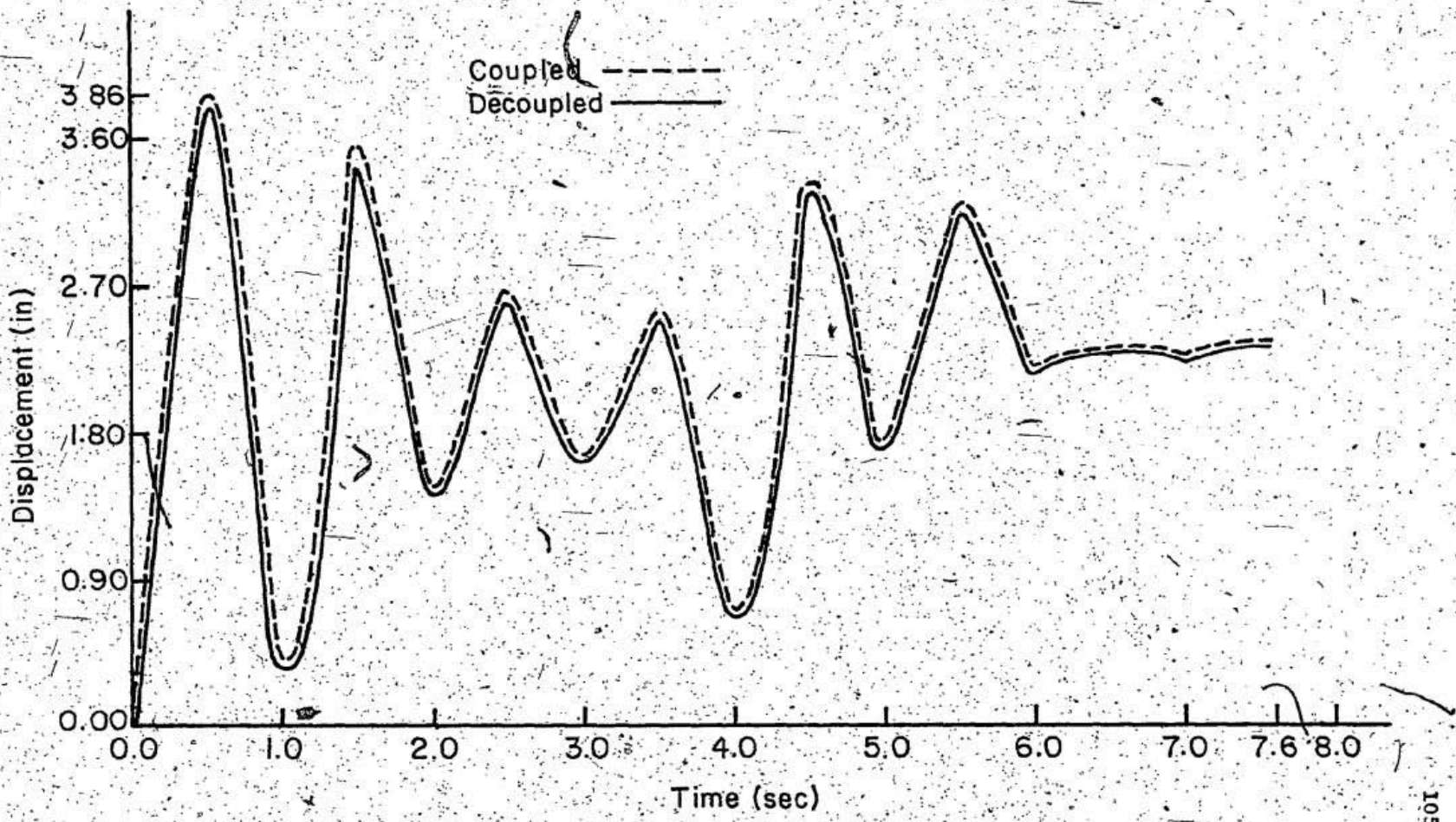

Fig. 6.6 Time-Histories for Horizontal Displacement at Node 19 for Damping Ratios Given in Table 6.2

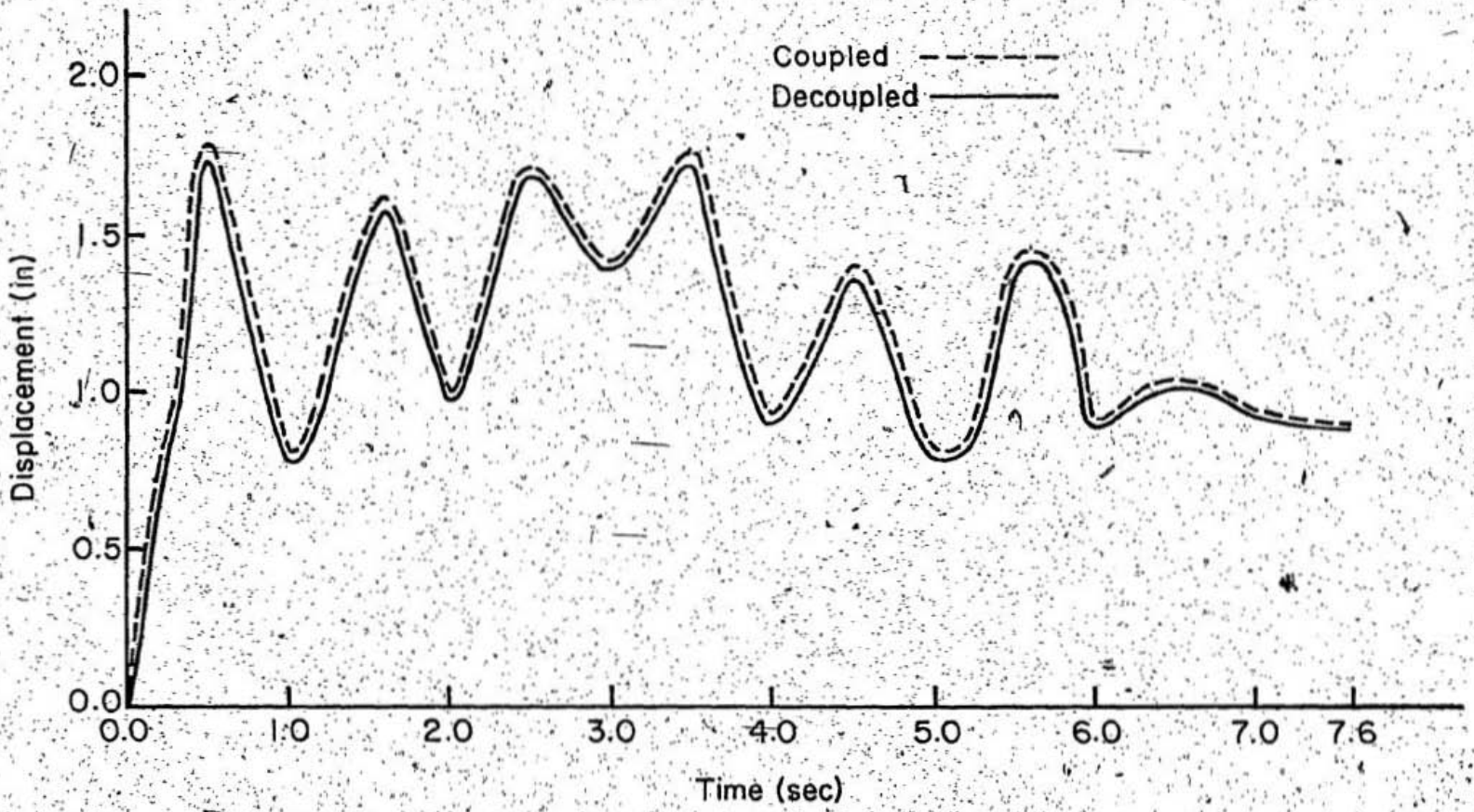

Fig. 6.7 Time-Histories for Horizontal Displacements at Node 14 for Damping Ratios Given in Table 6.2

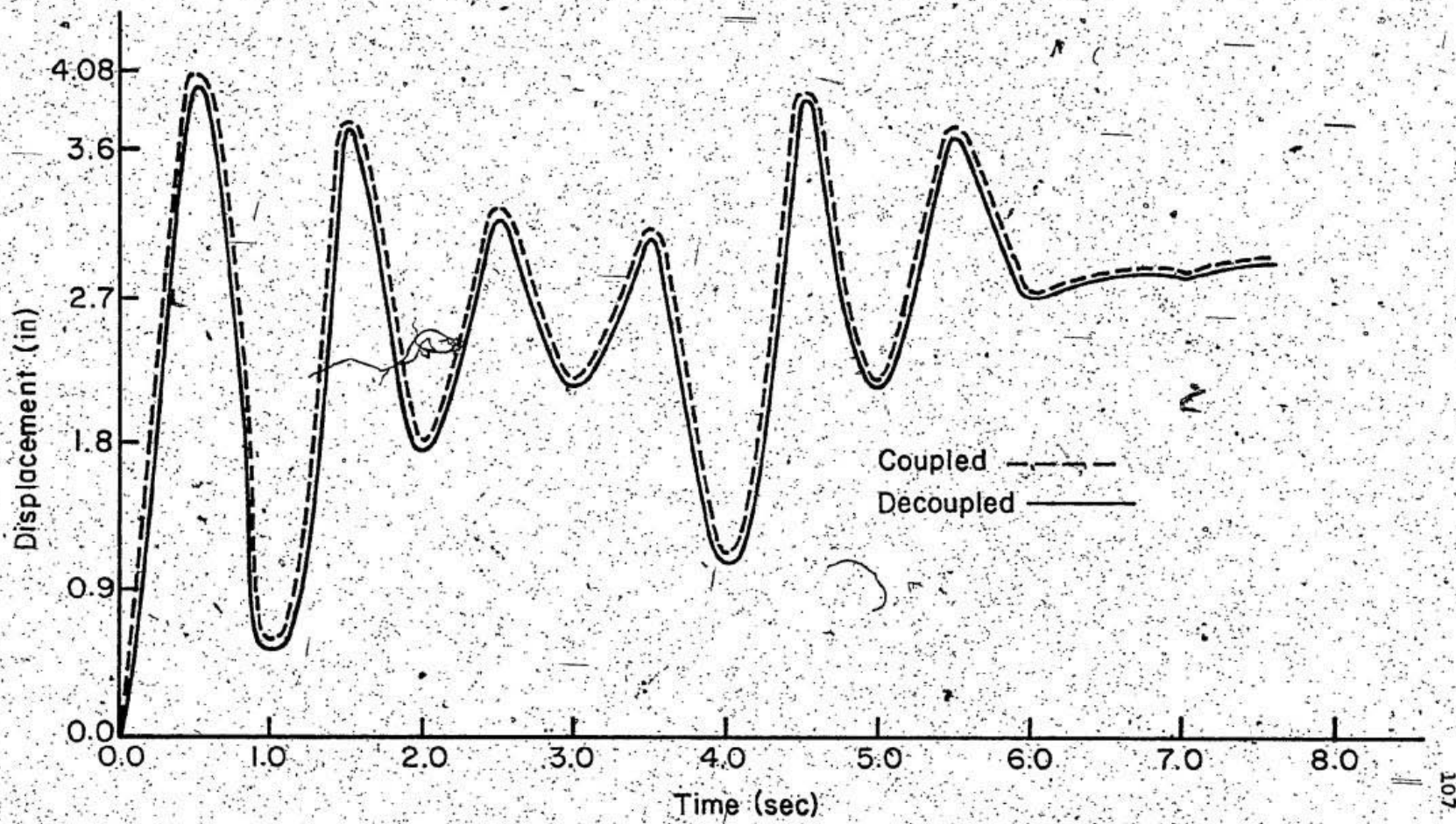

Fig. 6.8 Time-Histories for Horizontal Displacements at Node 19 for Damping Ratios Given in Table 6.3

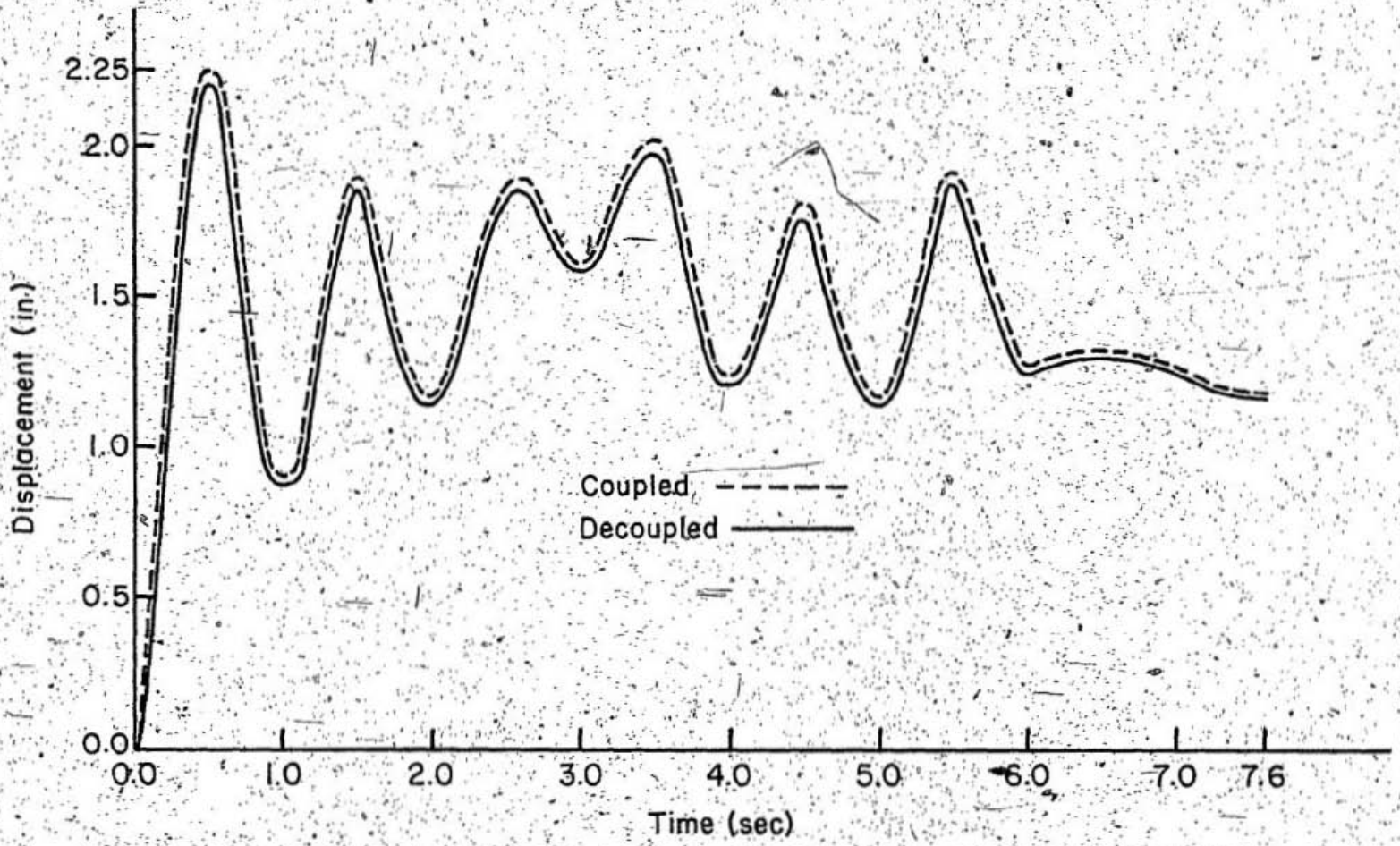

Fig. 6.9 Time-Histories for Horizontal Displacements at Node 14 for Damping Ratios Given in Table 6.3

BIBLIOGRAPHY

1. Veletsos, A. S. and Newmark, N. M., 'Natural Frequencies of Continuous Flexural Members', Proc. ASCE, Vol. 81 paper 735, July 1955.

2. Simpson, A. and Tabarrok, B., 'On Kron's Eigenvalue Procedure and Related Methods of Frequency Analysis'. Quart. Journ. Mech. and Applied Math.

3. Armstrong, I.D., 'The Natural Frequencies of Multistorey Frames', The Structural Engineer, 1969 No. 8 Volume 47.

4. Williams, F. W. and Wittrick, W. H., 'An Automatic Computational Procedure For Calculating Natural Frequencies of Skeletal Structure', Int. J. Mech. Sci: Pergamon Press. 1970. Vol. 12, pp. 781-791.

5. Armstrong, I.D., 'The Natural Frequencies of Grillages', Int. J. Mech. Sci. Pergamon Press. 1968. Vol. 10, pp. 43-55.

6. Williams, F. W. and Wittrick, W. H., "Computional Procedures For A Matrix Analysis of the Stability And Vibration of Thin Flat-Walled Structures in Compresion', Int. J. Mech. Sci. Pergamon Press. 1969. Vol. 11, pp. 979-998.

7. Wittrick, W. H. and Curzon, P. L. V., 'Stability Functions For the Local Buckling of Thin Flat-Walled Structures With the Walls in Combined Shear and Compression', The Aeronautical Quarterly Press. 1968. pp. 327-349.

8. Wittrick, W. H. and Williams, F. W. 'A General Algorithm For Computing Natural Frequencies of Elastic Structures. Q.J. Mech. App. Math., Vol. 14, 1971, pp. 263-284.

9. Rayleigh, J. W. S., 'The Theory of Sound', Vol. I, pp. 119. Dover, New York, 1945.

10. Wittrick, W. H. and Williams, F. W., 'New Procedures for Structural Eigenvalue Calculations Fourth Australasian Conference on the Mechanics of Structures and Materials', University of Queensland, Aug. 1973.

11. Wilkinson, J. H., 'The Algebraic Eigenvalue Problem', Oxford Univ. Press, 1965.

12. Sainsbury, R. N. and King, D., 'The Flow Induced Oscillation of Marine Structures', Proc. I. Civil E., Vol 49, 1971, pp. 269-302, Disscussion, Proc. I. Civ. E., Vol. 51, 1972, pp. 621-627.

13. Swannell, P., 'The Automatic Computation of the Natural Frequencies of Structural Frames Using an Exact Matrix Technique', Theory and Practice in Finite Element Structural

Analysis, Tokyo, 1973.

14. Timoshenko, S., Young, D. H., and Weaver, W., 'Vibration Problems in Engineering', Fourth Edition.

15. Clough, R. W. and Penzien, J., 'Dynamics of Structures', 1975 by McGraw-Hill, inc..

16. Kolousek, V., 'Dynamices in Engineering Structures'.

17. Thomson, W. T., 'Theory of Vibration with Applications'.

18. Swannell, P., 'Computer Methods for Buckling and Free Vibration with Distributed Mass', Buckling in Low-rise Industrial Buildings', 17th August 1976.

19. Tranberg, C. H., 'On the Free and Forced Vibration of Engineering Structures', Ph.D. Thesis; Univ. of Qld. Dept. of Civil Engineering.

20. Hurty, W. C., 'Vibration of Structural Systems by Component Mode Synthesis', Proc. Am. Soc. Civil Engrs., Vol. 86, EM4, August 1960.

21. Hurty, W. C., 'Dynamic Analysis of Structural Systems by Component Mode Synthesis', TR 32-530, January 1964, Jet Propulsion Laboratory, Pasadena, California.

22. Hurty, W. C., 'Dynamic Analysis of Structural Systems Using Component Modes', 'AIAA Journal', Vol. 3, No. 4, April 1965.

23. Hurty, W. C., 'A Criterion for Selecting Realistic Natural Modes of a Structure', TR 33-364, November 1967, Jet Propulsion Laboratory, Pasadena, California.

24. Bajan, R. L., Feng, C. C. and Jaszlics, I. J., 'Vibration Analysis of Complex Structural Systems by Modal Substitution', The Shock and Vibration Bulletin, No. 39, January 1969, Naval Research Laboratory, Washington, D.C..

25. Goldman, R. L., 'Vibration Analysis by Dynamic Partitioning', RM 305, May 1966, Martin Co., Baltimore, Maryland.

26. Goldman, R. L., 'Vibration Analysis by Dynamic Partitioning', AIAA Journal, Vol. 7, No. 6, June 1969.

27. Gwin, L. B., 'Methodology Report for Docking Loads', TR ED 2002-595, August 1968, Martin Marietta Corp., Denver, Colorado.

28. Skjelbreia, L. and Hendrickson, J. A., 'Fifth order gravity wave theory. Proceedings of 7th Conference on Coastal Engineering, Tokyo, 1960. Council on Wave Research. Richmond, California, 1961, pp. 184-196.

29. Hogben, N., Miller, B. L., Searle, J. W., and Ward, G., 'Estimation of Fluid Loading on Offshore Structures', Proc. Instn. Civ. Engrs., Part 2, 1977, 63, Sept., pp. 515-562.

30. Morison, J. R. et al., 'The Force Exerted by Surface Waves on Piles. Trans. Am. Inst. Min. Metall. Engrs., Petroleum Brach, 1950, 189, pp. 149-154.

31. Hogben, N., 'Fluid Loading on Offshore Structures, a state of art appraisal: wave loads. Royal Institution of Naval Architects, London, 1974, Maritime Technology Monograph 1.

32. Chakrabarti, S. K. and Tam, W. A., Cross and Local Wave Loads on a Large Vertical Cylinder - Theory and Experiment, Proc. 7th Offshore Technol. Conf., Houston 1973, Paper 1818.

33. Myers, J. J. et al., 'Handbook of Ocean Engineering, McGraw -Hill, New York, 1969.

34. Evans, D. J., 'Analysis of Wave Forces Data', Proc. 7th Offshore Technol. Conf., Houston, 1969, Paper 1005.

35. Hudspeth, R. T. et al., 'Comparison of Wave Forces Computed by Linear and Stream Function Methods, Proc. 7th Offshore Technol. Conf., Houstin, 1974, Paper 2037.

36. Rance, P. J., 'Wave Forces on Cylindrical Members of Structures', Hyd. Res. 1969, Hydraulics Research Station, Wallingford, 1970, pp. 14-17.

37. Chakrabarti, S. K. et al., 'Wave Forces on a Randomly Oriented Tube', Proc. 7th Offshore Technol. Conf., Houston, 1975, Paper 2190.

38. Zubov, N.N., 1945, Arctic Ice. Izdatel'Stvo Glavsevmoi eti, Moscow (1945), Tansl. by the U.S. Navy Oceanographic Office and the American Meteorological Society (1963), pp. 489.

39. Korzhavin, K. N., 1962. Action of Ice on Engineering Structures. Novosibirsk 1962. Draft Transl. 260 Corps of Engineers, CRREL, Hanover, New Hampshire, pp. 319, 1971.

40. Dromin, M. and Michel, B., 1974, Pressures of Thermal Origin Exerted by Ice Sheets upon Hydraulic Structures, Draft Translations 427 Corps of Engineers, CRREL, Hanover, New, Hampshire, pp. 405.

41. Michel, B., 1970, Ice Pressure on Engineering Structures. Cold Regions Science and Engineering, Monograph III - Bib., CRREL, Hanover, New Hampshire, U.S.A., pp. 71.

42. Blenkarn, K.A. and Knapp, A.E., 1969. Ice Conditions on the Grand Banks. Ice Seminar Sponsored by Petroleum Society of Canadian Institute of Mining and Metallurgy and the American Petroleum Institute, Calgary, Alberta, Canada, pp. 61-72.

43. Kopaigorodski, E.M., Vershinin, S.A., and Nifontov, S.A., 1972. Model Investigations of the Effect of an Ice Field Pushed Against the Piles of Offshore Oil Platforms, IAHR/AIRH Symp. on Ice and Its Action on Hydraulic Structures, Leningrad, U.S.S.R., pp. 100-102.

44. Hirayama, K., Schwarz, J., and Wu, H.C., 1973. Model Technique for the Investigation of the Forces on Structures. Proc. Second POAC Conference, Reykjavik, Iceland, pp. 332-344.

45. Hirayama, K., Schwarz, J., and Wu, H.C., 1974. An Investigation of Ice Forces on Vertical Structures. Iowa Inst. Hyd. Res. Report, No. 158.

46. Afanas'ev, V.P., 1973. Ice Pressure on Vertical Structures. Technical Translations 1708, National Research Council, Ottawa, Canada, pp. 6.

47. American Petroleum Institute, New York, 1971. API Recommended Practice for Planning, Designing, and Construction of Fixed Offshore Platforms.

48. Blumberg, R. and Strader, N. R. II, 1969. Dynamic Analysis of Offshore Structures. Proc. Offshore Technology Conference (OTC), Houston, Texas, Vol. I, Paper No. OTC 1009, pp. 107-126.

49. Matlock, H., Dawkins, W.P., and Panak, J.J., 1971. Analytical Model for Ice Structure Interaction. Proc. ASCE, Engineering Mechanics Division, Vol. 97, No. EM4, pp. 1083-1092.

50. Peyton, H.R., 1968. Ice and Marine Structures, Part I - The Magnitude of Ice Forces Involved in Design. Ocean Industry, 3, pp. 404-444.

51. Sudararajan, C. and Reddy, D.V., 1973 Stochastic Analysis Of ice Structure Interaction. Proc. Second. POAC Conference, Reykjavik, Iceland, pp. 345-353.

52. Blenkarn, K.A., 1970. Measurement and Analysis of Ice Forces on Cook Inlet Structures, Proc. Offshore Technology Conference (OTC), Houston, Texas, Vol. 2, pp. 365-378.

53. Reddy, D.V., and Chemma, P.S., 1974. Response of an Offshore Structure to Random Ice Forces. Proc. IEEE, International Conference on Engineering in the Ocean Environment, Halifax Vol. 1, pp. 84-88.

54. Reddy, D. V., Cheema, P. S., and Swamidas, A. S. J., 1975. Ice Force Response Spectrum Modal Analysis of Offshore Towers. Proc. Third POAC Conference, University of Alaska, Alaska, August.

55. King, R., 1974. Hydroelastic Models and Offshore Design, Civil Engineering, pp. 43-47/

56. Reddy, D. V., Cheema, P. S., Swamidas, A. S. J., and Haldar, A.K., 1975. Stochastic Response of a Three-Dimensional Offshore Tower to Ice Force. IAHR/AIRH Third International Symp. on Ice Problems, Hanover, New Hampshire, U.S.A., pp. 499-514.

57. Swamidas, A. S. J. and Reddy, D. V., 1976. Dynamic Ice Structure Interaction of Offshore Monopod Towers by Hybridisation of the Computer Programs EATSW and SAP-IV. Proc. First SAP-IV User's Conference, Los Angeles, California, pp. 33.

58. Liaw, C.Y. and Chopra, A. K., 1973. Earthquake Response of Axisymmetric Tower Structures Surrounded by Water. Report No. EERC 73-25, University of California, Berkeley, pp. 171.

59. Swamidas, A. S. J., Reddy, D. V., and Purcell, G., 1976. Ice Structure Interaction with Artificially Generated Force Records. Presented at the Symposium on Applied Glaciology Orgainized by the International Glaciological Society, Cambridge, England, September 12-17, 1976.

60. Thomson, W. T., Calkins, T., and Caravani, P., 'A Numerical Study of Damping', Int. J. Earthq. Engng. Struct. Dyn. 3, pp. 97-103 (1974).

61. Cronin, D. L., 'Approximation for Determining Harmonically Excited Response of Nonclassically Damped Systems', J. Engng. for Industry, Trans. ASME, 98B, pp. 43-47 (1976).

62. Beredugo, Y. O., 'Modal Analysis of Coupled Motion of Horizontally Excited Embedded Footings', Int. J. Earthq. Engng. Struct. Dyn. 4, pp. 403-410 (1976).

63. Bielak, J., 'Modal Analysis for Building - Soil Interaction', Instituto de Ingenieria, Universidad Nocional Autonoma de Mexico, 1975.

64. Clough, R. W., and Mojtahedi, S., 'Earthquake Response Analysis Considering Non-proportional Damping', Int. J. Earthq. Engng. Struct. Dyn. 4, pp. 489-496 (1976).

65. Corotis, R. B., and Martin, C. H., 1975. Approximate Dynamic Modelling of an Offshore Tower. Preprint 2439, ASCE National Struct. Engg. Convention, New Orleans.

66. Swannell, P., 'A Fortran IV Package to Compute the Natural Frequencies and Mode Shapes of Plane Frame Work., University of Queensland, 1972.

67. Feibusch, R. J., and Keith, E. J., 1969. Analysis of Offshore Structures Including Coupled Structure, Pile and Inelastic Soil Supports. Offshore Tech. Conf., Houston, Texas, Paper No. OTC 1054.

68. Haldar, A. K., Swamidas, A. S. J., Reddy, D.V., and Arockiasamy M., Dynamic Ice-Water-Soil-Structure Interaction of Offshore Towers Including Nonlinear Soil Behavior 9th Annual OTC in Houston, Texas, May 1977.

69. Shou-nien, H., Review of Modal Synthesis Techniques and a New Approach, Bellcomm, Inc., Washington, D.C., pp. 25-39.

70. Hancock, J. L., Peevey, R.M., 'New Concepts in Offshore Platforms', Amoco Production Co., Paper No. OTC 2265 pp. 235.242, Offshore Technology Conference 6200 North Central Expressway, Dallas, Texas 75206.

71. Seed, H.B. and Idriss, I.M., 1969. Influence of Soil Conditions on Ground Motion During Earthquakes. Proc. ASCE, Journal of Soil Mechanics and Foundation Division, Vol. 95, No. SML, pp. 99-137.

APPENDICES

APPENDIX I

I.1 Dynamic Member Stiffness Matrix

$$\{s\} = [s_{1x}\ s_{1y}\ m_1\ s_{2x}\ s_{2y}\ m_2]$$
$$\{v\} = [v_{1x}\ v_{1y}\ \theta_1\ v_{2x}\ v_{2y}\ \theta_2] \qquad \text{(I.1)}$$

$$k_{11} = \begin{bmatrix} a & o & o \\ o & b & d \\ o & d & c \end{bmatrix} \text{ and } k_{12} = \begin{bmatrix} e & o & o \\ o & f & h \\ o & -h & g \end{bmatrix} \qquad \text{(I.2)}$$

k_{22} is obtained from k_{11} by writing $-d$ for d and $k_{21} = k_{12}^T$.

Also, in Eqn. 3.18 and with reference to Fig. I.1.

$$T = \begin{bmatrix} \text{Cos}\bar{\beta} & \text{Sin}\bar{\beta} & o \\ -\text{Sin}\bar{\beta} & \text{Cos}\bar{\beta} & o \\ o & o & 1 \end{bmatrix} \qquad \text{(I.3)}$$

In vibration problems

$a = (EA/L)\ u\ \text{cotu}$

$b = (EI\lambda^3/L^3)\ (\text{Sin}\lambda\ \text{Cosh}\lambda + \text{Cos}\lambda\ \text{Sinh}\lambda)/Z$

$\bar{c} = (EI\lambda/L)\ (\text{Sin}\lambda\ \text{Cosh}\lambda - \text{Cos}\lambda\ \text{Sinh}\lambda)/Z$

$d = (EI\lambda^2/L^2)\ \text{Sin}\lambda\ \text{Sinh}\lambda/Z$

$e = -(EA/L)\ v\ \text{Cosec}\ v$

$f = -(EI\lambda^3/L^3)\ (\text{Sin}\lambda + \text{Sinh}\lambda)/Z$

$g = (EI\lambda/L)\ (\text{Sinh}\lambda - \text{Sin}\lambda)/Z$

$h = (EI\lambda^2/L^2)\ (\text{Cosh}\lambda - \text{Cos}\lambda)/Z$

with

$v = \omega L\ (U/EA)^{1/2}$

$$\lambda = (\omega^2 L^4 u/EI)^{1/4}$$

$$Z = (1 - \cos\lambda \cosh\lambda)$$

where ω is the circular frequency and L, u, EA and EI are the member length, mass per unit length, extensional rigidity and flexural rigidity, respectively. Also, in Eqn. 3.16

$$J_m(\omega) = J_a(\omega)\ i - 1/2\ [1 - (-1)^i\ sg(Z)] \qquad (I.4)$$

where J_a and i are, respectively, the highest integer $< v/\pi$ and the highest integer $< \lambda/\pi$. Also, $sg(Z) = 1$ or -1, taking the sign of Z.

I.2 The Dynamic Stiffness Matrix Including Axial Load, Shear Deformation and Rotary Inertia Effects

Definition of Symbols:

b = section thickness at neutral axis

Q = 1st moment of area of section above N.A.

P = Axial Load

G = Modulus of Rigidity

$$f_1 = (1 - u\omega^2 Q/Gab)/(1 - PQ/GIb)$$

$$f_2 = u\omega^2\ (I/a + QE/Gb)/(1 - PQ/GIb)$$

$$\left.\begin{matrix} E_1 \\ E_2 \end{matrix}\right\} = L \left\{ [u\omega^2/EI\ f_1 + (P/2EI)^2\ (f_1 + f_2)^2]^{1/2} \pm P/2EI\ (f_1 + f_2) \right\}^{1/2}$$

$$\beta = L(u\omega^2/Ea)^{1/2}$$

$$\bar{E}_1 = E_1(1 - PQ/GIb + u\omega^2 L^2 Q/GIb\ E_1^2)$$

$$\bar{E}_2 = E_2\left(1 - PQ/GIb - u\omega^2 L^2 Q/GIb\, E_2^2\right)$$

$$D = 2\,\bar{E}_1\,\bar{E}_2(1 - \text{Cosh}\,E_1\,\text{Cos}\,E_2) + (\bar{E}_1^2 - \bar{E}_2^2)\,\text{Sinh}E_1\,\text{Sin}E_2$$

$$H = \bar{E}_1\,E_1 + \bar{E}_2\,E_2$$

$$G = \left[\bar{E}_2\,E_2 - \bar{E}_1\,E_1\right]\bar{E}_1\bar{E}_2$$

$$M = \bar{E}_2\,E_1 + \bar{E}_1\,E_2$$

The elements of k_{11} and k_{12} are

$$a = EA/L\,(\beta\,\text{Cot}\beta)$$

$$b = E_1\,E_2\,H(EI/L^3)\,(\bar{E}_1\,\text{Sinh}E_1\,\text{Cos}E_2 + \bar{E}_2\,\text{Cosh}E_1\,\text{Sin}E_2)/Df_1$$

$$c = (EI/L)\,H(\bar{E}_1\,\text{Cosh}E_1\,\text{Sin}E_2 - \bar{E}_2\,\text{Sinh}E_1\,\text{Cos}E_2)/D$$

$$d = \left\{(EI/L^2)\,G(1 - \text{Cosh}E_1\,\text{Cos}E_2) + \bar{E}_1\,\bar{E}_2\,(M)\,(\text{Sinh}E_1\,\text{Sin}E_2)\right\}/D$$

$$e = -(EA/L)\,(\beta/\text{Sin}\beta)$$

$$f = -(EI/L^3)\,(E_1\,E_2\,H)\,(\bar{E}_1\,\text{Sinh}E_1 + \bar{E}_2\,\text{Sin}E_2)/Df_1$$

$$g = (EI/L)\,(H)\,(\bar{E}_2\,\text{Sinh}E_1 - \bar{E}_1\,\text{Sin}E_2)/D$$

$$h = (EI/L^2)\,(\bar{E}_1\,\bar{E}_2\,H)\,(\text{Cosh}E_1 - \text{Cos}E_2)/D$$

I.3 The Dynamic Stiffness Matrix, Allowing for Viscous Damping

For the damping coefficient = c_1 and $c_o = c/2u$, the elements of matrices k_{11} and k_{12} are identical to those given in I.2 above, if ω^2 is replaced by $(\omega^2 + c_o^2)$ in the expressions for E_1, E_2, $\bar{E}_1$, $\bar{E}_2$, f_1, f_2 and β.

APPENDIX II

II.1 Analysis of Non-linear Systems

Procedure

In the step-by-step integration method for nonlinear analysis, the condition of dynamic equilibrium is established at the beginning and end of each interval, Δt; the motion of the system during the time increment is evaluated approximately on the basis of an assumed response mechanism. The complete response is obtained by using the velocity and displacement computed at the end of one compuational interval as the initial conditions for the next interval; thus the process may be continued step-by-step from the initiation of loading to any desired time, approximating the nonlinear relationship by successive linear systems.

II.2 Incremental Equation of Equilibrium

For a MDOF system the equation of motion is:

$$[F_I(t)] + [F_D(t)] + [F_s(t)] = [P(t)] \qquad \text{(II.1)}$$

For a time increment, Δt,

$$[F_I(t + \Delta t)] + [F_D(t + \Delta t)] + [F_s(t + \Delta t)] = [P(t + \Delta t)] \qquad \text{(II.2)}$$

Subtracting Eqn. II.1 from Eqn. II.2 yeilds the incremental relationship:

$$[\Delta F_I(t)] + [\Delta F_D(t)] + [\Delta F_s(t)] = [\Delta P(t)] \qquad \text{(II.3)}$$

The incremental forces may be expressed as follows:

$$[\Delta F_I(t)] = [F_I(t+\Delta t)] - [F_I(t)] = [M]\,[\Delta \ddot{X}(t)]$$

$$[\Delta F_D(t)] = [F_D(t+\Delta t)] - [F_D(t)] = [c(t)]\,[\Delta \dot{X}(t)] \qquad \text{(II.4)}$$

$$[\Delta F_s(t)] = [F_s(t+\Delta t)] - [F_s(t)] = [k(t)]\,[\Delta X(t)]$$

$$[\Delta P(t)] = [P(t+\Delta t)] - [P(t)]$$

where it is assumed that the mass, M, does not change with time.

The elements of the incremental damping and stiffness matrices [c(t)] and [k(t)] are the influence coefficients $c_{ij}(t)$ and $k_{ij}(t)$, defined for the time increment; typical representations of these coefficients are shown in Fig. II.1.

The influence coefficients are given by

$$c_{ij}(t) = (dF_{Di}/d\dot{X}_i)_t, \quad k_{ij}(t) = (dF_{si}/dX_i)_t \qquad \text{(II.5)}$$

Substitution of Eqns. II.4 into Eqn. II.3 gives

$$[M]\,[\Delta \ddot{X}(t)] + [c(t)]\,[\Delta \dot{X}(t)] + [k(t)]\,[X(t)] = [\Delta P(t)] \qquad \text{(II.6)}$$

II.3 Step-By-Step Integration: Linear-Acceleration Method

The basic operation in the step-by-step solution of simultaneous differential equations of motion Eqs. (II.6) is their transformation to a set of simultaneous algebraic equations. This is accomplished by introducing a simple relationship between displacement, velocity and acceleration which may be assumed to be valid for a small time increment. In this method, the acceleration varies linearly with time leading to a quadratic and cubic variations of the

velocity and displacement vectors respectively. The final equations can be written as

$$[\tilde{k}(t)]\ [\Delta X(t)] = [\tilde{\Delta P}(t)] \qquad \text{(II.7)}$$

in which

$$[\tilde{k}(t)] = [k(t)] + 6/\Delta t^2\ [M] + 3/\Delta t\ [c(t)] \qquad \text{(II.8)}$$

and

$$[\tilde{\Delta P}(t)] = [\Delta P(t)] + [M]\ [6/\Delta t\ [\dot{X}(t)] + 3[\ddot{X}(t)]] + [c(t)]\ [3[\dot{X}(t)] + \Delta t/2\,[\ddot{X}(t)]] \qquad \text{(II.9)}$$

From the displacement $\Delta X(t)$, the velocity increment is found as

$$[\Delta\dot{X}(t)] = 3/\Delta t\ [\Delta X(t)] - 3[\dot{X}(t)] - \Delta t/2\ [\ddot{X}(t)] \qquad \text{(II.10)}$$

The displacement and the velocity vectors at the end of the time increment are then given by

$$[X(t+\Delta t)] = [X(t)] + [\Delta X(t)]$$
$$[\dot{X}(t+\Delta t)] = [\dot{X}(t)] + [\Delta\dot{X}(t)] \qquad \text{(II.11)}$$

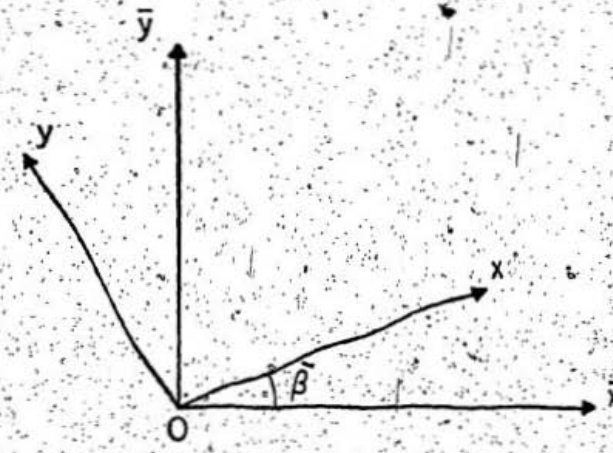

Fig. I.1 Relative Alignment of Member (Oxy) and Global (Oxȳ) Coordinate Systems

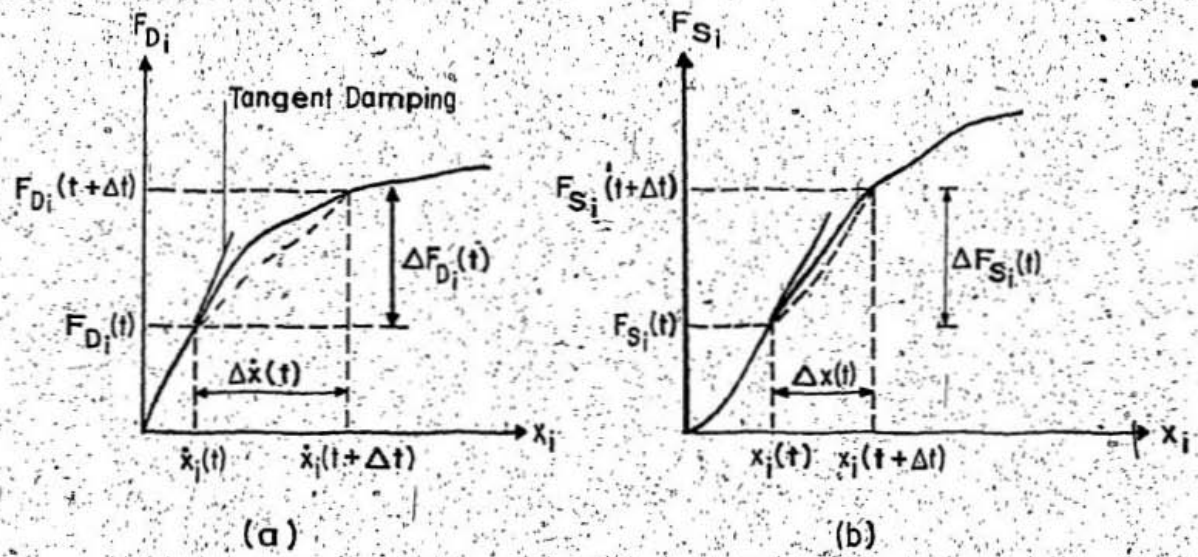

Fig. II.1 Variation of Damping and Spring Forces with Velocity and Displacement

APPENDIX III

COMPUTER DOCUMENTATION

Flow Chart for the Free Vibration - From Ref. 66

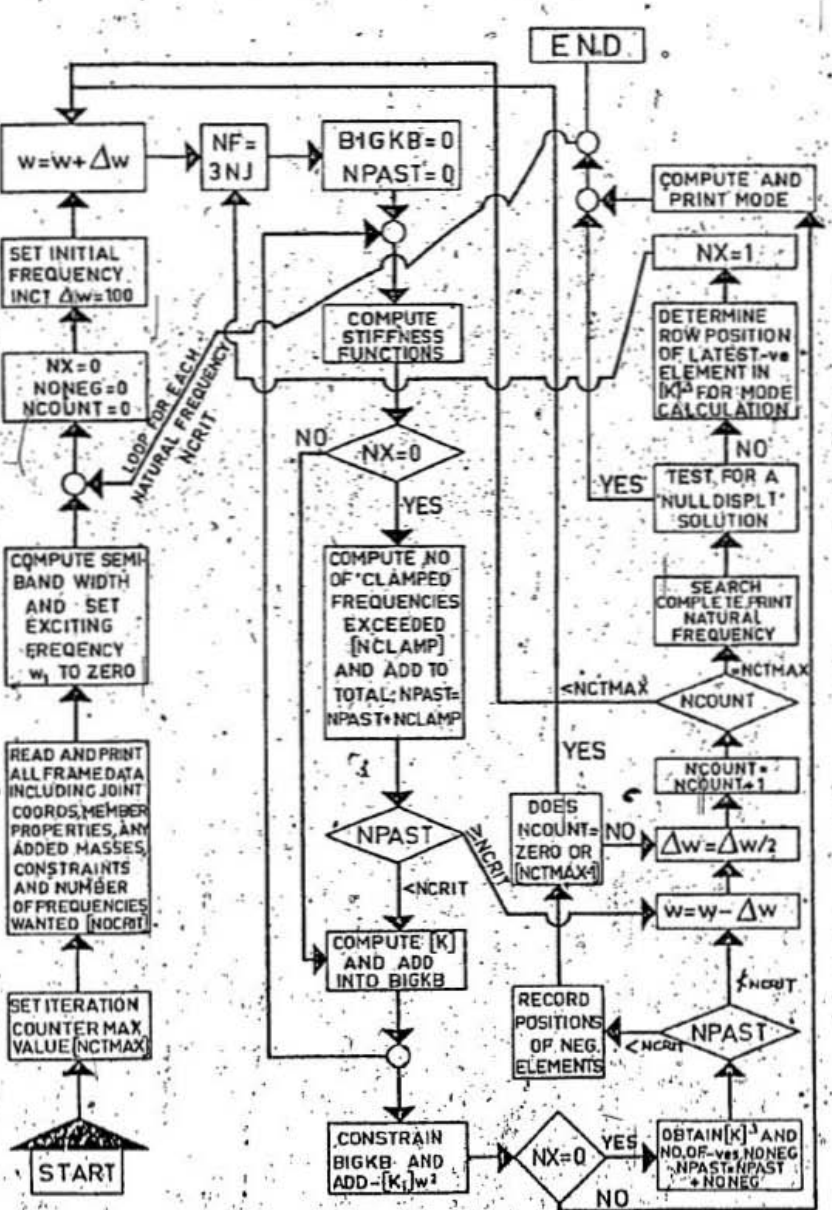

Flow Chart for Free Vibration Including Modal Synthesis

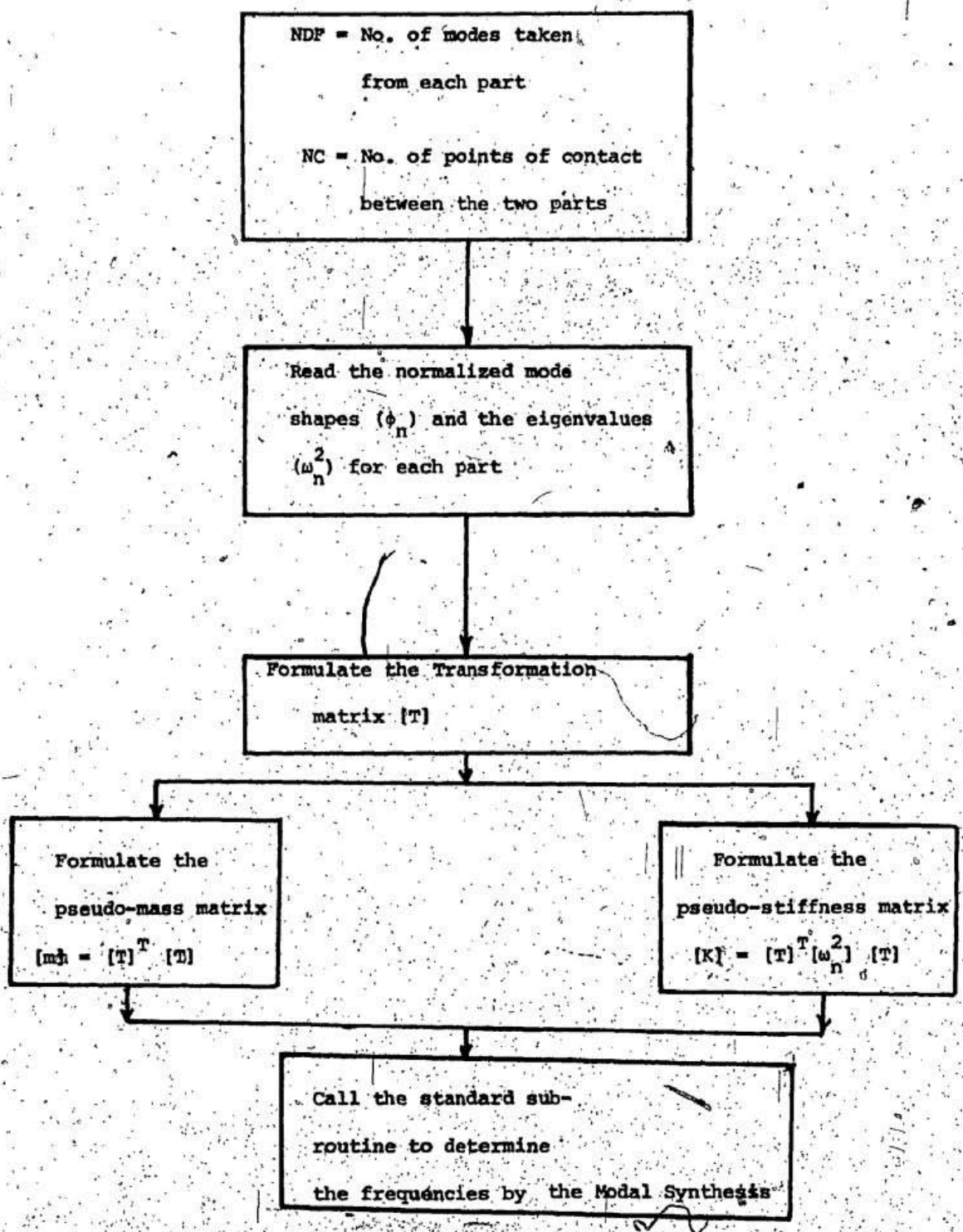

```
C                PROGRAMME TO FIND THE FREQUENCIES FOR OFFSHORE STRUCTURE.
C-----------------------------------------------------------------------
C
C                      USING MODAL SYNTHESIS TECHNIQUE
C
C-----------------------------------------------------------------------
      DIMENSION AZ(2,6),FAS(2,2),FAR(2,4),BZ(2,6),FB(2,6),
     *  FASN(2,2),X(2,2),Y(2,4),AM(12,10),WA(6),WB(6),AN(10,12),
     *  AMS(10,10),SK(12,12),SSK(10,12),WKAREA(2),OMEGA(10),FRQ(10),
     *  IR(10)
      DIMENSION AK(10,10),TAMS(10,10),ALFA(10),BETA(10),Z(10,10),WK(20)
      M=4
      NDF=6
      NC=2
      NN=M+NC
      MK=NN*2
      NK=MK-NC
C-----------------------------------------------------------------------
C
C     INPUT DATA
C     TO READ THE NORMALIZED EIGEN VECTOR FOR EACH PART OF STRUCTURE
      DO 2 I=1,NC
      DO 2 J=1,NDF
    2 READ(5,3) (AZ(I,J),J=1,NDF)
    3 FORMAT(6E10.3)
      DO 12  I=1,NC
      DO 12 J=1,NDF
   12 READ(5,14)(BZ(I,J),J=1,NDF)
   14 FORMAT(6E10.3)
      DO 4 I=1,NC
      DO 4 J=1,NC
    4 FAS(I,J)=AZ(I,J)
      DO 6 I=1,NC
      DO 6   J=1,M
      JJ=J+NC
    6 FAR(I,J)=AZ(I,JJ)
      DO 10 I=1,NC
      DO 10 J=1,NN
   10 FB(I,J)=BZ(I,J)
      CALL LINV1F(FAS,NC,NC,FASN,0,WKAREA,IER)
C-----------------------------------------------------------------------
      IA=NK
      IB=NK
      N=NK
      IZ=NK
      IJOB=1
      COMPLEX ALFA,Z
```

```
C
C
C     TO FORM PSEUDO MASS MATRIX FOR THE STRUCTURE
C
      DO 30 I=1,NC
      DO 30 J=1,M
      X(I,J)=0.0
      DO 30 K=1,NC
   30 X(I,J)=X(I,J)+FASN(I,K)*FAR(K,J)
      DO 40 I=1,NC
      DO 40 J=1,NN
      Y(I,J)=0.0
      DO 40 K=1,NC
   40 Y(I,J)=Y(I,J)+FASN(I,K)*FB(K,J)
      DO 50 I=1,MK
      DO 50 J=1,NK
   50 AM(I,J)=0.0
      DO 60 I=1,NC
      DO 60 J=1,M
   60 AM(I,J)=-X(I,J)
      DO 70 I=1,NC
      DO 70 J=1,NN
      JJ=J+M
   70 AM(I,JJ)=Y(I,J)
      DO 80 I=1,NK
      II=I+NC
   80 AM(II,I)=1.0
C
C     TO READ THE EIGEN VALUE FOR EACH PART OF THE STRUCTURE
C
      READ(5,90)(WA(I),I=1,NN)
      READ(5,90)(WB(I),I=1,NN)
   90 FORMAT(6E10.3)
      DO 100  I=1,MK
      DO 100 J=1,NK
  100 AN(J,I)=AM(I,J)
      DO 110 I=1,NK
      DO 110 J=1,NK
      AMS(I,J)=0.0
      DO 110  K=1,MK
  110 AMS(I,J)=AMS(I,J)+AN(I,K)*AM(K,J)
C
C     TO FORM THE PSEUDO STIFNESS MATRIX FOR THE STRUCTURE
C
      DO 120 I=1,MK
      DO 120 J=1,MK
  120 SK(I,J)=0.0
      DO 130 I=1,NN
  130 SK(I,I)=WA(I)
      DO 140 I=1,NN
      II=I+NN
  140 SK(II,II)=WB(I)
      DO 150 I=1,NK
```

```
      DO 150 J=1,MK
      SSK(I,J)=0.0
      DO 150 K=1,MK
  150 SSK(I,J)=SSK(I,J)+AN(I,K)*SK(K,J)
      DO 160  I=1,NK
      DO 160 J=1,NK
      AK(I,J)=0.0
      DO 160  K=1,NK
  160 AK(I,J)=AK(I,J)+SSK(I,K)*AM(K,J)
      WRITE(6,340)
      DO 165 I=1,NK
      DO 165 J=1,NK
  165 TAMS(I,J)=AMS(I,J)
C-----------------------------------------------------------------------
CCC
CCC   TO GET THE EIGEN VALUE FOR THE STRUCTURE
CCC
C-----------------------------------------------------------------------
      CALL EIGZF(AK,IA,TAMS,IB,N,IJOB,ALFA,BETA,Z,IZ,WK,IER)
      WRITE(6,170)
  170 FORMAT(1H1)
      DO 190 I=1,NK
      OMEGA(I)=SQRT(REAL(ALFA(I))/(BETA(I)))
      FRQ(I)=OMEGA(I)/6.28
  190 CONTINUE
C-----------------------------------------------------------------------
CCC
CCC   TO ARRANGE THE EIGEN VALUE IN ASCENDING ORDER
CCC
C-----------------------------------------------------------------------
      DO 195  I=1,NK
  195 IR(I)=I
      CALL VSORTP(OMEGA,NK,IR)
      DO 197 I=1,4
  197 WRITE(6,200) I,FRQ(IR(I))
  200 FORMAT(10X,'FRQ (',I1,')= ',E12.4)
      STOP
      END
```